Characterization of black spot resistance in diploid roses with QTL detection, meta-analysis and candidate-gene identification

D. Lopez Arias, A. Chastellier, T. Thouroude, J. Bradeen, L. van Eck, Yannick de Oliveira, S. Paillard, F. Foucher, L. Hibrand-Saint Oyant, Vanessa Soufflet-Freslon

CHARACTERIZATION OF BLACK SPOT RESISTANCE IN DIPLOID ROSES WITH QTL DETECTION, META-ANALYSIS AND CANDIDATE-GENE IDENTIFICATION

D. C. Lopez Arias[1], A. Chastellier[1], T. Thouroude[1], J. Bradeen[2], L. Van Ech[2], Yannick De Oliveira[3], S. Paillard[1], F. Foucher[1], L. Hibrand-Saint Oyant[1] and V. Soufflet-Freslon[1]

[1]IRHS-UMR1345, Université d'Angers, INRAE, Institut Agro, SFR 4207 QuaSaV, 49071, Beaucouzé, France

[2]Department of Plant Pathology and The Stakman-Borlaug Center for Sustainable Plant Health, University of Minnesota, St. Paul, MN, USA

[3] Génétique Quantitative et Évolution - Le Moulon, INRAE - Université Paris-Sud - CNRS - AgroParisTech, Ferme du Moulon, F-91190 Gif-sur-Yvette, France

*Corresponding author: Diana Carolina Lopez Arias, diana.lopez-arias@inrae.fr

Email list of the authors:

D. C. Lopez Arias[1]: diana.lopez-arias@inrae.fr, A. Chastellier[1]: annie.chastelier@inrae.fr, T. Thouroude[1]: tatiana.thouroude@inrae.fr, J. Bradeen[2]: jbradeen@umn.edu, L. Van Eck[2]: vaneck@augsburg.edu, Yannick De Oliveira[3]: yannick.de-oliveira@inrae.fr. S. Paillard[1]: sophie.paillard@inrae.fr, F. Foucher[1]: fabrice.foucher@inrae.fr, L. Hibrand-Saint Oyant[1]: laurence.hibrand-saint-oyant@inrae.fr and V. Soufflet-Freslon[1]: vanessa.soufflet-freslon@Agrocampus-ouest.fr.

Author's ORCID:

D. C. Lopez Arias: https://orcid.org/0000-0001-8129-2786, J. Bradeen: https://orcid.org/0000-0003-1930-4728, L. Van Ech: https://orcid.org/0000-0002-3073-1344, S. Paillard: https://orcid.org/0000-0001-7516-848X, F.

Foucher: https://orcid.org/0000-0002-3693-7183, L. Hibrand-Saint Oyant: https://orcid.org/0000-0002-7604-3811 and V. Soufflet-Freslon: https://orcid.org/0000-0002-1264-7595.

Key message

Two environmentally stable QTLs linked to black spot disease resistance in the *Rosa wichurana* genetic background were detected, in different connected populations, on linkage groups 3 and 5. Co-localization between *R*-genes and defense response genes was revealed via meta-analysis.

Abstract

The widespread rose black spot disease (BSD) caused by the hemibiotrophic fungus *Diplocarpon rosae* Wolf. is efficiently controlled with fungicides. However, in the actual context of reducing agrochemical use, the demand for rose bushes with higher levels of resistance has increased. Qualitative resistance conferred by major genes (*Rdr* genes) has been widely studied but quantitative resistance to BSD requires further investigation. In this study, segregating populations connected through the BSD resistant *Rosa wichurana* male parent were phenotyped for disease resistance over several years and locations. A pseudo-testcross approach was used, resulting in six parental maps across three populations. A total of 45 individual QTLs with significant effect on BSD resistance were mapped on the male maps (on linkage groups (LG) B3, B4, B5 and B6), and 12 on the female maps (on LG A1, A2, A3, A4 and A5). Two major regions linked to BSD resistance were identified on LG B3 and B5 of the male maps and were integrated into a consensus map built from all three of the male maps. A meta-analysis was used to narrow down the confidence intervals of individual QTLs from three populations by generating meta-QTLs. Two “hot spots” or meta-QTLs were found per LG, enabling reduction of the confidence interval to 10.42 cM for B3 and 11.47 cM for B5. An expert annotation of NBS-LRR encoding genes of the genome assembly of Hibrand et al. was performed and used to explore potential co-localization with *R*-genes. Co-localization with defense response genes was also investigated.

Keywords

Rosa, quantitative resistance, natural infection, *Diplocarpon rosae*, QTL mapping, meta-analysis

Conflict of interest

All authors declare that they have no conflicts of interests.

Ethical standards

We declare that these experiments complied with the ethical standards in France.

Availability of data and material

Genetic maps and QTL tables are available as supplementary data.

Author contribution

DCLA participated in the phenotyping, performed the genetic and statistical analyses and wrote the paper. VSF, FF and LHSO conceived the AC provided a technical support in the SSR genotyping and participated in the phenotyping. TT coordinated the field trials and participated in the phenotyping. LVE and JB performed the manual annotation and provided revision of the manuscript. YDO provided support in software Biomercator and the meta-analysis approach. FF provided extensive revisions of the manuscript. SP, LHSO and VSF participated in the phenotyping and provided extensive revisions of the manuscript. All authors read the final version of the manuscript and approved its publication.

Introduction

Cultivated roses are among the most popular garden plants (Waliczek et al. 2015a; Wang et al. 2017). In France, 16% of shrubs bought by the final consumers are garden roses, with a market value of 50.6 million Euros in 2017. Due in part to susceptibility to BSD, sales of garden roses in France declined 10% in 2017 compared with 2016 (VAL'HOR and FranceAgriMer 2017). As such, BSD causes large economic losses and is, therefore, considered the most serious disease of cultivated roses grown outdoors.

BSD in roses, caused by the hemibiotrophic fungus *Diplocarpon rosae* Wolf, is globally distributed and affects nearly all modern varieties. To date, 13 races have been reported (Carlson-Nilsson 2001; Gachomo et al. 2006; Whitaker et al. 2007, 2010b; Zlesak et al. 2010; Zurn et al. 2018). Typical symptoms of this disease include dark rounded spots with fringed margins on the adaxial side of the leaves followed by chlorosis around the lesion and

premature defoliation (Blechert and Debener 2005; Gachomo et al. 2006; Horst and Cloyd 2007). Reduced vigor in susceptible varieties can be observed, sometimes leading to death due to increased susceptibility to other stresses, like frost (Smith et al. 1989; Black et al. 1994). It is, then, important to study the rose-*Diplocarpon rosae* pathosystem.

The BSD fungus is obligate to the genus *Rosa*, though other *Diplocarpon* species are pathogenic on different crop species in the *Rosaceae* genus (Horst and Cloyd 2007). *Diplocarpon rosae* is spread mainly through asexual spores that are water-borne. During the infection process, the spores germinate, develop a germ tube with a melanized appresorium and penetrate the leaf cuticle (Gachomo 2005; Gachomo et al. 2006, 2010; Gachomo and Kotchoni 2007). During the biotrophic phase, subcuticular hyphae are formed followed by intercellular hyphae. Haustoria can be observed in this first stage of infection (Gachomo 2005; Gachomo and Kotchoni 2007). Then, the pathogen switches from a biotrophic lifestyle to a necrotrophic one and forms necrotrophic intracellular hyphae, followed in short order by a production of acervuli and second-generation conidia. On susceptible plants, a new generation of conidia is produced within nine days after inoculation (Gachomo 2005; Gachomo et al. 2006; Gachomo and Kotchoni 2007). Conidia are then spread by water-splash to start a whole new infection process on other leaves. Effective infection requires free water and humid conditions (Saunders 1966; Wiggers et al. 1997). Consequently, BSD is especially problematic in areas with high annual precipitation and humidity (Debener 2017).

BSD is rarely observed in greenhouse production as humidity can be carefully regulated. Garden rose multiplication and grafting are mainly done in the field, and rose bushes are generally used in gardens and landscaping for aesthetic value and low maintenance requirements. Due to the perennial habit of garden roses and *D. rosae* overwintering in fallen leaves, new infections can appear each year if the disease is not well managed (Münnekhoff et al. 2017) and can impact final consumers such as private gardeners and public garden managers. BSD is traditionally managed with fungicide applications. To reduce risk of chemical exposure, added costs and labor associated with this type of management, today's consumers are increasingly asking for natural resistance in rose plants (Harp et al. 2009; Zlesak et al. 2010, 2017; Waliczek et al. 2015b; Byrne et al. 2019). Moreover, European countries have adopted new laws to preserve the environment that aim to decrease agrochemical use. For example in France, measures such as the Ecophyto Plan (Labbé 2014) have forbidden the use of chemicals in public landscaping and private gardens since January 2017 and 2019, respectively (Labbé 2014). These concerns have encouraged breeders and researchers to study BSD and to develop varieties with sustainable and higher levels of resistance.

Indeed, genetic resistance is a critical challenge to successful disease management in an environmentally friendly and cost-effective manner. Researchers have studied the genetic resistance to BSD, helping to identify modern rose varieties and wild species with high levels of resistance (Wiggers et al. 1997; Carlson-Nilsson 2001; Boontiang 2003; Blechert and Debener 2005; Uggla and Carlson-Nilsson 2005; Harp et al. 2009; Schulz et al. 2009; Soufflet-Freslon et al. 2019). However, breeding for BSD resistance is complex due to the development of new pathogenic races and different ploidy levels in the genus *Rosa* (Debener et al. 1998; Uggla and Carlson-Nilsson 2005; Whitaker et al. 2007; Debener 2017). Four major loci associated with BSD resistance were identified mostly using detached leaf assays: *Rdr1* and *Rdr2* on chromosome 1 (Malek and Debener 1998; Yokoya et al. 2000; Malek et al. 2000; Kaufmann et al. 2003, 2010; Hattendorf et al. 2004; Whitaker et al. 2010a; Terefe-Ayana et al. 2011; Menz et al. 2018, 2020), *Rdr3* recently found to be located on chromosome 6 (Whitaker et al. 2010a; Zurn et al. 2020) and *Rdr4* possibly located on chromosome 5 (Zurn et al. 2018). Evidence of partial resistance to BSD was reported in several cases and seems to be race-non-specific (Xue and Davidson 1998; Shupert 2006; Whitaker and Hokanson 2009; Whitaker et al. 2010b; Allum et al. 2010; Dong et al. 2017). Quantitative resistance often confers a partial level of resistance to the plant by reducing pathogen multiplication, plant colonization, disease spread or symptom severity (Pilet-Nayel et al. 2017). This type of resistance is usually controlled by several genes and is associated with genomic regions termed Quantitative Trait Loci (QTLs). Over the last 20 years, many QTL experiments for disease resistance have been carried out on major crops (Lacape et al. 2010; Qi et al. 2011; Holland and Coles 2011; Yadava et al. 2012; Hamon et al. 2013; Semagn et al. 2013; Said et al. 2013; Pilet-Nayel et al. 2017). More recently, QTL analyses have been conducted on ornamental crops such as carnations, gerberas or roses (Yagi et al. 2006, 2012; Leus et al. 2015; Fu et al. 2017; Yan et al. 2019). On-going research suggests QTLs conferring resistance to BSD. Yan et al. (Yan et al. 2019) have identified a possible major QTL on LG 3, based on one year of phenotypic data and a pedigree based map of 15 diploid genotypes while Soufflet-Freslon et al. (Soufflet-Freslon et al. 2019) identified possible QTLs in two populations in France. These emerging studies aside, quantitative resistance to BSD has not been extensively studied, yet it remains a powerful tool to identify genomic regions involved in complex traits such as disease resistance.

The validity of QTL mapping results is influenced by many factors, including experimental conditions, choice of parents, rating scale, environmental conditions during the scored years, type and size of mapping populations, map density and statistical methods (Lanaud et al. 2009; Liu et al. 2009; Vasconcellos et al. 2017; Guo et al. 2018). Thus, QTL mapping of one trait across multiple populations and environments can frequently yield heterogeneous results

comprising different genomic positions and large confidence intervals. Further refinement of these intervals and synthesis of all QTL information are difficult but necessary steps prior to QTL cloning attempts and MAS breeding application. Meta-analysis is an effective approach to combine QTL results from independent studies and refine QTL positions on a consensus genetic map (Goffinet and Gerber 2000; Veyrieras et al. 2007). This method was useful in characterizing the genetic determinants of complex traits for a variety of crops such as drought stress in rice (Khowaja et al. 2009), ear emergence in wheat (Griffiths et al. 2009), yield and anthesis silking in maize (Semagn et al. 2013), yield associated traits in *Brassica juncea* (Yadava et al. 2012), seed weight and resistance to soybean cyst nematode in soybean (Guo et al. 2006; Qi et al. 2011), partial resistance to *Aphanomyces euteiches* in pea (Hamon et al. 2013) or fiber quality, yield, drought tolerance and disease resistance in cotton (Lacape et al. 2010; Said et al. 2013). With plant genome sequences becoming increasingly available, it is now possible to apply comparative analysis between genetic and physical maps to identify candidate genes underlying MetaQTLs. This approach has not yet been explored for an ornamental crop such as roses.

The main objective of our study was to explore the genetic determinants of BSD resistance in *Rosa wichurana* (RW). We identified QTLs linked to BSD resistance in RW using three different populations phenotyped over several years and locations. We next evaluated the stability of these QTLs and their inheritance in different genetic backgrounds. Finally, we explored sets of candidate genes at BSD resistance QTL locations using one of the recently published rose genome assembly from Hibrand-Saint Oyant et al. in 2018.

Material and methods

Mapping populations

We used *R. wichurana* (RW) as a source of resistance. Indeed, RW was described to be highly resistant to BSD (Debener et al. 1998; Yan et al. 2019). RW was crossed with different cultivars to develop three F1 progenies:

- OW population (151 individuals) was obtained from a cross between *R. chinensis* 'Old Blush' (OB), susceptible to BSD, and RW (Lopez Arias et al. in press; Hibrand-Saint Oyant et al. 2018; Soufflet-Freslon et al. 2019),

- HW population (209 individuals) was generated from a cross between a dihaploid rose named H190 (Meynet et al. 1994), susceptible to BSD, and RW (Soufflet-Freslon et al. 2019),

- FW population (96 individuals) resulted from a cross between the cultivar ‘The Fairy’ (TF) and RW (Kawamura et al. 2015). In the Earth-Kind® Trials using detached leaf assay, TF was shown to be susceptible to pathogen races 3, 8 and 9 (Zlesak et al. 2010).

The OW and FW populations were planted on their own roots in the field at INRA Horticulture Experimental Facility (Beaucouzé, France). The HW population was grafted on to *Rosa canina* 'Laxa' rootstock and planted in three French sites (Soufflet-Freslon et al. 2019):

- Nursery France Pilté (45270 Quiers-sur-Bezonde, Loiret, France), henceforth referred to as Bellegarde,
- Nursery/Breeder Meilland Richardier (Diémoz, Isère, France), henceforth referred to as Diémoz,
- Horticulture Experimental Facility (Beaucouzé, France), henceforth referred to as Angers.

Pruning was performed in November followed by a copper treatment to protect against canker. One to two applications of the fungicide NIMROD® were made according to manufacturer’s recommendations in the Spring to prevent powdery mildew development, and an aphicide spray was used if necessary. NIMROD® is not effective against *D. rosae* and no broad-spectrum fungicide was used.

For the HW and FW populations, field trials were performed in a randomized complete block design with three replicates. Due to production problems, only one replicate per individual for the OW population was used.

Disease scoring and statistical analyses

BSD was visually scored for each population two years after planting them in the field and at the peak of disease (between July and September depending on the year). BSD was scored on the lower part of the plant using a visual rating scale from 0 to 5 presented in Supplementary figure 1 (Marolleau et al. 2020; Soufflet-Freslon et al. 2019). These scores correspond to a percentage of infected leaves and a degree of defoliation (scores 4 and 5). Disease resistance or susceptibility on field trials was assessed using the visual rating scale described above. First, plants with a score lower than 1 were considered “resistant”. Indeed, the response to the *D. rosae* infection seemed to prevent pathogen development on the leaves or considerably reduce pathogen growth on the plant, leading to no visible symptoms (score 0) or to the infection of a small portion of leaves (less than 25% of the lower part of the plant). Then, plants with a score lower than 4 were considered “intermediate” as less than 75% of the lower part of the plant was infected but no defoliation had yet occurred. Finally, susceptible plants were scored 4 to 5 with more than 75% of the

lower part of the plant showing symptoms and/or a sever defoliation at that time, meaning that the response to the infection did not efficiently impair pathogen development.

The OW population was scored from 2014 to 2018 (Lopez Arias et al. in press), the HW population was scored from 2012 to 2014 (Soufflet-Freslon et al. 2019) and in 2018, and the FW population was scored in 2014 and 2018.

All phenotypic data were analyzed with Rstudio interface (version 1.1.463, http://www.rstudio.com/) of R software (http://www.r-project.org/), version 3.5.1 (2018-07-02).

An overall mean for each population was calculated for each year of scoring to assess whether or not the disease incidence was uniform over the years using a Kruskal-Wallis test (for OW and HW populations) and a Wilcoxon test (for FW population).

The normality of residuals was tested using a Shapiro-Wilk test and the homogeneity of variance was assessed with a Bartlett's test. However, in field situations, plants can die or disease scoring can be missing, resulting in unbalanced experimental designs. Unlike analysis of variance (ANOVA), maximum likelihood methods, such as Restricted Maximum Likelihood (REML), provide unbiased estimators without any demand on the design and balance of data (Patterson and Thompson 1971; Corbeil and Searle 1976; Harville 1977; Lynch and Walsh 1998; Holland et al. 2010). Based on the data distribution, REML was used in place of ANOVA to estimate variance components using the package 'sommer' (Covarrubias-Pazaran 2019) in R. The broad-sense heritability was calculated for each population based on the following formula:

$H^2 = \sigma_g^2 / (\sigma_g^2 + \frac{\sigma_{gxe}^2}{a} + \frac{\sigma_\varepsilon^2}{ar})$, where σ_g^2 is the genotypic variance among populations, σ_{gxe}^2 is the variance of the interaction between genotype and environment (year/location for HW and year for FW and OW), σ_ε^2 is the residual variance, *a* is the number of scoring years and *r* the number of replicates in each population.

Genetic data and linkage mapping

It is not possible to obtain homozygous parental lines in rose by self-fertilizing due to strong inbreeding depression. As such, a "double pseudo-testcross strategy" developed for highly heterozygous plants (Grattapaglia and Sederoff 1994; Weber et al. 2003; Fischer et al. 2004; Hibrand-Saint Oyant et al. 2007; Roman et al. 2015; Zurn et al. 2018; Bourke et al. 2018; Yan et al. 2019) was used in the current study. This strategy involves a controlled cross between two genotypes, with heterozygous genetic markers originating from either parents, followed in their F1

generation. Multiple maximum likelihood mapping was conducting using JoinMap V4.1(Van Ooijen 2011) using the CP (Cross population = outbreed full-sib family) population setting. In this analysis, molecular markers can segregate in one or both parents, with maps comprising dominant and co-dominant markers calculated separately for each parent followed by construction of an integrated consensus map.

Parental linkage maps for FW and HW populations were constructed from previously published data (Kawamura et al. 2015; Roman et al. 2015). Constructed maps were checked for apparent genotyping errors and/or poor fitting loci by looking at aberrant number of double crossing, high values of 'Nearest Neighbor fit' (N.N fit) and genotype probabilities (-Log10(P)). When outstanding loci were found, genotyping was controlled either with SNP/probeset categories according to cluster properties or raw genotyping from GeneMapper software and removed when necessary. Maps were then re-calculated. The consensus map released by (Spiller et al. 2011) was used to check LG names and whole LG inversions for consistency.

Parental linkage maps for the OW population were developed using previously reported single nucleotide polymorphism (SNP) marker data (Hibrand-Saint Oyant et al. 2018). Short sequence repeat (SSR) markers previously genotyped in this population were also included (Lopez Arias et al. in press) and used as common markers for the Meta-QTL analysis. Parental maps were calculated using JoinMap 4.1 (Van Ooijen 2011) but due to insufficient "anchor loci" (i.e. makers heterozygous in both parents) an integrated map could not be obtained for this population. Following calculation of pair-wise recombination frequencies, seven LGs were identified using the logarithm of odds (LOD) score of independence between pairs of loci at a threshold of 4. Due to a large number of markers per LG (from 171 to 1,134 markers), the maximum-likelihood mapping algorithm method was used to order markers on LGs. Indeed, this method is more suitable than regression mapping for large marker datasets (Cheema and Dicks 2009). The maximum-likelihood mapping algorithm method was carried out under default JoinMap calculation settings (i.e. simulated annealing chain length of 10,000 with an acceptance probability threshold of 0.25, Gibbs sampling for estimation of multipoint recombination frequencies with a burn-in chain length of 10,000 and a chain length per Monte Carlo EM algorithm of 1,000). The same procedure previously described was carried out to identify and remove markers with genotyping errors and poor fitting.

QTL mapping

QTL mapping was performed using the parental maps for each population (OW, FW and HW) and data from different years were analyzed separately. The R/QTL package (Broman and Sen 2009; Broman and Wu 2019) was used to map QTLs and specific analyses were carried out for each set of phenotypic data according to the distribution of disease scores. For all populations, scoring years and locations, a "one dimensional QTL scan" was carried out using different specific models that best fit the data using the package R/QTL on the Rstudio interface (Broman and Sen 2009).

For data distributed normally, a three-step strategy was employed using a normal model for simple interval mapping (SIM) and composite interval mapping (CIM). First, the multiple imputation method was used to overcome issues with missing data as it fills in all missing genotype data even at sites between markers on a defined grid along LGs (Broman and Sen 2009). For this, the function 'sim.geno' was used with 200 imputations and a step size of 1cM. Next, using the previous simulated data, a genome scan with a single QTL model (SIM) was performed with the function 'scanone' (parameters: normal model and imputation method). Finally, a permutation test with 1,000 permutations of the data was used to identify genome-wide significance thresholds for declaring the presence of a QTL (Doerge and Churchill 1996). When QTLs were identified, CIM was performed to improve further QTL detections by including a marker at the peak of QTL with large effect as covariate (Broman and Sen 2009).

For data exhibiting a substantial peak at zero, the mapping strategy was based on a two-part model used to better characterize the influence of a QTL presence on BSD (Broman 2003; Broman and Sen 2009; Holland and Coles 2011). For this approach, the phenotypic data were analyzed in two parts. First, individuals with scoring values above zero were analyzed using a normal phenotype model. Second, the trait was considered as binary (0 and >0) (Broman 2003; Broman and Sen 2009). The two-part model performs the following three calculations, each with a resulting LOD score: (1) the hypothesis that a given QTL increased the probability that an individual had a null phenotype (LODπ), and so was resistant (which can also be referred as the penetrance of the disease); (2) the hypothesis that a detected QTL influenced the average phenotype among individuals with non-null phenotypes (LODμ), so it affected the severity of the disease; (3) the probability of having a QTL at a given position (LODμ,π) (simply the sum of LOD scores from the preceding analyses).

To characterize detected QTLs, approximate 95% Bayesian credible intervals, phenotypic variation and QTL effects were estimated using the functions bayesint, makeqtl/fitqtl and effectplot respectively.

Meta-QTL analysis

The meta-QTL analysis was conducted with Biomercator v4.2.2 software (Arcade et al. 2004; Sosnowski et al. 2012). The total number of QTLs per LG for all three populations was recorded. LGs with more than three QTLs and with QTLs from all the populations were considered for the meta-analysis. Input map files and QTL files for Biomercator v4.2.2 were prepared for the male parent map of each population according to its requirements.

Using the male map of OW population as the reference linkage map to fix locus order, a consensus male map was constructed using ConsMap (based on a weighted least square (WLS) strategy). To identify meta-QTLs, we pursued the approach proposed by Goffinet and Gerber in 2000. Due to the fact that our mapping populations share a common male parent and because the same plants were phenotyped across years, our data are not completely independent. In simulation tests, the Goffinet approach proved to be robust, obviating the need for further manipulation of non-independent data (Goffinet and Gerber 2000). The method first tests the likelihood of QTL grouping in maximum four groups and then selects the optimum number of groups using an 'Akaike' information criterion (AIC) (Arcade et al. 2004; Sosnowski et al. 2012). Estimated positions and confidence intervals (CI) of all consensus QTLs were provided and the resulting meta-QTLs were projected on the previously constructed consensus map using QTLProj.

NB-encoding genes and candidate-gene mining

In version 4.2.2 of Biomercator, genetic maps can be linked to genome annotation using anchor markers. Genes underlying QTL or meta-QTL confidence intervals (CI) can be listed and basic gene ontology (GO) term representation within CI, chromosome or whole genome can be applied. In this study, we compared the lists of genes underlying meta-QTLs for the recently released rose genome sequence (Hibrand-Saint Oyant et al. 2018).

To detect potential candidate-genes, a detailed analysis of NBS-LRR genes was performed. Protein sequences from Rosa chinensis (Hibrand-Saint Oyant et al. 2018) were scanned for the presence of R-gene-related domains using the hmmscan algorithm in HMMER v3.1b2 (Finn et al. 2015). These domains included NB-ARC (PF00931), TIR (PF01582, PF13676) and LRR (PF00560, PF07723, PF07725, PF12799, PF13306, PF13516, PF13855, PF14580) domains as defined in the Pfam database (Finn et al. 2016). Only proteins with an NB-ARC domain hit longer than 20 amino acid residues and with E-value $< 1 \times 10{-}05$ were retained for subsequent analysis. These sequences were

scanned for the presence of additional, non-canonical domains. The presence of coiled-coil domains was determined for each protein using ncoils with the arguments "-c -w -win 21 -min_P 0.75" and "-c -w -win 28 -min_P 0.75" (Lupas et al. 1991). Custom python scripts were developed to parse, tile and filter the scan output to obtain detailed domain configuration for each protein sequence. NB-ARC domains were extracted from each sequence according to the hmmscan results, and used for subsequent phylogenetic analysis. NB-ARC sequences were coalesced into homology groups using USEARCH with the arguments "-cluster_agg %s -id 0.8 -linkage min" (Edgar 2010). A multiple sequence alignment was constructed for each homology group using MUSCLE (Edgar 2004), and consensus sequences obtained using HMMBUILD and HMMEMIT in HMMER v3.1b2. A multiple sequence alignment was constructed from all consensus sequences using MUSCLE and converted to the PHYLIP format (Felsenstein 1989). RaxML was used to construct the phylogeny (Stamatakis 2014), using 100 bootstrap replicates and an NB-ARC consensus sequence from Arabidopsis thaliana as outgroup, with the arguments "-m PROTCATDAYHOFF -T 24 -f a -x 98 -p f -N 100". Chromosomal positions for candidate *R*-genes were used to construct a physical map of *R*-gene distribution within the genome, using CIRCOS (Krzywinski et al. 2009).

Results

Disease scoring and statistical analyses

BSD was recorded in all three studied populations over several environments (years and locations) under natural infection in fields with no chemical treatment. Across all scoring years, the parents RW and TF were found resistant to BSD with a mean score of 0.50 and 0.33, respectively. The H190 female parent was classified as intermediate with a mean score of 3.44 for all locations whereas OB had a mean score of 4.7 and was classified as susceptible to BSD.

For the OW population, the mean annual BSD scores from 2014 to 2018 were not significantly different from each other ($H=7.2759$, 4 d.f., $P=0.122$, see Supplementary figure 2) indicating that the disease impact on the OW population was homogeneous over 2014-2015-2016-2017 and 2018. The disease scores in the OW population ranged from 0 to the maximum score 5. The median of 2018 scoring was higher than for other years. Residuals for the OW population showed a distribution close to normal ($W=0.99509$, $P=0.02045$) but the homogeneity of variance across years was not validated by a Bartlett's test ($K=298.1$, 9 d.f., $P<0.001$).

For the FW population, BSD scores in 2014 were significantly different from those in 2018 ($Z=-12.648$, 5 d.f., $P<0.001$, see Supplementary figure 2). In general, the FW population was more resistant than the two other populations with scores ranging from 0 to 4. Additionally, FW was the only population showing no defoliation due to disease. The phenotypic distribution of the FW population showed a peak at 0 and the residuals did not follow a normal distribution ($W=0.93557$, $P<0.001$). However, homogeneity of variance across years was validated ($K=298.1$, 9 d.f., $P<0.001$).

For the HW population, the mean of BSD scores in different locations was significantly different ($H=476.52$, 2 d.f., $P<0.001$, data not shown), so all three locations were considered separately. In the three locations (Angers, Bellegarde and Diémoz), BSD was scored over several years (four, three and three years respectively) and infection levels for each year within a location were significantly different from each other ($Ha=346.74$, 3 d.f., $P<0.001$; $Hb=308.8$, 2 d.f., $P<0.001$ and $Hd=212.43$, 2 d.f., $P<0.001$; respectively, see Supplementary figure 2). BSD scores ranged from 0 to 4 for Angers and Bellegarde, and no individual was found completely resistant in Diémoz in all scoring years with BSD scores ranging from 0.67 to 4. A spike-like distribution was observed in 2018 in Angers, 2014 in Bellegarde and 2013 in Diémoz. Normality of residuals as well as homogeneity of variance were not validated (respectively $W=0.99618$, $P<0.001$ and $K=35.799$, 9 d.f., $P<0.001$). Interestingly, scoring year 2012 was lower than 2013 and 2014 for all three locations, and for Angers in 2018, many individuals presented a high resistance. However, the mean of BSD over the three years (2012, 2013 and 2014) was always the lowest in Angers, intermediate in Bellegarde and the highest in Diémoz.

Since normality and variance homogeneity assumptions were not validated for all three populations, the calculation of variance components was obtained using the REML method. The broad sense heritability of BSD resistance was estimated to be 0.79, 0.86 and 0.65 for the OW, HW and FW populations, respectively, indicating that BSD resistance is mainly controlled by genetic factors in all three populations. Moreover, the proportion of phenotypic variance due to genetic effects, here the variance in response to *D. rosae* infection due to genetic background of the individuals, seems to be higher for HW than for OW and lower for FW.

Linkage mapping of parental maps

Parent-based maps were constructed for the HW and FW populations using previously published data (Kawamura et al. 2011, 2015; Roman et al. 2015). For both populations, seven LGs were defined and named according

to the rose integrated consensus map of (Spiller et al. 2011). For the HW population, the male map comprised 56 markers covering 418.58 cM, and the female map comprised 37 markers covering 313.89 cM. On LG6 of the female map, only two markers were found heterozygous and were mapped. For the FW population, the male map comprised 94 markers covering 457.94 cM and the female map comprised 75 markers with a coverage of 369.91 cM.

For the OW population, we generated linkage maps with already published data by (Hibrand-Saint Oyant et al. 2018) and SSR markers selected to facilitate meta-analysis. A total of 497 SNP and 36 SSR markers were mapped on the male map. The resulting map comprises 402 unique loci assigned to seven LGs, designated B1-B7. The average marker interval was 1.14 cM (Table 1 and Supplementary figure 4) and the entire map covered 453.62 cM. LGs range in size from 42.6 (B3) to 84.34 cM (B2). A total of 692 SNP markers, 31 SSR markers and one gene (*NP* also known as *RoAP2*, see Table 1 and Supplementary figure 3) were mapped in the female of the OW population. The resulting map included 513 unique loci assigned to seven LGs (named A1-A7). The average distance between markers is 0.96 cM and LGs range in size from 33.42 (A2) to 97.65 cM (A5). The female map for the OW population is 473.85 cM in total length.

Common markers were the ones shared by at least two populations. In total, 72 markers (41 common markers found for the male maps and 31 for the female maps) were used as "bridge markers" to connect the OW, FW and HW linkage maps (Table 1, listed on Supplementary table 1). The number of common markers per LG ranged from three (B1-B6 and A1-A6-A7) to nine (B3) (Table 1). Of 41 markers shared by at least two of the male linkage map, 21 were shared by all three male maps. Only eight markers were shared by the three female maps (Supplementary table 1). There was at least one common marker between the three populations for all LGs of the male and the female (except for A1) maps.

QTL analysis

First, QTL detections within populations were performed using the parental genetic maps and phenotypic data of BSD resistance from the OW, HW and FW populations. In each population, individuals showed variable resistance responses across environments and years, so locations and years were considered separately in QTL analysis (Supplementary figure 2).

Two methods were adopted to perform QTL detection according to data distribution. Phenotypic data for the OW population and the HW population, with the exception of Angers 2018, Bellegarde 2014 and Diémoz 2013

phenotypic data (Figure 1) were analyzed using a normal model for simple interval mapping (SIM) and composite interval mapping (CIM). All other data exhibiting spike-like distribution were analyzed with a two-part model, henceforth referred as "2p" (Broman 2003). In addition, a mean across years was applied for each population (and for the HW population for each location separately). Then a normal method for QTL detection was used.

In total with the method for normally distributed phenotypes, 35 QTLs associated with BSD resistance were detected for the male maps, and eight QTLs were detected for the female maps. For spike-like distributions, ten QTLs were detected with the male maps and four with the female maps.

Male maps

For all three populations, across years and locations combined, a total of 45 QTLs with significant effects on BSD resistance were identified on LGs B3, B4, B5 and B6 (Table 1 and Supplementary figures 5, 6, 7 and 8). QTLs on B3 and B5 were found for all three populations, whereas QTLs on B4 and B6 were population-specific (OW and HW, respectively).

QTLs on B3 were identified for all years and locations with both detection methods. Phenotypic variance within-population explained by individual QTLs on B3 varied from 3.9% to 23.6% and the LOD values varied from 2.73 to 15.23 (Table 2). For the OW population, five marker peaks were found in a region from 4cM to 26cM for the different years (Supplementary figure 5 and Table 2); for the HW population, five marker peaks were also found in a region from 3 to 19cM for all scoring years and locations (Supplementary figures 7 and 8). For spike-like distributions, 2p model provides more information on the effect of the QTLs found. Indeed, for 2018 BSD scores of FW and HW in Angers and 2014 BSD scores of HW in Bellegarde, both LOD scores calculated for the 2p model exceeded their respective LOD thresholds (respectively Supplementary figures 6B, 8A and 8B, Table 2). This means that the QTLs found on B3 affects the penetrance (appearance of the symptoms) as well as the severity of the disease. However, for HW Diémoz 2013, only the LODπ reached its corresponding threshold meaning that the QTL found on B3 for 2013 affected only the penetrance. The 2p model gave a better precision on the QTL location on B3 from the beginning of the LG to 9.67cM (Table 2).

QTLs on B5 were found repeatedly for each scoring year and location in the HW population (Supplementary figures 7 and 8), and were year dependent in the OW population (detected for scoring years 2016, 2017 and 2018, see Supplementary figure 5). A QTL on B5 was also detected on FW for scoring year 2018. The LOD peak values varied from 3.43 to 12.14, and the phenotypic variance ranged from 2.89% to 19.82% (Table 2). For the OW population, two

close peaks were found for scoring years 2017, 2018 and the mean in a region from 8.71cM to 10cM. For all scoring years and locations for the HW population, four marker peaks were found in a region from 23cM to 41cM (Supplementary figures 7 and 8). Interestingly, in the OW population in 2016, the FW population in 2018, and for all years and locations for the HW population, a second peak on the distal end of B5 can also be observed (Supplementary figures 5, 6B, 7 and 8).

Two QTLs were identified on B4 in 2017 and with the mean across years for the OW population, explaining 5.1 to 7.6% of the phenotypic variance. The location of the B4 QTL was defined more precisely using BSD scores averaged across years (10cM region) than a single year scores (entire LG based on 2017 data, see table 2).

QTLs with significant but small effects on BSD resistance were mapped on B6 in most years and locations for the HW population as well as for the average BSD scores. These QTLs were population-specific and were only detected when RW was crossed with H190 (Supplementary figures 7 and 8). The LOD peaks ranged from 2.6 to 5.92 explaining 3.6 to 4.63% of phenotypic variance (Table 2). For data from HW Angers 2018 and HW Bellegarde 2014, the QTL on B6 affected the penetrance of the trait (Supplementary figure 8). No interactions between QTLs were observed across years and locations (data not shown). As B6 and B4 QTLs had small effects on BSD resistance and were population-specific and year-specific, they were not considered for the subsequent meta-analysis.

Female maps

No QTL common across all three populations was identified on the female maps (Table 3), but QTLs were shared by pairs of populations. The OW and FW populations displayed a common QTL on A1, while for the HW and FW populations displayed two common QTLs, both on A4.

In the OW population, a significant QTL on A1 was identified in 2017, explaining 6.53% of the total phenotypic variance and was located at the end of the LG (Lopez Arias et al. in press).

For the FW population, three QTLs were detected with 2018 data using 2p method. These QTLs, located on A1, A2 and A4, explained 4.06%, 2.57% and 3.61% of the phenotypic variance, respectively (Table 3). Interestingly, QTLs on A1 and A4 had an effect on the penetrance of the trait (LOD 2.59 and 4.09 respectively; see Table 3) whereas the QTL on A2 had an effect on both severity and penetrance (Supplementary figure 9A).

To position the QTL detected in the OW and FW populations on LG A1, markers at the confidence interval limits and markers at the peak of the QTLs were positioned on a physical map (Supplementary figure 10). TIR-NB-LRR (*TNL*) genes and cluster of genes from this regions identified by Menz et al. in 2020 were also mapped. Two

clusters of *TNL* genes, named cluster 1 (genes OB2_C to OB2_H) and cluster 2 (genes OB2_J to OB2_S), were localized near the end of chromosome 1 (supplementary figure 10). The *Rdr1* resistance gene from *Rosa multiflora* is part of cluster 2 (Malek et al. 2000; Kaufmann et al. 2003; Hattendorf et al. 2004; Terefe-Ayana et al. 2011; Menz et al. 2020). Importantly, the QTLs derived from the female parents TF and OB co-localized with both clusters of *TNL* genes (Supplementary figure 10).

For the HW population, QTLs were identified on LG A3 in 2012 and 2014 in Angers, 2013 in Bellegarde, 2014 in Diémoz and the averages across years for each location explaining 4.4% to 5.8% of the phenotypic variation (Table 3). One QTL explaining 5.91% of phenotypic variation was also identified on A3 in Bellegarde in 2014 using the 2p model. This QTL had an effect on the penetrance of the trait (Supplementary figure 9B). Also in Bellegarde, a QTL explaining 5.39% of the phenotypic variance was identified on A5 in 2012. In Diémoz, a QTL explaining 5.77% of the phenotypic variance was identified on A4 in 2014 (Table 3).

For both male and female maps, further QTLs and epistasis between QTLs were investigated using a two dimensional genome scan and no epistasis was significantly detected for any scoring year with normal distribution (data not shown). The percent explained by all QTLs is, then, the sum of all the phenotypic variance explained by the individual QTLs of each scoring years (Table 3).

Meta-analysis

A meta-analysis of B3 and B5 QTLs was conducted. First, a consensus male map across all populations was constructed using 41 common markers (Table 1 and Supplementary table 1). In total, B3 comprised nine markers common across the OW, FW and HW male maps and B5 comprised eight markers common across all male maps (Table 1). LG3 and LG5 of the consensus map were represented in Figure 2. Secondly, QTLs of the original maps were projected on the chosen reference map (OW population map) by the map-projection function of Biomercator 4.2.2. In total, 20 QTLs of BSD resistance were projected on the reference LG3 and 17 QTLs on the reference LG5 (Figure 2). The meta-QTL optimum number was ensured by the AIC. Two meta-QTLs were identified on both LG3 and LG5 (represented by two different colors on the LGs of figure 2). For LG3, the first meta-QTL (named Meta_1_3) had a confidence interval (CI) of 2.72 cM and the second meta-QTL (named Meta_2_3) had a CI of 7.70 cM (Table 4 and Figure 2). The CI for the meta-QTL on LG5 (named Meta_1_5) was 3.95 cM and 7.52 cM for the second one (Meta_2_5). The average CI of the 20 individual QTLs found in B3 was 20.1 cM whereas for both predicted meta-

QTLs together it was 10.42 cM. For B5, the individual QTL average CI was 26.62 cM and only 11.47 cM for both predicted meta-QTLs (Figure 2 and Table 4). The CI were approximately twice as small with the meta-analysis, which allowed us to be more precise in the location of QTLs linked to BSD resistance.

When looking at the meta-QTL contributions, we can see that the first meta-QTL (Meta_1_5) was represented exclusively by OW population QTLs that showed large peaks at the beginning of the LG (except OWpop_RW_16B5 QTL that showed two distinct peaks separated by 30cM, see Supplementary figure 5) whereas the QTLs of HW and FW populations contributed to the second meta-QTL (Meta_2_5). Curiously, individual QTLs with a wide interval and double peaks separated by 10 to 30cM were detected on B5 (Supplementary figure 5 to 8). The configuration suggests the presence of linked QTLs, requiring additional or alternative analytical approaches (Nakamichi et al. 2001; Kao and Zeng 2010). Accordingly, we attempted a two-dimensional analytical approach for normally distributed data but failed to separate more precisely the putatively linked QTLs in this region (data not shown).

Gene mining from meta-QTL intervals and *NB*-encoding genes in *Rosa* genome

All SNP markers were mapped to the *Rosa chinensis* reference genome of Hibrand-Saint Oyant et al. (2018) and were used to project the consensus genetic map onto the reference genome. The first meta-QTL on LG3, Meta_1_3, corresponds to an approximately 2.86 Mb genome region encompassing 291 annotated genes. The second one, Meta_2_3, represents a 3.5 Mb genome region comprising 450 annotated genes. On LG5, the first predicted meta-QTL, Meta_1_5, represents 1.80 Mb comprising 271 annotated genes, while the second meta-QTL, Meta_2_5, represents 6.06 Mb comprising 557 genes (Table 4).

We explored genes associated with predicted meta-QTLs, focusing specifically on potential disease resistance genes. First, we annotated the predicted *NB*-encoding (Nucleotide Binding) genes in the rose genome, identifying 493 candidate *R*-genes (Supplementary table 2). Candidate *NB-LRR* genes were mapped onto the assembled pseudochromosomes of *R. chinensis* (Figure 3). *NB*-encoding genes mapped to every chromosome of the rose genome. Only nine genes mapped onto the unassembled scaffolds (rc00). Chromosome 1 contained the largest number of *NB*-encoding genes (106). Overall, the mean number of *R*-genes per chromosome was 69. However, *NB*-encoding genes were not homogeneously distributed across chromosomes, with clustering evident, especially on the distal end of chromosomes 1, 5 and 7 (Figure 3).

On LG3, 11 automatically annotated R-genes and four manually annotated NBS-encoding genes (*RC3G0136400*, *RC3G0136500*, *RC3G0136600*, *RC3G0145900*) co-localized with the first meta-QTL, Meta_1_3 (Table 4, Figure 3 and Supplementary table 2). The manual and the automated annotations identified nearly the same number of NBS-encoding genes in the interval of the second B3 meta-QTL (Meta_2_3) encompassing four RGAs for the automated annotation and three *NB*-coding genes (*RC3G0272000*, *RC3G0277900*, and *RC3G0280800*) for the manual annotation (see table 4). In addition to these NBS-encoding genes, we investigated co-localizations of defense response genes with the Meta-QTLs. Interestingly, a gene involved in response to fungal infection (*RC3G0142400*) is associated with the meta-QTL Meta_1_3. This gene encodes an EMSY-LIKE 1 protein that is known to contribute to RPP7-mediated and basal immunity against a specific strain Hiks1 of *Peronospora parasitica* in *Arabidopsis* (Tsuchiya and Eulgem 2011), possibly by regulating chromatin states. Two genes encoding for P450 cytochrome also co-localized with the first meta-QTL Meta_1_3. Cytochromes P450 monooxygenases (CYP) are known to be involved in plant defense mechanisms as they mediate secondary metabolism compounds of the xenobiotic detoxification pathway. For example, the *CYP* gene *CYP736B* in grapevine is involved in defense responses against *Xylella fastidiosa* and the wheat *CYP72A* is involved in the defense responses to *Fusarium graminearum* (Schuler and Werck-Reichhart 2003; Schuler et al. 2006). Similarly, in the Solanaceae, two cytochromes P450 participate in fungal pathogen resistance (Morant et al. 2003) and a *Phytophthora infestans*-induced cytochrome P450 is associated with quantitative resistance to late blight in potato (Trognitz et al. 2002). Moreover, a transcription factor from the WRKY family (*RC3G0261500*) upstream of the NBS-encoding gene (*RC3G0261700*) also co-localize with the Meta_2_3. WRKY transcription factors are known to play an important role in plant immunity and have been identified as major components of the resistance to fungi (Yang et al. 2009; Pandey and Somssich 2009; Lui et al. 2017). A pathogenesis-related (PR) thaumatin gene (*RC3G0264400*) was also found to co-localized with Meta_2_3. This gene codes for a PR-5 type protein (also called TLP for thaumatin-like protein) that has been reported for its antifungal activity against various filamentous fungi (Chu and Ng 2003; Ho et al. 2007; Singh et al. 2013; Zhang et al. 2018).

For LG B5, 17 QTLs were mapped on the consensus LG and two meta-QTL clusters were identified. The same genes (*RC5G0059300*, *RC5G0061300*, and *RC5G0061600*) were annotated as *R*-genes with the expert annotation and the automatic one for Meta_1_5 (Table 4). However, in Meta_2_5 region, five genes were not found to be *NB*-encoding genes (RC5G0227800, RC5G0228700, RC5G0231700, RC5G0232700, RC5G0245000) with the expert annotation. Interestingly, Meta_2_5 is close to the region where the newly identified *Rdr4* gene giving resistance to all races of *D.*

rosae, except the race 12, was located (Zurn et al. 2018). The meta-QTL, Meta_2_5, did not co-localize with the possible location of *Rdr4* but the marker peak of the QTL found in 2016 for OW population co-localized with it (Lopez Arias et al. in press) as well as the marker peak of the QTL found in Diémoz 2013 scoring year of HW population. Moreover, a glucan synthase like gene (*RC5G0249400*; *GLS4* gene or also called *CalS8*), known to be involved in the formation of callose-containing papillae in response to pathogen attack (Enrique et al.; Dong 2005; Enns et al. 2005; Dong et al. 2008; Voigt and Somerville 2009; Ellinger et al. 2013; Voigt 2014, 2016), co-localized with Meta_2_5. Finally, a cluster of ten genes coding for cytochrome P450 also co-localized with Meta_2_5.

Discussion

Importance of environmental effects on BSD scores

Since the expression of quantitative resistance can be affected by the environment, quantitative disease resistance (QDR) is best studied under field conditions with phenotypic measurements collected over different locations and years (Kelly and Vallejo 2006; Niks et al. 2015; Corwin and Kliebenstein 2017). In the current study, a difference of inoculum pressure or fungal strains between locations (Soufflet-Freslon et al. 2019) could explain why, for the HW population, the disease incidence was generally lower in Angers than in Bellegarde and Diémoz for a given year (Supplementary figure 2C). On the other hand, the effects of environmental conditions such as temperature, humidity or rainfall on BSD development in fields are well documented (Saunders 1966; Knight 1975; Gachomo 2005). In particular, (Saunders 1966) showed that climatic conditions play a critical role in the accumulation and spread of *D. rosae* inoculum. Heavy rainfalls and temperature above 14°C during trigger inoculum accumulation and spread of conidia from infected leaves (Saunders 1966). During the scoring period from 2012 to 2018, average precipitation in August and September of a given year was consistently lower in Angers and Bellegarde than in Diémoz. Similarly, for all populations, variation in disease impacts between years was observed, with low rainfall in August-September correlating with lower BSD scores. Conversely, in wetter locations or years (e.g., Diémoz in 2013 and Bellegarde in 2014), more individuals presented disease symptoms with BSD score distributions skewed to the left (with a lot of individuals presenting more symptoms than normal) like Diémoz. Specifically, the year 2013 (with a spike at score 4) could be explained by heavy rainfalls in August-September. Similarly, Bellegarde in 2014 presenting similar rainfall than Diémoz (97.25 mm) also showed a spike at score 4 and a distribution skewed to the left (Figure 1C).

New QTLs detected on parental genetic maps

Our main objective was to identify genomic regions conditioning resistance to *D. rosae*. We generated and analyzed phenotypic BSD data gathered across seven years, three locations, and three genetic populations.

The three populations used in this study were originated from interspecific crosses. The highly heterozygous nature of *Rosa* species is a complicating factor when it comes to genetic mapping. The pseudo-test cross mapping approach (Grattapaglia and Sederoff 1994; Kirst et al. 2004; Adam-Blondon et al. 2016), developed for highly heterozygous species, allows development of parental maps that are then combined into an integrated map. However, (Gartner et al. 2013) showed that, although integrating homologous chromosomes that have been rearranged can produce mathematically and statistically correct maps, they do not necessarily reflect the biological reality of chromosomal rearrangements and meiotic recombination that had happened during the outbred cross. Therefore, even if the gene position is highly conserved between species, genome rearrangements may exist in interspecific crosses. This can lead to significant changes in collinearity between parental genomes (Lespinasse et al. 2000; Gartner et al. 2013). For example, recently released, independently generated rose genome assemblies suggest chromosome rearrangements (Raymond et al. 2018; Hibrand-Saint Oyant et al. 2018; Smulders et al. 2019). In the current study, we observed rearrangements between the parents OB and RW, especially on chromosome 3. For these reasons, we decided to apply pseudo-test cross mapping approach without integrating the parental maps at the end. QTL analyses were then carried out using two different methods of detection on separated parental maps.

Overall, many QTLs for resistance to BSD were detected in this study. Consistent with natural variation in inoculum pressure, pathogen race, and environmental conditions encountered in field studies over several years, some QTLs identified in this study were only found in a given population, location or year. For example, BSD resistance QTLs on B6 were found specifically on the male map of the HW population across all environments (Table 2). Since all three populations share the RW male parent, identification of the B6 QTLs only in the HW population for several years and locations suggests that expression of these QTLs also depends on genetic background that is crossed with *R. wichurana*. Moreover, the marker peak CTG623 of B6 QTL was found to co-localize with the possible location of *Rdr3* (Zurn et al. 2020).

Importantly, other QTLs were more consistently detected across populations, locations, and years, suggesting a more robust impact on disease resistance. First, a QTL on LG A1 was mapped in two populations (FW and OW) (Supplementary figure 10), originating from the female parents TF and OB. This QTL co-localizes with a cluster of

NB-LRR genes, including the previously reported BSD resistance gene *Rdr1* (Lopez Arias et al. in press; Hattendorf et al. 2004; Terefe-Ayana et al. 2011). This observation suggests the intriguing possibility that the underlying genetic basis of the A1 QTL might be a canonical NB-LRR gene, in whole or in part. In addition, regarding the difference of BSD score between both female parents (with OB very susceptible to BSD and TF resistant to it), we can hypothesize that an allelic variation in the causal gene could originate a difference in the observed phenotype. Then, a QTL conditioning BSD resistance on LG B4 was identified for two different environments and two different populations: the OW population in Angers in 2017 (male map) and the HW population in Diémoz in 2014 (H190 female map; Table 2 and 3). Resistance conditioned by this QTL may be environment- and pathogen race-dependent. Finally, QTLs on LGs B3 and B5 were found for all populations, years and locations in the male resistant parent RW but also in the H190 female map (Table 2 and 3). At the moment, the apparent mapping of QTLs from these two parents, with a clear difference in BSD resistance, on the same linkage groups could be explained by one of these two hypothesis: (1) RW and H190 QTLs co-localized meaning that both parents shared the same resistance source and the difference observed in the phenotype could be due to an allelic variation between them or (2) the QTLs originated from both parents do not co-localize meaning that the resistance source is different. Unfortunately, the maps quality did not allow us to determine precisely if the male and female QTLs on linkage group 3 and 5 co-localized (data not shown). However, consistent expression of QTLs on linkage groups 3 and 5 across environments and genetic backgrounds suggest that they are stable enough to be useful in the genetic improvement of rose resistance to *D. rosae.* In the end, we can see with this study that separated maps allowed us to identify two main QTLs on B3 and B5 with large effect on the resistance to BSD as well as small effect QTLs on parents that were considered tolerant or susceptible.

QTLs characterization and two-part model result interpretation

Substantial peaks in the distribution of genotype mean values are fairly common and represent one of the principal departure from the assumption of normality required to perform QTL analysis (Lander and Botstein 1989). When working with disease resistance, individuals may show high resistance so a peak at 0 can be observed. In this case, the standard QTL detection approach behave poorly and can detect spurious QTLs in regions with low genetic information (Broman 2003; Feenstra and Skovgaard 2004). To deal with this problem, Broman proposed in 2003 a "Two-part model" that combines a binary analysis (absence *vs* presence) and a normal analysis for individuals with non-null phenotype. The trait is divided in two components: penetrance and severity (Broman 2003; Broman and Sen

2009). That way, more information about the part of trait that is affected by the QTL can be obtained. This model has so far been applied for reproductive barriers with male sterility in house mouse and ear tip masculinization in maize (White et al. 2011, 2012; Holland and Coles 2011). In our study, we adapted when necessary the model used to perform the QTL analyses, so data distributions with a substantial spike were analyzed with the two-part model. When both the penetrance and the severity of the trait were affected by the QTLs, it meant that these positions have an effect on the appearance of the BSD symptoms or penetrance (when treated as binomial; with no symptoms *vs* symptoms) as well as the severity of symptoms (BSD score > 0).

The 2p model provided interesting information for the B3 and B5 QTLs found on the male parent maps. For Angers 2018 data from the HW and FW populations, both the penetrance and the severity of the trait were affected by the B3 QTLs, meaning that these regions impact both appearance of BSD symptoms and symptom severity. Interestingly, for the B5 QTLs in both populations, only penetrance (absence/presence of the symptoms) was impacted. For the resistant female parent TF, the A2 QTL impacts both the penetrance and the severity of the trait whereas the A1 and A4 QTLs impact only penetrance.

Meta-analysis and gene mining

With recent progress in mapping algorithms and models that can handle a wide diversity of phenotypic data, quantitative trait mapping has become the first step in the dissection of the genetic factors underlying complex and quantitative traits such as disease resistance (Zhu and Zhao 2007; Rawat 2016). That way, many studies mapped quantitative disease resistance loci of crop plants over the past decades (Lacape et al. 2010; Qi et al. 2011; Holland and Coles 2011; Yadava et al. 2012; Hamon et al. 2013; Semagn et al. 2013; Said et al. 2013; Pilet-Nayel et al. 2017). Cloning and functional validation of causal gene(s) or quantitative trait nucleotide polymorphism underlying QTLs has been accomplished in maize (Yang et al. 2017) but remains a long and difficult process. Indeed, the biological bases of QDR in the defense responses are still unknown, so several reviews proposed hypotheses of mechanisms underlying Quantitative resistance loci (QRL) (Poland et al. 2009; St Clair 2010; Roux et al. 2014; Corwin and Kliebenstein 2017).

First, one crucial step facilitating cloning and validation of causal genes is the QRL position refinement. Towards this goal, in this study, we narrow the confidence interval of the most phenotypically stable and reproducible QTLs on a common consensus map and perform a meta-analysis of the corresponding LGs, B3 and B5. Two meta-

QTL clusters were identified for both LG B3 and B5 (Figure 2 and Table 4). This method allowed us to refine the genomic regions linked to BSD resistance and to study the influence of genetic background and environment on QRL detection (Table 4). However, combination of QTL mapping results across several studies that differ with marker density, linkage, sample size, etc. is still a challenge. Even though Goffinet and Gerber's method aims to resolve the number of QTL and their location using a model selection, questions on the real number of QTL subsist. On one hand, for LG B3, both clusters found during the meta-analysis can be either two real QTLs or an artefact due to the possible rearrangement that happened in this region. For instance, not far from the meta-QTL Meta_1_3 on B3, a large rearrangement was described between the two alleles in OB (corresponding to recurrent blooming locus and the rearrangement of *copia*-like retrotransposon, Hibrand-Saint Oyant et al. 2018). On the other hand, on LG B5, uncertainty remains on whether or not the QTLs located within the same genomic region are the same QTLs. Specially, because individual QTLs present double LOD peaks characteristic of linked QTLs. Increasing the sample size of the populations in future experiments may provide a better power to separate closely linked QTLs on LG B5. Therefore, at this moment, only hypotheses can be made. For example: both clusters being completely new QTLs different from the newly identified *Rdr4* resistance gene (Zurn et al. 2018) or the first meta-QTL Meta_1_5 being a new QTL and the Meta_2_5 being *Rdr4* locus that did not co-localized with it due to map imprecisions.

Second, elucidating the molecular mechanisms underlying QRLs can assist breeders in developing cultivars with more durable levels of resistance by "making more informed and prudent decisions" (Kelly and Vallejo 2006). Indeed, it has been shown that QRLs can co-localize with major R-genes as well as defense response genes (Poland et al. 2009; St Clair 2010; Roux et al. 2014; Corwin and Kliebenstein 2017). In this study, we used the meta-QTL physical positions to inform gene mining efforts based on whole genome sequence data (Hibrand-Saint Oyant et al. 2018), specifically searching for associations between defined genetic regions and NBS-LRR and defense response genes. However, the resistance loci originated from RW and the genomic differences between both genotypes could impact our efforts. Nevertheless, the use of the haploid OB genome sequence to identify candidate genes underlying BSD resistance meta-QTLs has promise. Genes involved in pathogen recognition, signal transduction, transcription modulation and detoxification pathways were identified in the chromosomal regions linked to BSD resistance. Interestingly, Blechert and Debener in 2005 classified the interaction between *D. rosae* and the wild type *R. wichurana* as type 7 meaning that the fungus germinates and penetrates the cuticle but is not capable of producing hyphal structures on the host. Indeed, cell-wall appositions were observed on one to three cells resulting in visible necrotic

areas akin to hypersensitivity reactions (HR). Genes involved in the activation of cell death (WRKY, PR-proteins, ROS pathway, etc.) as well as in detoxification pathways (with cytochrome P450) seem to be good candidates. Thus, the possibility of RGAs being responsible for the observed resistance on RW is also not to be ruled out as they are in the first line of biotic stress responses like the one observed for RW by Blechert and Debener (2005).

In this study, confidence intervals of chromosomal regions conditioning quantitative resistance to *D. rosae* were reduced thanks to the meta-analysis approach. Unfortunately, at this stage of the study, no consistent markers linked to BSD resistance have been identified as the CI regions and peaks of detected QTLs vary slightly over the years and locations. A refinement of the QTL location of stable QTLs on B3 and B5 is needed prior to marker detection for marker assisted breeding and/or causal gene identification. Using the genomic resources now available such as the rose genome and the data provided in this article such as the manually annotated RGAs, the first hypothesis on the genetic basis of QDR in Rose-*D. rosae* pathosystem were made. However, at this stage, only a large number of candidate genes were identified. Further evidence supporting their involvement in the observed resistance of RW genotype need to be provided so the potential candidate genes can be narrowed down to a number that can allow experimental validation through qPCR expression profiles and/or gene inactivation. Finally, the large number of QTL detected in this study, together with the fact that some QTL did not co-colocalize with known *Rdr* genes, suggests that the number of QTL could be even larger than what has been detected with these limited populations, offering the promise of wide spectrum of resistance sources to rose breeder and scientists.

Conclusion

In this study, we report the first discovery and genetic characterization of quantitative resistance to BSD. We examined the contributions of a common resistant parent over several years, locations, and genetic populations. We confirm the presence of a strong effect QTLs on LG B3 and B5 from the genotype *R. wichurana*, consistent with complementary on-going research (Yan et al. 2019). The LG B3 and LG B5 QTLs are stable over years and effective against a wide range of *D. rosae* races and across various environments (Lopez Arias et al. in press; Yan et al. 2019; Soufflet-Freslon et al. 2019). We demonstrate a method to leverage meta-analyses to reduce CI of single QTLs. This method was specifically chosen for its robustness to non-full independency and it allowed us to integrate data from three different populations of perennial rose bushes. BSD data collected over seven years and multiple locations,

provided validation of QTLs on B3 and B5, demonstrating their stability and robustness. Genes underlying these QTLs are potential breeding targets for the development of BSD resistant rose cultivars.

References

Adam-Blondon A-F, Martinez-Zapater J-M, Kole C (2016) Genetics, genomics, and breeding of grapes. CRC Press

Allum JF, Bringloe HD, Roberts AV (2010) Interactions of four pathotypes of *Diplocarpon rosae* with species and hybrids of Rosa. Plant Pathol 59:516–522. https://doi.org/10.1111/j.1365-3059.2009.02222.x

Arcade A, Labourdette A, Falque M, et al (2004) BioMercator: integrating genetic maps and QTL towards discovery of candidate genes. Bioinforma Oxf Engl 20:2324–2326. https://doi.org/10.1093/bioinformatics/bth230

Black WA, Byrne DH, Pemberton HB (1994) Field study of black spot resistance in rose. HortScience 29:

Blechert O, Debener T (2005) Morphological characterization of the interaction between *Diplocarpon rosae* and various rose species. Plant Pathol 54:82–90. https://doi.org/10.1111/j.1365-3059.2005.01118.x

Boontiang K (2003) Breeding of black spot disease resistance of garden and florist rose. PhD Thesis, 愛媛大学

Bourke PM, Gitonga VW, Voorrips RE, et al (2018) Multi-environment QTL analysis of plant and flower morphological traits in tetraploid rose. TAG Theor Appl Genet Theor Angew Genet 131:2055–2069. https://doi.org/10.1007/s00122-018-3132-4

Broman K, Sen S (2009) A Guide to QTL Mapping with R/qtl. Springer-Verlag, New York

Broman KW (2003) Mapping quantitative trait loci in the case of a spike in the phenotype distribution. Genetics 163:1169–1175

Broman KW, Wu H (2019) Qtl: tools for analyzing qtl experiments. Version 1.44-9URL https://CRAN.R-project.org/package=qtl

Byrne DH, Pemberton HB, Holeman DJ, et al (2019) Survey of the rose community: desired rose traits and research issues. Acta Hortic 189–192. https://doi.org/10.17660/ActaHortic.2019.1232.28

Carlson-Nilsson BU (2001) Evaluation of rose species and cultivars for resistance to *Marssonina rosae* (*Diplocarpon rosae*). Acta Hortic 413–417. https://doi.org/10.17660/ActaHortic.2001.547.53

Cheema J, Dicks J (2009) Computational approaches and software tools for genetic linkage map estimation in plants. Brief Bioinform 10:595–608. https://doi.org/10.1093/bib/bbp045

Chu KT, Ng TB (2003) Isolation of a large thaumatin-like antifungal protein from seeds of the Kweilin chestnut Castanopsis chinensis. Biochem Biophys Res Commun 301:364–370. https://doi.org/10.1016/S0006-291X(02)02998-4

Corbeil RR, Searle SR (1976) Restricted maximum likelihood (REML) estimation of variance components in the mixed model. Technometrics 18:31–38. https://doi.org/10.2307/1267913

Corwin JA, Kliebenstein DJ (2017) Quantitative resistance: more than just perception of a pathogen. Plant Cell tpc.00915.2016. https://doi.org/10.1105/tpc.16.00915

718 Covarrubias-Pazaran G (2019) Sommer: solving mixed model equations in R. Version 4.0.1URL https://CRAN.R-
719 project.org/package=sommer

720 Debener T (2017) Inheritance of characteristics. In: Reference Module in Life Sciences. Elsevier, Hannover, Germany,
721 pp 1–7

722 Debener T, Drewes-Alvarez R, Rockstroh K (1998) Identification of five physiological races of blackspot,
723 *Diplocarpon rosae* Wolf, on roses. Plant Breed 117:267–270. https://doi.org/10.1111/j.1439-
724 0523.1998.tb01937.x

725 Doerge RW, Churchill GA (1996) Permutation tests for multiple loci affecting a quantitative character. Genetics
726 142:285–294

727 Dong Q, Wang X, Byrne DH, Ong K (2017) Characterization of Partial Resistance to Black Spot Disease of *Rosa* sp.
728 HortScience 52:49–53. https://doi.org/10.21273/HORTSCI11349-16

729 Dong X (2005) Functional investigation of Arabidopsis callose synthases and the signal transduction pathway. The
730 Ohio State University

731 Dong X, Hong Z, Chatterjee J, et al (2008) Expression of callose synthase genes and its connection with *Npr1* signaling
732 pathway during pathogen infection. Planta 229:87–98. https://doi.org/10.1007/s00425-008-0812-3

733 Edgar RC (2010) Search and clustering orders of magnitude faster than BLAST. Bioinformatics 26:2460–2461.
734 https://doi.org/10.1093/bioinformatics/btq461

735 Edgar RC (2004) MUSCLE: Multiple sequence alignment with high accuracy and high throughput. Nucleic Acids Res
736 32:1792–1797. https://doi.org/10.1093/nar/gkh340

737 Ellinger D, Naumann M, Falter C, et al (2013) Elevated early callose deposition results in complete penetration
738 resistance to powdery mildew in Arabidopsis. Plant Physiol 161:1433–1444.
739 https://doi.org/10.1104/pp.112.211011

740 Enns LC, Kanaoka MM, Torii KU, et al (2005) Two callose synthases, *GSL1* and *GSL5*, play an essential and redundant
741 role in plant and pollen development and in fertility. Plant Mol Biol 58:333–349.
742 https://doi.org/10.1007/s11103-005-4526-7

743 Enrique R, Siciliano F, Favaro MA, et al Novel demonstration of RNAi in citrus reveals importance of citrus callose
744 synthase in defence against *Xanthomonas citri* subsp. citri. Plant Biotechnol J 9:394–407

745 Feenstra B, Skovgaard IM (2004) A quantitative trait locus mixture model that avoids spurious LOD score peaks.
746 Genetics 167:959–965. https://doi.org/10.1534/genetics.103.025437

747 Felsenstein J (1989) PHYLIP - Phylogeny Inference Package (Version 3.2). Cladistics 5:164–166.
748 https://doi.org/10.1111/j.1096-0031.1989.tb00562.x

749 Finn RD, Clements J, Arndt W, et al (2015) HMMER web server: 2015 update. Nucleic Acids Res 43:W30–W38.
750 https://doi.org/10.1093/nar/gkv397

751 Finn RD, Coggill P, Eberhardt RY, et al (2016) The Pfam protein families database: towards a more sustainable future.
752 Nucleic Acids Res 44:D279–D285. https://doi.org/10.1093/nar/gkv1344

753 Fischer BM, Salakhutdinov I, Akkurt M, et al (2004) Quantitative trait locus analysis of fungal disease resistance
754 factors on a molecular map of grapevine. Theor Appl Genet 108:501–515. https://doi.org/10.1007/s00122-
755 003-1445-3

Fu Y, van Silfhout A, Shahin A, et al (2017) Genetic mapping and QTL analysis of Botrytis resistance in *Gerbera hybrid*a. Mol Breed 37:. https://doi.org/10.1007/s11032-016-0617-1

Gachomo EW (2005) Studies of the life cycle of *Diplocarpon rosae* Wolf on roses and the effectiveness of fungicides on pathogenesis. Cuvillier Verlag

Gachomo EW, Dehne H-W, Steiner U (2006) Microscopic evidence for the hemibiotrophic nature of D*iplocarpon rosae*, cause of black spot disease of rose. Physiol Mol Plant Pathol 1–3:86–92. https://doi.org/10.1016/j.pmpp.2007.02.002

Gachomo EW, Kotchoni SO (2007) Detailed description of developmental growth stages of *Diplocarpon rosae* in Rosa: a core building block for efficient disease management. Ann Appl Biol 151:233–243. https://doi.org/10.1111/j.1744-7348.2007.00167.x

Gachomo EW, Seufferheld MJ, Kotchoni SO (2010) Melanization of appressoria is critical for the pathogenicity of *Diplocarpon rosae*. Mol Biol Rep 37:3583–3591. https://doi.org/10.1007/s11033-010-0007-4

Gartner GAL, McCouch SR, Moncada MDP (2013) A genetic map of an interspecific diploid pseudo testcross population of coffee. Euphytica 192:305–323. https://doi.org/10.1007/s10681-013-0926-y

Goffinet B, Gerber S (2000) Quantitative trait loci: a meta-analysis. Genetics 155:463–473

Grattapaglia D, Sederoff R (1994) Genetic linkage maps of *Eucalyptus grandis* and *Eucalyptus urophylla* using a pseudo-testcross: mapping strategy and RAPD markers. Genetics 137:1121–1137

Griffiths S, Simmonds J, Leverington M, et al (2009) Meta-QTL analysis of the genetic control of ear emergence in elite European winter wheat germplasm. TAG Theor Appl Genet Theor Angew Genet 119:383–395. https://doi.org/10.1007/s00122-009-1046-x

Guo B, Sleper DA, Lu P, et al (2006) QTLs associated with resistance to soybean cyst nematode in soybean: meta-analysis of QTL locations. Crop Sci

Guo J, Chen L, Li Y, et al (2018) Meta-QTL analysis and identification of candidate genes related to root traits in maize. Euphytica 214:223. https://doi.org/10.1007/s10681-018-2283-3

Hamon C, Coyne CJ, McGee RJ, et al (2013) QTL meta-analysis provides a comprehensive view of loci controlling partial resistance to *Aphanomyces euteiches* in four sources of resistance in pea. BMC Plant Biol 13:45. https://doi.org/10.1186/1471-2229-13-45

Harp DA, Zlesak DC, Hammond G, et al (2009) Earth-Kind® rose trials – identifying the world's strongest, most beautiful landscape roses. 10

Harville DA (1977) Maximum likelihood approaches to variance component estimation and to related problems. J Am Stat Assoc 72:320–338. https://doi.org/10.2307/2286796

Hattendorf A, Linde M, Mattiesch L, et al (2004) Genetic analysis of rose resistance genes and their localisation in the rose genome. Acta Hortic 123–130. https://doi.org/10.17660/ActaHortic.2004.651.14

Hibrand-Saint Oyant L, Crespel L, Rajapakse S, et al (2007) Genetic linkage maps of rose constructed with new microsatellite markers and locating QTL controlling flowering traits. Tree Genet Genomes 4:11. https://doi.org/10.1007/s11295-007-0084-2

Hibrand-Saint Oyant L, Ruttink T, Hamama L, et al (2018) A high-quality genome sequence of *Rosa chinensis* to elucidate ornamental traits. Nat Plants 4:473–484. https://doi.org/10.1038/s41477-018-0166-1

794 Ho VSM, Wong JH, Ng TB (2007) A thaumatin-like antifungal protein from the emperor banana. Peptides 28:760–
795 766. https://doi.org/10.1016/j.peptides.2007.01.005

796 Holland JB, Coles ND (2011) QTL controlling masculinization of ear tips in a maize (zea mays l.) intraspecific cross.
797 G3 GenesGenomesGenetics 1:337–341. https://doi.org/10.1534/g3.111.000786

798 Holland JB, Nyquist WE, Cervantes-Martínez CT (2010) Estimating and interpreting heritability for plant breeding:
799 an update. Plant Breed Rev 9–112. https://doi.org/10.1002/9780470650202.ch2

800 Horst RK, Cloyd RA (2007) Compendium of rose diseases and pests. APS Press

801 Kao C-H, Zeng M-H (2010) An investigation of the power for separating closely linked QTL in experimental
802 populations. Genet Res 92:283–294. https://doi.org/10.1017/S0016672310000273

803 Kaufmann H, Mattiesch L, Lörz H, Debener T (2003) Construction of a BAC library of *Rosa rugosa* Thunb. and
804 assembly of a contig spanning Rdr1, a gene that confers resistance to blackspot. Mol Genet Genomics
805 268:666–674. https://doi.org/10.1007/s00438-002-0784-0

806 Kaufmann H, Terefe D, Yasmin A, et al (2010) Cloning and analysis of *Rdr1*, a black spot resistance gene from roses.
807 Acta Hortic 191–196. https://doi.org/10.17660/ActaHortic.2010.870.25

808 Kawamura K, Hibrand-Saint Oyant L, Crespel L, et al (2011) Quantitative trait loci for flowering time and
809 inflorescence architecture in rose. TAG Theor Appl Genet Theor Angew Genet 122:661–675.
810 https://doi.org/10.1007/s00122-010-1476-5

811 Kawamura K, Hibrand-Saint Oyant L, Thouroude T, et al (2015) Inheritance of garden rose architecture and its
812 association with flowering behaviour. Tree Genet Genomes 11:1–12. https://doi.org/10.1007/s11295-015-
813 0844-3

814 Kelly JD, Vallejo V (2006) QTL analysis of multigenic disease resistance in plant breeding. In: Tuzun S, Bent E (eds)
815 Multigenic and Induced Systemic Resistance in Plants. Springer US, Boston, MA, pp 21–48

816 Khowaja FS, Norton GJ, Courtois B, Price AH (2009) Improved resolution in the position of drought-related QTLs in
817 a single mapping population of rice by meta-analysis. BMC Genomics 10:276. https://doi.org/10.1186/1471-
818 2164-10-276

819 Kirst M, Myburg A, Sederoff R (2004) Genetic mapping in forest trees: markers, linkage analysis and genomics. In:
820 Setlow JK (ed) Genetic Engineering: Principles and Methods. Springer US, Boston, MA, pp 105–141

821 Knight C (1975) Development of *Diplocarpon rosae* on different rose cultivars. PhD Thesis, London University

822 Krzywinski M, Schein J, Birol I, et al (2009) Circos: An information aesthetic for comparative genomics. Genome Res
823 19:1639–1645. https://doi.org/10.1101/gr.092759.109

824 Labbé J (2014) LOI n° 2014-110 du 6 février 2014 visant à mieux encadrer l'utilisation des produits phytosanitaires
825 sur le territoire national

826 Lacape J-M, Llewellyn D, Jacobs J, et al (2010) Meta-analysis of cotton fiber quality QTLs across diverse
827 environments in a *Gossypium hirsutum* x *G. barbadense* RIL population. BMC Plant Biol 10:132.
828 https://doi.org/10.1186/1471-2229-10-132

829 Lanaud C, Fouet O, Clément D, et al (2009) A meta–QTL analysis of disease resistance traits of *Theobroma cacao* L.
830 Mol Breed 24:361–374. https://doi.org/10.1007/s11032-009-9297-4

Lander ES, Botstein D (1989) Mapping mendelian factors underlying quantitative traits using RFLP linkage maps. Genetics 121:185–199

Lespinasse D, Rodier-Goud M, Grivet L, et al (2000) A saturated genetic linkage map of rubber tree (Hevea spp.) based on RFLP, AFLP, microsatellite, and isozyme markers. Theor Appl Genet 100:127–138. https://doi.org/10.1007/s001220050018

Leus L, Hosseini Moghaddam H, Van Huylenbroeck J, De Riek J (2015) QTLs associated with powdery mildew resistance responses in roses. Acta Hortic 287–293. https://doi.org/10.17660/ActaHortic.2015.1064.34

Liu S, Hall MD, Griffey CA, McKendry AL (2009) Meta-analysis of qtl associated with fusarium head blight resistance in wheat. Crop Sci 49:1955–1968. https://doi.org/10.2135/cropsci2009.03.0115

Lopez Arias DC, Chastellier A, Thouroude T, et al (in press) High density SNP and SSR linkage map and QTL analysis for resistance to black spot in segregating rose population. Acta Hortic

Lui S, Luo C, Zhu L, et al (2017) Identification and expression analysis of *WRKY* transcription factor genes in response to fungal pathogen and hormone treatments in apple (Malus domestica). J Plant Biol 60:215–230. https://doi.org/10.1007/s12374-016-0577-3

Lupas A, Van Dyke M, Stock J (1991) Predicting coiled coils from protein sequences. Science 252:1162–1164. https://doi.org/10.1126/science.252.5009.1162

Lynch M, Walsh B (1998) Genetics and analysis of quantitative traits. Sunderland, Mass. : Sinauer

Malek B von, Debener T (1998) Genetic analysis of resistance to blackspot (*Diplocarpon rosae*) in tetraploid roses. Theor Appl Genet 96:228–231. https://doi.org/10.1007/s001220050731

Malek B von, Weber WE, Debener T (2000) Identification of molecular markers linked to Rdr1 blackspot in roses. Theor Appl Genet 101:977–983. https://doi.org/10.1007/s001220051570

Marolleau B, Petiteau A, Bellanger MN, et al (2020) Strong differentiation within *Diplocarpon rosae* strains based on microsatellite markers and greenhouse-based inoculation protocol on Rosa. Plant Pathol

Menz I, Lakhwani D, Clotault J, et al (2020) Analysis of the *Rdr1* gene family in different *Rosaceae* genomes reveals an origin of an *R*-gene cluster after the split of Rubeae within the *Rosoideae* subfamily. PLOS ONE 15:e0227428. https://doi.org/10.1371/journal.pone.0227428

Menz I, Straube J, Linde M, Debener T (2018) The TNL gene *Rdr1* confers broad-spectrum resistance to Diplocarpon rosae. Mol Plant Pathol. https://doi.org/10.1111/mpp.12589

Meynet J (Institut N de la RA, Barrade R, Duclos A, Siadous R (1994) Dihaploid plants of roses (*Rosa x hybrida* , cv "Sonia") obtained by parthenogenesis induced using irradiated pollen and in vitro culture of immature seeds. Agron Fr

Morant M, Bak S, Møller BL, Werck-Reichhart D (2003) Plant cytochromes P450: tools for pharmacology, plant protection and phytoremediation. Curr Opin Biotechnol 14:151–162. https://doi.org/10.1016/S0958-1669(03)00024-7

Münnekhoff A-K, Linde M, Debener T (2017) The gene diversity pattern of *Diplocarpon rosae* populations is shaped by the age, diversity and fungicide treatment of their host populations. Plant Pathol 66:1288–1298. https://doi.org/10.1111/ppa.12681

Nakamichi R, Ukai Y, Kishino H (2001) Detection of closely linked multiple quantitative trait loci using a genetic algorithm. Genetics 158:463–475

870 Niks RE, Qi X, Marcel TC (2015) Quantitative resistance to biotrophic filamentous plant pathogens: concepts,
871 misconceptions, and mechanisms. Annu Rev Phytopathol 53:445–470. https://doi.org/10.1146/annurev-
872 phyto-080614-115928

873 Pandey SP, Somssich IE (2009) The Role of *WRKY* Transcription Factors in Plant Immunity. Plant Physiol 150:1648–
874 1655. https://doi.org/10.1104/pp.109.138990

875 Patterson HD, Thompson R (1971) Recovery of inter-block information when block sizes are unequal. Biometrika
876 58:545–554. https://doi.org/10.2307/2334389

877 Pilet-Nayel M-L, Moury B, Caffier V, et al (2017) Quantitative resistance to plant pathogens in pyramiding strategies
878 for durable crop protection. Front Plant Sci 8:1838. https://doi.org/10.3389/fpls.2017.01838

879 Poland JA, Balint-Kurti PJ, Wisser RJ, et al (2009) Shades of gray: the world of quantitative disease resistance. Trends
880 Plant Sci 14:21–29. https://doi.org/10.1016/j.tplants.2008.10.006

881 Qi Z, Sun Y, Wang J, et al (2011) Meta-Analysis of 100-Seed Weight QTLs in Soybean. Agric Sci China 10:327–334.
882 https://doi.org/10.1016/S1671-2927(11)60011-4

883 Rawat N (2016) Approaches for disease resistant candidate genes identification in plants: recent techniques and trends.
884 Austin Food Sci 1:1010

885 Raymond O, Gouzy J, Just J, et al (2018) The Rosa genome provides new insights into the domestication of modern
886 roses. Nat Genet 50:772. https://doi.org/10.1038/s41588-018-0110-3

887 Roman H, Rapicault M, Miclot AS, et al (2015) Genetic analysis of the flowering date and number of petals in rose.
888 Tree Genet Genomes 11:85. https://doi.org/10.1007/s11295-015-0906-6

889 Roux F, Voisin D, Badet T, et al (2014) Resistance to phytopathogens *e tutti quanti*: placing plant quantitative disease
890 resistance on the map. Mol Plant Pathol 15:427–432. https://doi.org/10.1111/mpp.12138

891 Said JI, Lin Z, Zhang X, et al (2013) A comprehensive meta QTL analysis for fiber quality, yield, yield related and
892 morphological traits, drought tolerance, and disease resistance in tetraploid cotton. BMC Genomics 14:776.
893 https://doi.org/10.1186/1471-2164-14-776

894 Saunders (1966) Epidemiological aspects of blackspot disease of roses caused by *Diplocarpon rosae* Wolf. Ann Appl
895 Biol 58:115–122. https://doi.org/10.1111/j.1744-7348.1966.tb05076.x

896 Schuler MA, Duan H, Bilgin M, Ali S (2006) Arabidopsis cytochrome P450s through the looking glass: a window on
897 plant biochemistry. Phytochem Rev 5:205–237. https://doi.org/10.1007/s11101-006-9035-z

898 Schuler MA, Werck-Reichhart D (2003) Functional genomics of P450s. Annu Rev Plant Biol 54:629–667.
899 https://doi.org/10.1146/annurev.arplant.54.031902.134840

900 Schulz DF, Linde M, Blechert O, Debener T (2009) Evaluation of genus *Rosa* germplasm for resistance to black spot,
901 downy mildew and powdery mildew. Eur J Hortic Sci 74:1–9

902 Semagn K, Beyene Y, Warburton ML, et al (2013) Meta-analyses of QTL for grain yield and anthesis silking interval
903 in 18 maize populations evaluated under water-stressed and well-watered environments. BMC Genomics
904 14:313. https://doi.org/10.1186/1471-2164-14-313

905 Shupert DA (2006) Inheritance of flower, stem, leaf, and disease traits in three diploid interspecific rose populations.
906 Texas A&M University

907 Singh NK, Kumar KRR, Kumar D, et al (2013) Characterization of a Pathogen Induced Thaumatin-Like Protein Gene
908 *AdTLP* from *Arachis diogoi*, a Wild Peanut. PLOS ONE 8:e83963.
909 https://doi.org/10.1371/journal.pone.0083963

910 Smith IM, Dunez J, Philips DH, et al (1989) European handbook of plant diseases. Q Rev Biol 64:200–200.
911 https://doi.org/10.1086/416271

912 Smulders MJM, Arens P, Bourke PM, et al (2019) In the name of the rose: a roadmap for rose research in the genome
913 era. Hortic Res 6:65–65. https://doi.org/10.1038/s41438-019-0156-0

914 Sosnowski O, Charcosset A, Joets J (2012) BioMercator V3: an upgrade of genetic map compilation and quantitative
915 trait loci meta-analysis algorithms. Bioinforma Oxf Engl 28:2082–2083.
916 https://doi.org/10.1093/bioinformatics/bts313

917 Soufflet-Freslon V, Marolleau B, Thouroude T, et al (2019) Development of tools to study rose resistance to black
918 spot. Acta Hortic 213–220. https://doi.org/10.17660/ActaHortic.2019.1232.31

919 Spiller M, Linde M, Hibrand-Saint Oyant L, et al (2011) Towards a unified genetic map for diploid roses. Theor Appl
920 Genet 122:489–500. https://doi.org/10.1007/s00122-010-1463-x

921 St Clair DA (2010) Quantitative disease resistance and quantitative resistance Loci in breeding. Annu Rev Phytopathol
922 48:247–268. https://doi.org/10.1146/annurev-phyto-080508-081904

923 Stamatakis A (2014) RAxML version 8: a tool for phylogenetic analysis and post-analysis of large phylogenies.
924 Bioinformatics 30:1312–1313. https://doi.org/10.1093/bioinformatics/btu033

925 Terefe-Ayana D, Yasmin A, Le TL, et al (2011) Mining disease-resistance genes in roses: functional and molecular
926 characterization of the *Rdr1* locus. Front Plant Sci 2:. https://doi.org/10.3389/fpls.2011.00035

927 Trognitz F, Manosalva P, Gysin R, et al (2002) Plant defense genes associated with quantitative resistance to potato
928 late blight in Solanum phureja x dihaploid S. tuberosum hybrids. Mol Plant-Microbe Interact MPMI 15:587–
929 597. https://doi.org/10.1094/MPMI.2002.15.6.587

930 Tsuchiya T, Eulgem T (2011) EMSY-like genes are required for full *RPP7*-mediated race-specific immunity and basal
931 defense in Arabidopsis. Mol Plant-Microbe Interact MPMI 24:1573–1581. https://doi.org/10.1094/MPMI-
932 05-11-0123

933 Uggla M, Carlson-Nilsson BU (2005) Screening of fungal diseases in offspring from crosses between Rosa sections
934 Caninae and Cinnamomeae. Sci Hortic 104:493–504. https://doi.org/10.1016/j.scienta.2004.11.001

935 VAL'HOR, FranceAgriMer (2017) Bilan complet achats de végétaux

936 Van Ooijen JW (2011) Multipoint maximum likelihood mapping in a full-sib family of an outbreeding species. Genet
937 Res 93:343–349. https://doi.org/10.1017/S0016672311000279

938 Vasconcellos RCC, Oraguzie OB, Soler A, et al (2017) Meta-QTL for resistance to white mold in common bean. PLOS
939 ONE 12:e0171685. https://doi.org/10.1371/journal.pone.0171685

940 Veyrieras J-B, Goffinet B, Charcosset A (2007) MetaQTL: a package of new computational methods for the meta-
941 analysis of QTL mapping experiments. BMC Bioinformatics 8:49. https://doi.org/10.1186/1471-2105-8-49

942 Voigt CA (2014) Callose-mediated resistance to pathogenic intruders in plant defense-related papillae. Front Plant Sci
943 5:. https://doi.org/10.3389/fpls.2014.00168

Voigt CA (2016) Cellulose/callose glucan networks: the key to powdery mildew resistance in plants? New Phytol 212:303–305. https://doi.org/10.1111/nph.14198

Voigt CA, Somerville SC (2009) Chapter 4.4.5 - Callose in Biotic Stress (Pathogenesis): Biology, biochemistry and molecular biology of callose in plant defence: callose deposition and turnover in plant–pathogen interactions. In: Bacic A, Fincher GB, Stone BA (eds) Chemistry, Biochemistry, and Biology of 1-3 Beta Glucans and Related Polysaccharides. Academic Press, San Diego, pp 525–562

Waliczek TM, Byrne DH, Holeman DJ (2015a) Growers' and consumers' knowledge, attitudes and opinions regarding roses available for purchase. Acta Hortic

Waliczek TM, Byrne DH, Holeman DJ (2015b) Growers' and consumers' knowledge, attitudes and opinions regarding roses available for purchase. Acta Hortic 235–239. https://doi.org/10.17660/ActaHortic.2015.1064.26

Wang H, Yang Y, Li M, et al (2017) Residents' preferences for roses, features of rose plantings and the relations between them in built-up areas of Beijing, China. Urban For Urban Green 27:1–8. https://doi.org/10.1016/j.ufug.2017.06.011

Weber CA, Moore GA, Deng Z, Gmitter FG (2003) Mapping Freeze Tolerance Quantitative Trait Loci in a *Citrus grandis* × *Poncirus trifoliata* F1 Pseudo-testcross Using Molecular Markers. J Am Soc Hortic Sci 128:508–514. https://doi.org/10.21273/JASHS.128.4.0508

Whitaker VM, Bradeen JM, Debener T, et al (2010a) Rdr3, a novel locus conferring black spot disease resistance in tetraploid rose: genetic analysis, LRR profiling, and SCAR marker development. TAG Theor Appl Genet Theor Angew Genet 120:573–585. https://doi.org/10.1007/s00122-009-1177-0

Whitaker VM, Debener T, Roberts AV, Hokanson SC (2010b) A standard set of host differentials and unified nomenclature for an international collection of *Diplocarpon rosae* races. Plant Pathol 59:745–752. https://doi.org/10.1111/j.1365-3059.2010.02281.x

Whitaker VM, Hokanson SC (2009) Partial resistance to black spot disease in diploid and tetraploid roses: general combining ability and implications for breeding and selection. Euphytica 169:421–429. https://doi.org/10.1007/s10681-009-9976-6

Whitaker VM, Hokanson SC, Bradeen J (2007) Distribution of Rose Black Spot (*Diplocarpon rosae*) Genetic Diversity in Eastern North America Using Amplified Fragment Length Polymorphism and Implications for Resistance Screening. J Am Soc Hortic Sci 132:534–540

White MA, Steffy B, Wiltshire T, Payseur BA (2011) Genetic dissection of a key reproductive barrier between nascent species of house mice. Genetics 189:289–304. https://doi.org/10.1534/genetics.111.129171

White MA, Stubbings M, Dumont BL, Payseur BA (2012) Genetics and evolution of hybrid male sterility in house mice. Genetics 191:917–934. https://doi.org/10.1534/genetics.112.140251

Wiggers RJ, West JG, Taylor J (1997) Conidial germination and infection by *Diplocarpon rosae* on susceptible and resistant rose species. Mycologia 89:103–108. https://doi.org/10.2307/3761178

Xue AG, Davidson CG (1998) Components of Partial Resistance to Black Spot Disease *(Diplocarpon rosae* Wolf) in Garden Roses. HortScience 33:96–99

Yadava SK, Arumugam N, Mukhopadhyay A, et al (2012) QTL mapping of yield-associated traits in *Brassica juncea*: meta-analysis and epistatic interactions using two different crosses between east European and Indian gene pool lines. TAG Theor Appl Genet Theor Angew Genet 125:1553–1564. https://doi.org/10.1007/s00122-012-1934-3

Yagi M, Kimura T, Yamamoto T, et al (2012) QTL analysis for resistance to bacterial wilt (Burkholderia caryophylli) in carnation (Dianthus caryophyllus) using an SSR-based genetic linkage map. Mol Breed 30:495–509. https://doi.org/10.1007/s11032-011-9639-x

Yagi M (National I of FS, Onozaki T, Taneya M, et al (2006) Construction of a genetic linkage map for the carnation (*Dianthus caryophyllus* by using RAPD and SSR markers and mapping quantitative trait loci (QTL) for resistance to bacteria wilt caused by Burkholderia caryophylli. J Jpn Soc Hortic Sci Jpn

Yan M, Byrne DH, Klein PE, et al (2019) Black spot partial resistance in diploid roses: QTL discovery and linkage map creation. Acta Hortic 1232:135–141. https://doi.org/10.17660/ActaHortic.2019.1232.21

Yang B, Jiang Y, Rahman MH, et al (2009) Identification and expression analysis of *WRKY* transcription factor genes in canola (*Brassica napus* L.) in response to fungal pathogens and hormone treatments. BMC Plant Biol 9:68. https://doi.org/10.1186/1471-2229-9-68

Yang Q, Balint-Kurti P, Xu M (2017) Quantitative disease resistance: dissection and adoption in maize. Mol Plant 10:402–413. https://doi.org/10.1016/j.molp.2017.02.004

Yokoya K, Kandasamy KI, Walker S, et al (2000) Resistance of roses to pathotypes of *Diplocarpon rosae*. Ann Appl Biol 136:15–20. https://doi.org/10.1111/j.1744-7348.2000.tb00003.x

Zhang J, Wang F, Liang F, et al (2018) Functional analysis of a pathogenesis-related thaumatin-like protein gene *TaLr35PR5* from wheat induced by leaf rust fungus. BMC Plant Biol 18:76. https://doi.org/10.1186/s12870-018-1297-2

Zhu M, Zhao S (2007) Candidate gene identification approach: progress and challenges. Int J Biol Sci 3:420–427

Zlesak DC, Nelson R, Harp D, et al (2017) Performance of landscape roses grown with minimal input in the north-central, central, and south-central united states. HortTechnology 27:718–730. https://doi.org/10.21273/HORTTECH03681-17

Zlesak DC, Whitaker VM, George S, Hokanson SC (2010) Evaluation of roses from the Earth-Kind® trials: black spot (*Diplocarpon rosae* wolf) resistance and ploidy. HortScience 45:1779–1787. https://doi.org/10.21273/HORTSCI.45.12.1779

Zurn JD, Zlesak DC, Holen M, et al (2018) Mapping a novel black spot resistance locus in the climbing rose Brigth eyesTM ('radbrite'). Front Plant Sci 9:1730. https://doi.org/10.3389/fpls.2018.01730

Zurn JD, Zlesak DC, Holen M, et al (2020) Mapping the black spot resistance locus *Rdr3* in the shrub rose 'George Vancouver' allows for the development of improved diagnostic markers for DNA-informed breeding. Theor Appl Genet. https://doi.org/10.1007/s00122-020-03574-4

List of abbreviation

Black Spot Disease (BSD); Quantitative Trait Loci (QTLs); Marker Assisted Breeding (MAS); Linkage Groups (LG); *Rosa wichurana* (RW); *Rosa chinensis* 'Old blush' (OB); *Rosa hybrid* 'The Fairy' (TF); *Rosa chinensis* 'Old blush' x *Rosa wichurana* population (OB population); *Rosa hybrid* 'The Fairy' x *Rosa wichurana* population (FW population); H190 x *Rosa wichurana* population (HW population); Analysis of Variance (ANOVA); Restricted

Maximum Likelihood (REML); 'Nearest Neighbor fit' (N.N fit); Short Sequence Repeat (SSR); Single Nucleotide Polymorphism (SNP); Logarithm of Odds (LOD); Weighted Least Square (WLS); 'Akaike' Information Criterion (AIC); Confidence Intervals (CI); Centimorgans (cM); Gene Ontology (GO); Resistance gene (*R*-gene); Number of Petals (NP); Simple Interval Mapping (SIM); Composite Interval Mapping (CIM); Two-part model (2p model); TIR-NB-LRR (*TNL*); *NB*-encoding (Nucleotide Binding); Quantitative Disease Resistance (QDR); Quantitative resistance loci (QRL); Cytochromes P450 monooxygenases (CYP); Pathogenesis-Related (PR); Thaumatin-Like Protein (TLP)

Figure legends

Fig. 1 Black spot disease scoring data distribution for all years and locations for the three populations A: Scoring data for different years for OW population in Angers, B: Scoring data for different years for HW population in Angers, C: Scoring data for different years for HW population in Bellegarde, D: Scoring data for different years for HW population in Diémoz, and E: Scoring data for different years for FW population in Angers.

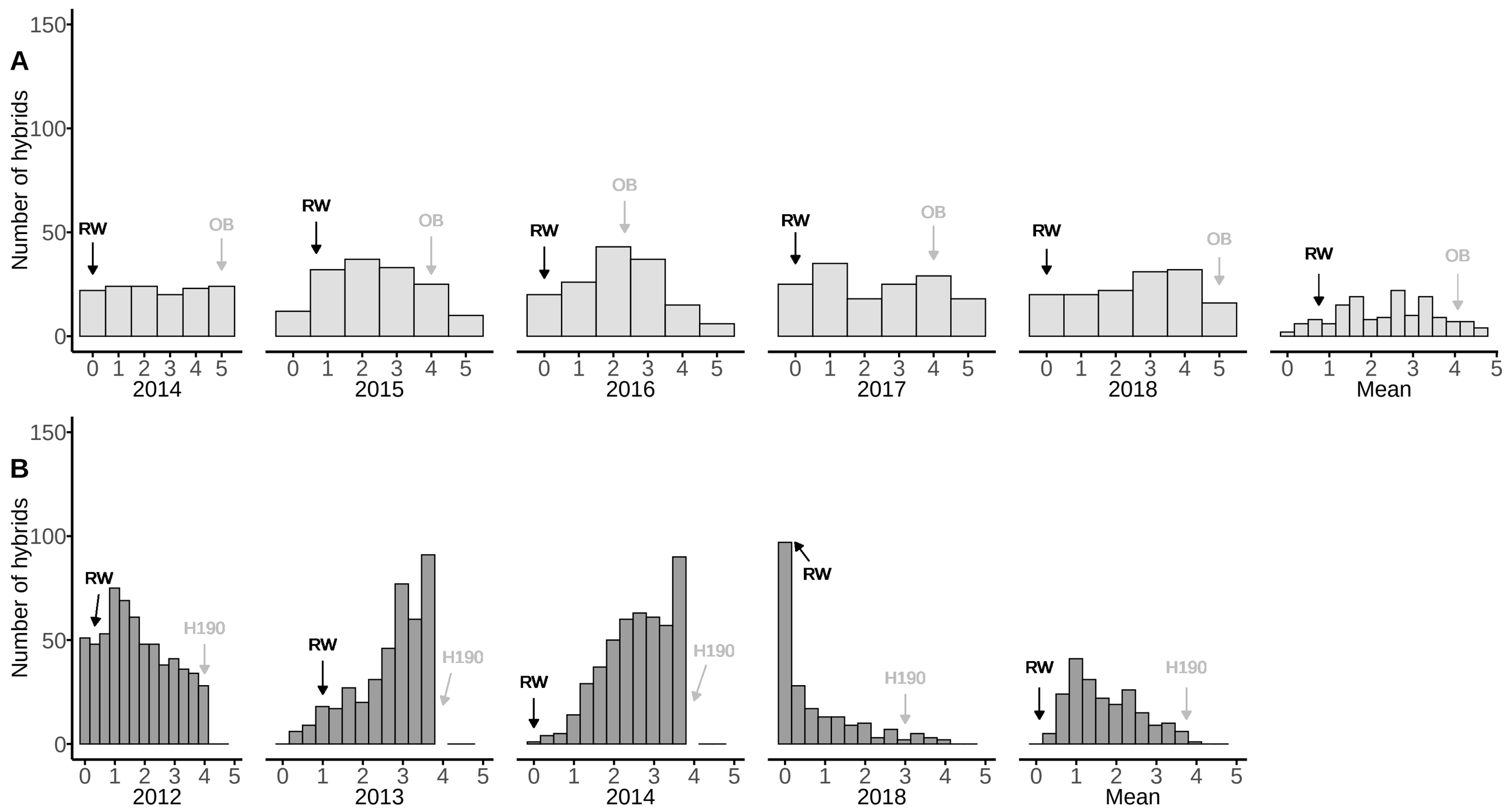
A
Number of hybrids
150
100
50
0
RW
OB
0 1 2 3 4 5
2014
2015
2016
2017
2018
Mean
B
H190
2012
2013
2014
2018
Mean
C
H190–NA
RW–NA
D
E
RW – NA
TF

Fig. 2 Representation of individual QTLs and meta-QTLs associated with black spot disease resistance for OW, FW and HW rose populations on the male consensus map

Names of markers are on the right and the genetic distances (in cM) on the left. The 19 and 17 QTLs detected on B3 and B5, respectively, on all three populations are projected onto a newly built consensus map. QTL names are coded as follows: PopName_map_YearLG_Location_method. 95% Bayesian confidence intervals are displayed with vertical bars where the length is proportional to the interval width, and the QTL peak is represented by a line. Meta-QTLs are represented in plain color on the LGs.

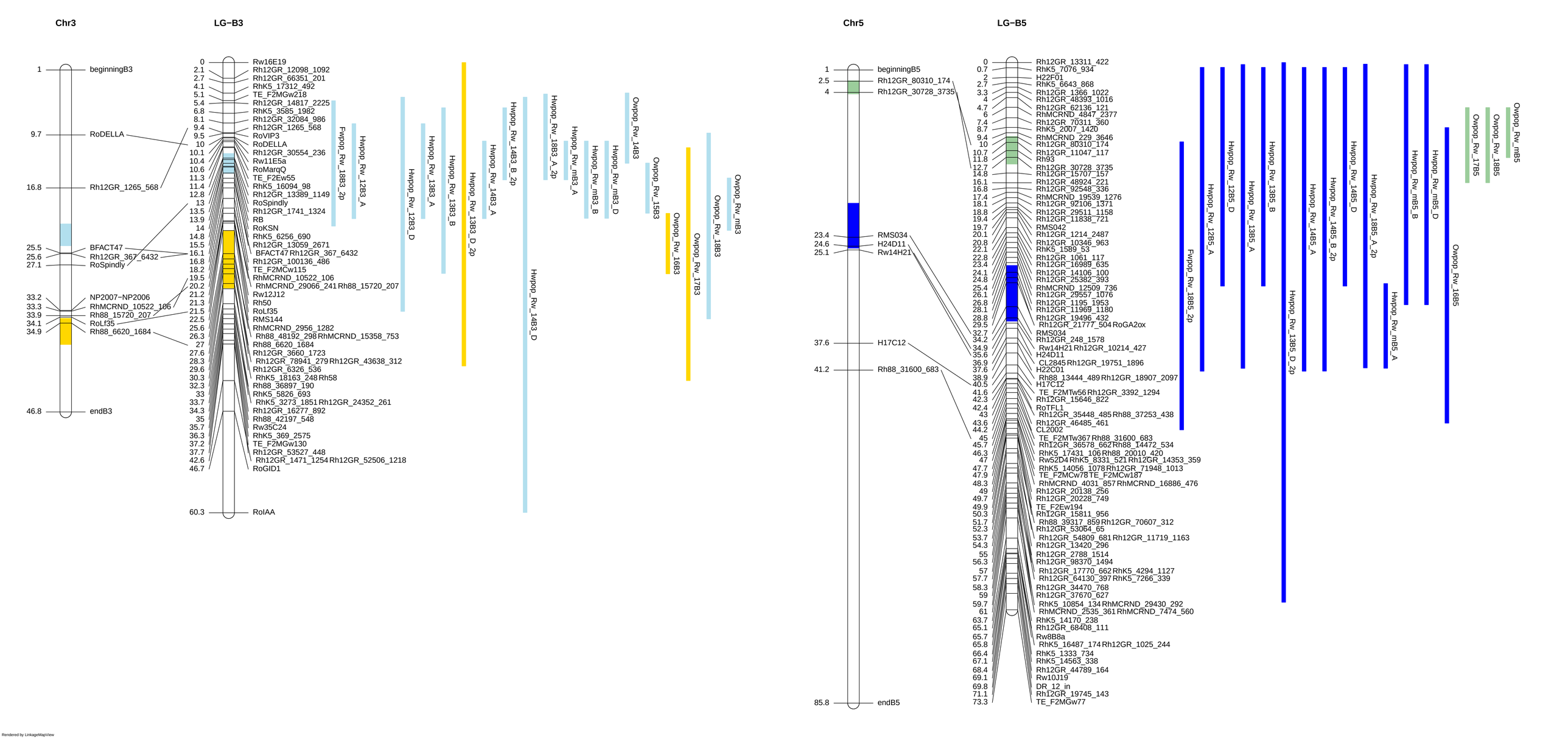

Fig. 3 Candidate R-genes placed on the pseudochromosomes of *Rosa chinensis* assembly and meta-QTL position

Each pseudochromosome is represented by a yellow bar, with the positions of the *R*-genes indicated as blue lines.

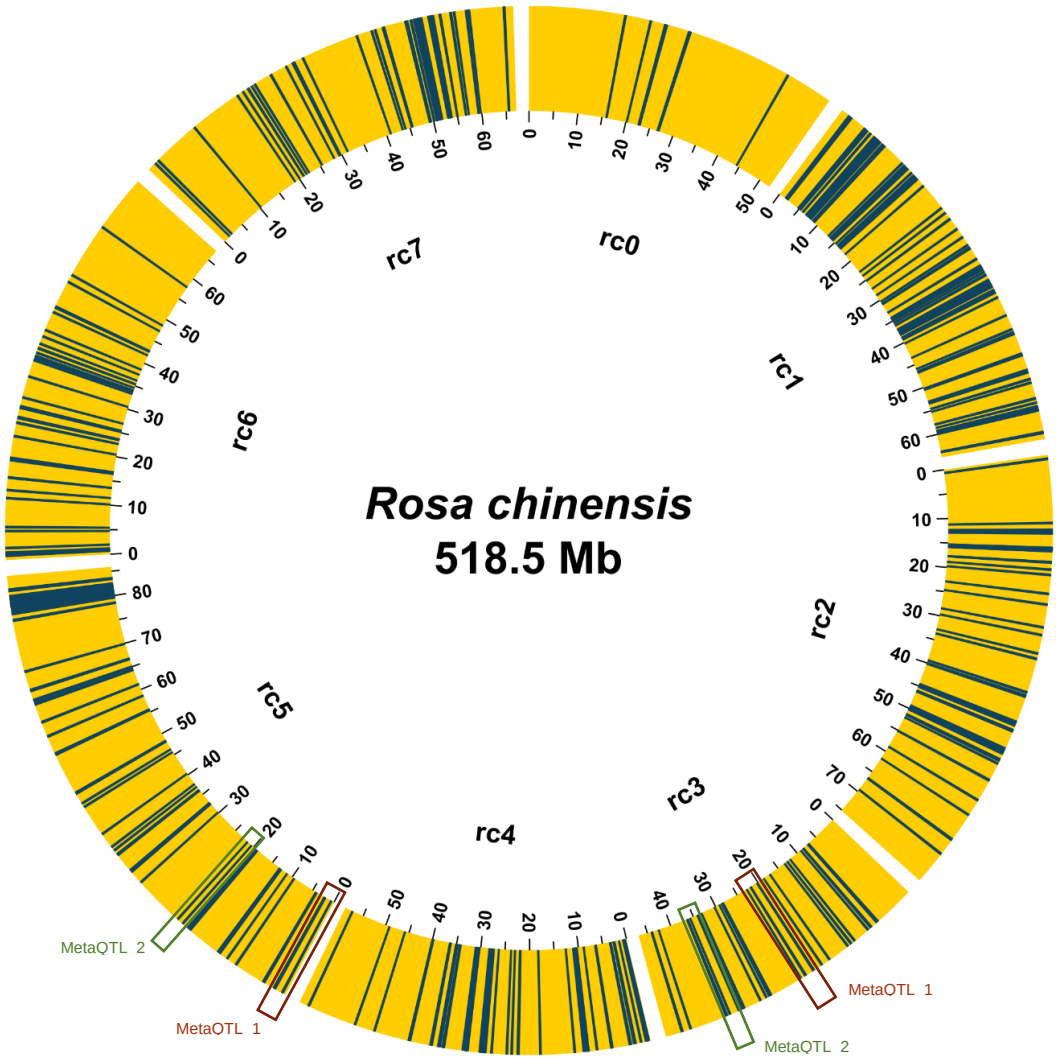
Rosa chinensis
518.5 Mb
rc0
rc1
rc2
rc3
rc4
rc5
rc6
rc7
MetaQTL 2
MetaQTL 1
MetaQTL 1
MetaQTL 2

Table legends

Table 1 Summary of the SSR and SNP-based linkage maps for OW population and the common markers with other populations

Linkage groups (LG) names for the female map (A1 to A7) and for the male map (B1 to B7) were assigned according to Spiller et al. 2011. Several markers were mapped at the same locus so the number of unique loci is displayed and in the total number, the number of markers with different phases (called identicals) are displayed in parenthesis. One gene marker was used for the female map and is represented with (+1) on the table. *Marker was counted as common when at minimum two of the three populations shared this same marker.

Table 1 Summary of the SSR and SNP-based linkage maps for OW population and the common markers with other populations

LG	Female map							LG	Male map						
	Length (cM)	Number of markers			Number of loci	Average marker interval (cM)	Number of common markers*		Length (cM)	Number of markers			Number of loci	Average marker interval (cM)	Number of common markers*
		SNP	SSR	Total (identicals)						SNP	SSR	Total (identicals)			
A1	71.71	115	2	117 (690)	79	0.91	3	B1	57.44	66	2	68 (171)	50	1.15	3
A2	33.42	69	3	72 (1100)	45	0.74	8	B2	84.34	90	7	97 (266)	65	1.30	8
A3	53.75	61	5 (+1)	68 (520)	53	1.01	5	B3	42.6	37	5	42 (518)	35	1.22	9
A4	58.79	41	5	46 (220)	40	1.47	4	B4	66.82	73	7	80 (371)	66	1.01	6
A5	97.68	148	7	155 (1007)	115	0.85	5	B5	71.12	83	7	90 (318)	74	0.96	8
A6	70.15	133	4	137 (1134)	91	0.77	3	B6	55.89	65	3	68 (210)	48	1.16	3
A7	88.36	126	5	131 (841)	90	0.98	3	B7	75.41	83	5	88 (217)	64	1.18	4
Total	473.85	692	31 (+1)	726 (5512)	513	0.96	31	Total	453.62	497	36	534 (2072)	402	1.14	41

Linkage groups (LG) names for the female map (A1 to A7) and for the male map (B1 to B7) were assigned according to Spiller et al. 2011. Several makers were mapped at the same locus so the number of unique loci is displayed and in the total number, the number of markers with different phases (called identicals) are displayed in parenthesis. One gene marker was used for the female map and is represented with (+1) on the table.

*Marker was count as common when minimum two of the three populations shared this same marker.

Table 2 Summary of QTL for black spot disease resistance in OW, FW and HW populations across multiple environments (years and locations) for male maps

[a] Normal indicates a QTL mapping using a normal model with CIM analysis and 2p indicates a two-part model that studies consecutively a binary model and a normal one, so three LOD were calculated: LOD.π (penetrance, equivalent to binary model), LOD.μ (severity, equivalent to normal model for non-spike phenotypes) and LOD.π.μ (sum, complete model). [b] Permutation test giving the LOD threshold calculated using 1,000 permutations over which a QTL was significant. [c] Linkage group number with B for the male map. [d] Proportion of phenotypic variation explained by the QTL. [e] Confidence interval calculated with the 95% Bayesian credible interval.

Table 2 Summary of QTL for black spot disease resistance in OW, FW and HW populations across multiple environments (years and locations) for male maps

Population	Method[a]	Location	Year	PT[b]	LG[c]	LOD[a]	Lod.π[a]	Lod.μ[a]	R^2 (%)[d]	95% Bayes CI (in cM) [e]		Peak	
										Interval start	Interval end	Closest marker	Position (cM)
OW	normal	Angers	2014	2.6	B3	3.16			10.1	4.07	13.5	Rh12GR_1265_568	9.34
			2015	2.6	B3	8.72			23.6	13.5	20.2	Rh12GR_367_6432	1613
			2016	2.5	B3	6.79			17.9	20.2	28.3	Rh88_6620_1684	26.96
					B5	4.11			9.8	8.71	48.3	Rh88_31600_683	44.99
			2017	2.6	B3	4.65			10.2	11.4	42.6	Rh88_15720_207	20.19
					B4	3.55			7.6	2	65.4	Rh12GR_14039_541	14.2
					B5	5.26			11.4	6.03	16.1	Rh12GR_80310_174	10.04
			2018	2.6	B3	3.17			8.8	9.44	34.3	RhMCRND_10522_106	19.52
					B5	3.43			9.3	6.03	16.1	Rh12GR_80310_174	10.04
			Mean	2.6	B3	11.18			22.1	15.46	22.49	Rh12GR_367_6432	16.33
					B4	3.02			5.1	13.95	23.6	Rh88_49087_478	20.9
					B5	5.42			11	6.03	12.74	Rh12GR_30728_3735	8.71
FW	2p	Angers	2018	2.15	B3	4.74	4.13	0.60	11.44	0	16.8	BFACT47	7.01
					B5	2.91	2.74	0.17	0.89	10.4	49	RoRGA2	29.34
HW	normal	Angers	2012	2.32	B3	7.67			15.74	3.97	16.7	RB	9.67
					B5	3.6			6.23	0	40.7	Rw14H21	25.13
			2013	2.21	B3	8.56			16.02	3.97	16.7	RB	9.67
					B5	9.94			14.82	0	40.7	RMS034	32.18
					B6	2.87			3.6	0	62.5	CTG623	8.28
			2014	2.23	B3	7.54			12.99	6.3	16.7	RB	9.67
					B5	6.36			9.66	0	40.7	RMS034	25.13
					B6	3.12			4.22	0	20.88	CTG623	8.28
			Mean	2.14	B3	15.23			21.43	6.3	11.5	RB	9.67
					B5	12.14			16.76	29.34	40.69	RMS034	32.18
					B6	3.92			4.63	0	20.88	CTG623	8.28
		Bellegarde	2013	2.30	B3	5.08			8.52	0	22.2	RoRGA/RoDELLA	3.97
					B5	9.86			19.6	0	29.3	Rw14H21	25.13

Table 2 (continued)

Population	Method[a]	Location	Year	PT[b]	LG[c]	LOD[a]	Lod.π[a]	Lod.μ[a]	R^2 (%)[d]	95% Bayes CI (in cM) [e]		Peak	
										Interval start	Interval end	Closest marker	Position (cM)
HW	normal	Bellegarde	Mean	2.33	B3	5.23			8.41	6.3	16.66	RoMarQ	6.3
					B5	4.99			5.35	0	32.18	Rw14H21	25.13
					B6	2.6			4.15	0	20.88	CTG623	8.28
		Diémoz	2012	2.25	B3	3.72			7.19	0	28.7	Rw14H21	25.13
					B5	4.21			9.14	0	29.3	CTG623	8.28
			2014	2.21	B3	2.73			3.9	0	60.6	BFACT47	11.5
					B5	4.64			8.72	0	29.3	Rw14H21	25.13
					B6	2.96			4.17	0	38.3	CTG623	8.28
			Mean	2.08	B3	5.55			9.7	6.3	16.66	BFACT47	11.5
					B5	8.43			12.78	0	32.18	Rw14H21	25.13
	2p	Angers	2018	3.03	B3	8.19	0.77	7.42	15.66	0	11.5	RoSpindly	8.96
					B5	9.92	0.7	9.22	19.82	0	40.69	H24D11	30.08
					B6	3.13	0.64	2.48	2.35	0	62.5	CTG623	8.28
		Bellegarde	2014	2.96	B3	12.55	9.62	2.95	13.69	0	9.67	RoRGA	3.97
					B5	6.39	4.84	1.59	8.17	0	40.69	Rw14H21	25.13
					B6	4.87	4.7	0.17	2.76	0	20.88	CTG623	8.28
		Diémoz	2013	3.06	B3	4	0.87	3.13	8.96	0	60.63	RoLf35	19.08
					B5	5.98	0.16	5.82	11.93	0	72.49	H17C12	40.69

[a] Normal indicates a QTL mapping using a normal model with CIM analysis and 2p indicates a two-part model that studies consecutively a binary model and a normal one, so three LOD were calculated: LOD.π (penetrance, equivalent to binary model), LOD.μ (severity, equivalent to normal model for non-spike phenotypes) and LOD.π.μ (sum, complete model).

[b] Permutation test giving the LOD threshold calculated using 1,000 permutations over which a QTL was significant.

[c] Linkage group number with B for the male map.

[d] Proportion of phenotypic variation explained by the QTL.

[e] Confidence interval calculated with the 95% Bayesian credible interval.

Table 3 Summary of QTL for black spot disease resistance in OW, FW and HW populations across multiple environments (years and locations) for female maps

[a] Normal indicates a QTL mapping using a normal model with CIM analysis and 2p indicates a two-part model that studies consecutively a binary model and a normal one, so three LOD were calculated: LOD.π (penetrance, equivalent to binary model), LOD.μ (severity, equivalent to normal model for non-spike phenotypes) and LOD.π.μ (sum, complete model). [b] Permutation test giving the LOD threshold calculated using 1,000 permutations over which a QTL was significant. [c] Linkage group number with B for the male map. [d] Proportion of phenotypic variation explained by the QTL. [e] Confidence interval calculated with the 95% Bayesian credible interval.

Table 3 Summary of QTL for black spot disease resistance in OW, FW and HW populations across multiple environments (years and locations) for female maps

Population	Method[a]	Location	Year	PT[b]	LG[c]	LOD[a]	Lod.π[a]	Lod.μ[a]	R^2 (%)[d]	95% Bayes CI (in cM) [e]		Peak	
										Interval Start	Interval End	Nearest marker	Position (cM)
OW	normal	Angers	2017	2.71	A1	4.12			6.53	42.89	60.3	Rh12GR_100474_250	54.3
FW	2p	Angers	2018	2.10	A1	2.6	2.59	0.01	4.06	15.92	44.87	Rw34L6	35
					A2	5.86	3.16	2.63	2.57	1.12	14.64	Rw59A12	1.12
					A4	4.18	4.09	0.01	3.61	32.53	44.28	Rw53O21	44.28
HW	normal	Angers	2012	2.04	A3	2.77			5.8	23.73	41.37	NP2007	33.71
		Angers	2014	2.09	A3	2.3			4.44	23.73	41.37	NP2007	33.71
		Bellegarde	2012	2.05	A5	2.51			5.39	0	36.04	H24D11	27.09
		Bellegarde	2013	1.95	A3	2.47			5.1	12.35	33.71	RoLf35H	23.73
		Diémoz	2014	2.08	A3	2.63			5.74	23.73	41.37	NP2007	33.71
					A4	2.87			5.77	0	37.36	Rw20l17	12.6
		Diémoz	Mean	2.09	A3	2.17			4.4	23.73	41.37	NP2007	33.71
	2p	Bellegarde	2014	2.73	A3	3.02	2.15	0.91	5.91	12.35	51.19	NP2006	33.71

[a] Normal indicates a QTL mapping using a normal model with CIM analysis and 2p indicates a two-part model that studies consecutively a binary model and a normal one, so three LOD were calculated: LOD.π (penetrance, equivalent to binary model), LOD.μ (severity, equivalent to normal model for non-spike phenotypes) and LOD.π.μ (sum, complete model).

[b] Permutation test giving the LOD threshold calculated using 1,000 permutations over which a QTL was significant.

[c] Linkage group number with B for the male map.

[d] Proportion of phenotypic variation explained by the QTL.

[e] Confidence interval calculated with the 95% Bayesian credible interval.

Table 4 Meta-QTL genomic position and gene mining

[a] Meta-QTL names using all the QTLs found with the normal and 2p method results. [b] Chromosome numbers from *Rosa chinensis* genome (Hibrand Saint-Oyant et al. 2018). [c] Genomic positions of the meta-QTLs after projection on *Rosa chinensis* genome (Hibrand Saint-Oyant et al. 2018). [d] Genes coding for disease resistance proteins from the automatic annotation of the genome. [e] Resistance gene analogs with *NB*-domain found with protein sequence scan (manual annotation). [f] Total number of annotated genes under meta-QTL intervals with Goffinet et al. (2000) method.

Table 4 Meta-QTL genomic position and gene mining

Meta_QTL[a]	Chr[b]	Genetic position (cM)		Interval position (bp)[c]		Number of genes in the interval		
		start	end	start	end	RGAs_auto[d]	RGAs_manual[e]	Total[f]
Meta_1_3	3	12.17	14.89	21605249	24567362	11	4	291
Meta_2_3	3	22.51	30.21	34220246	37772912	4	3	450
Meta_1_5	5	9.68	13.63	2414969	4219224	3	3	271
Meta_2_5	5	27.14	34.66	18827666	24889549	5	9	557

[a] Meta-QTL names using all the QTLs found with the normal and 2p method results.
[b] Chromosome numbers from *Rosa chinensis* genome (Hibrand Saint-Oyant et al. 2018).
[c] Genomic positions of the meta-QTLs after projection on *Rosa chinensis* genome (Hibrand Saint-Oyant et al. 2018).
[d] Genes coding for disease resistance proteins from the automatic annotation of the genome.
[e] Resistance gene analogs with *NB*-domain found with protein sequence scan (manual annotation).
[f] Total number of annotated genes under meta-QTL intervals with Goffinet et al. (2000) method.

Additional files

Supplementary tables

Supp. Table 1 Common marker list for all populations for the female and male maps

[a] Only SSR markers are listed. The markers shared by all three populations are displayed in green; [b] A1-A7 for the female maps and B1-B7 for the male maps.

Supp. table 1 Common marker list for all populations for the female and male maps

Male maps					Female maps				
Markers[a]	LG[b]	OW	HW	FW	Markers[a]	LG[b]	OW	HW	FW
RMS015	B1	X	X	X	RMS015	A1	X		X
Rw25J16	B1		X	X	Rw32K24	A1	X		X
Rw32K24	B1	X	X	X	Rw25J16	A1		X	X
CTG329	B2		X	X	RMS132	A2	X	X	X
CTG356	B2	X	X		CTG356	A2	X		X
RMS129	B2	X		X	RMS147	A2		X	X
RMS132	B2	X	X	X	Rw59A12	A2		X	X
RMS137	B2	X	X	X	Rw23F13	A2		X	X
RMS147	B2	X	X	X	RMS137	A2		X	X
Rw23F13	B2	X		X	CTG329	A2		X	X
Rw59A12	B2	X	X	X	Rh80	A2		X	X
BFACT47	B3	X	X	X	BFACT47	A3	X	X	
RoAP2	B3		X	X	Rh58	A3	X	X	X
Rh50	B3		X	X	Rw35C24	A3	X		X
Rh58	B3	X	X	X	CTG21	A3	X		X
RMS144	B3	X		X	Rh50	A3		X	X
RoIAA	B3		X	X	Rog5	A4	X	X	
RoVIP3	B3		X	X	Rw55E12	A4	X	X	
Rw16E19	B3	X	X	X	Cl3881	A4	X		X
Rw35C24	B3	X	X	X	Rh98	A4	X	X	X
Cl3881	B4	X	X	X	H22F01	A5	X	X	
H20D08	B4	X	X		H24D11	A5	X	X	
H2F12	B4	X	X	X	Rw14H21	A5	X	X	X
Rog5	B4	X		X	CL2845	A5	X	X	X
Rw53O21	B4	X	X	X	Rw10J19	A5	X		X
Rw55E12	B4	X	X	X	Rw22A3	A6	X		X
CL2845	B5	X	X	X	Rw61F2	A6	X		X
H17C12	B5		X	X	CTG623	A6	X	X	X
H22C01	B5	X	X		RMS003	A7	X	X	X
H22F01	B5	X	X	X	Rw10M24	A7	X	X	
H24D11	B5	X		X	Rw15D15	A7	X	X	X
RMS034	B5	X		X					
Rw10J19	B5	X	X	X					
Rw14H21	B5	X	X	X					
CTG623	B6	X	X	X					
Rw22A3	B6	X	X	X					
Rw61F2	B6	X	X						
H10D03	B7	X	X						
RMS003	B7	X	X	X					
Rw10M24	B7	X		X					
Rw15D15	B7	X	X	X					

[a] Only SSR markers are listed, the markers shared by all three populations are displayed in emphasized green; [b] A1-A7 for the female maps and B1-B7 for the male maps.

Supp. Table 2 NB-encoding genes information and position in Rose genome

Summary of NB-encoding genes identified in manual annotations. Listed are gene ID names, chromosomal affiliation, end and start positions, classification (CC=Coiled Coil; LRR=Leucine Rich Repeat; NBS=Nucleotide Binding Site; TIR=Toll Interleukin Like Receptor); non-canonical domains (i.e., conserved protein domains that are atypical of NBS-LRR proteins); configuration of identified conserved NB-ARC subdomains; and detailed domain configurations, complete with reported e-values from a Pfam analysis.

Gene ID	Chromosome	Start	End	Classification	Non-canonical domains	Configuration of subdomains within NB-ARC	Detailed domain configuration, including E-values from Pfam analysis
RC0G0129500	rc00	15921725	15925651	NBS-LRR		P-loop[465-473] Kin-2[546-553] RNBS-B[573-576] GLPL[629-635]	[440-721]NB-ARC:6.8e-40 [872-926]LRR_8:4.7e-07
RC0G0129700	rc00	15936605	15940195	NBS-LRR		P-loop[491-499] Kin-2[572-579] RNBS-B[599-605] GLPL[661-667]	[467-747]NB-ARC:1.3e-38 [908-964]LRR_8:9.6e-08
RC0G0157500	rc00	20165214	20168978	NBS		P-loop[100-108] Kin-2[181-188] RNBS-B[209-215] GLPL[276-282]	[76-370]NB-ARC:6.2e-73
RC0G0174400	rc00	22640609	22644651	NBS	RPW8	P-loop[186-194] Kin-2[267-274] RNBS-B[292-298] GLPL[347-353]	[4-135]RPW8:8.3e-22 [165-435]NB-ARC:1.7e-34
RC0G0176800	rc00	22873190	22878387	NBS-LRR	RPW8	P-loop[184-192] Kin-2[263-270] RNBS-B[288-294] GLPL[343-349]	[3-113]RPW8:7e-17 [165-429]NB-ARC:5.1e-34 [628-684]LRR_8:1.2e-05 [724-763]LRR_4:0.00046
RC0G0200900	rc00	26709295	26713250	NBS-LRR		P-loop[205-213] Kin-2[280-287] RNBS-B[310-316] GLPL[369-375]	[172-194]AAA_16:0.0003 [196-458]NB-ARC:7.2e-61 [578-615]LRR_8:0.0026 [620-656]LRR_8:0.0064
RC0G0201600	rc00	26778236	26782002	NBS-LRR		P-loop[205-213] Kin-2[280-287] RNBS-B[310-316] GLPL[369-375]	[172-194]AAA_16:1.9e-05 [196-455]NB-ARC:2.2e-60 [576-613]LRR_8:0.0037
RC0G0202800	rc00	26907214	26909933	NBS-LRR		P-loop[116-124] Kin-2[191-198] RNBS-B[221-227] GLPL[280-286]	[83-105]AAA_16:0.00016 [107-367]NB-ARC:7e-63 [490-527]LRR_4:0.0038 [528-564]LRR_8:0.006
RC0G0283700	rc00	44426071	44428206	CC-NBS-LRR		P-loop[205-213] Kin-2[282-289] RNBS-B[313-319] GLPL[376-382]	[184-464]NB-ARC:1.4e-59 [574-623]LRR_8:2e-07 [630-652]LRR_4:8.3e-05
RC1G0009500	rc01	1503964	1506714	NBS		P-loop[26-34] Kin-2[104-111] RNBS-B[132-138] GLPL[191-197]	[2-263]NB-ARC:6.7e-37
RC1G0012400	rc01	1742358	1745854	CC-NBS-LRR		P-loop[201-209] Kin-2[277-284] RNBS-B[307-313] GLPL[368-374]	[170-191]AAA_16:0.00058 [192-453]NB-ARC:9.3e-64 [583-639]LRR_8:0.00043
RC1G0015400	rc01	1977225	1978112	NBS		P-loop[43-51] Kin-2[119-126] RNBS-B[149-155] GLPL[210-216]	[21-294]NB-ARC:2.3e-66
RC1G0035900	rc01	4772090	4776326	NBS-LRR		P-loop[204-212] Kin-2[279-286] RNBS-B[310-316] GLPL[371-377]	[173-182]AAA_16:3.2e-05 [183-461]NB-ARC:2.5e-60 [877-933]LRR_8:0.00012 [950-1009]LRR_8:0.0013 [1009-1038]LRR_4:0.0023
RC1G0036600	rc01	4825651	4829916	NBS-LRR		P-loop[200-208] Kin-2[274-281] RNBS-B[305-311] GLPL[366-372]	[174-420]NB-ARC:1.2e-48 [934-975]LRR_4:0.00053
RC1G0037000	rc01	4845477	4854130	NBS-LRR		P-loop[202-210] Kin-2[277-284] RNBS-B[308-314] GLPL[369-375]	[171-180]AAA_16:0.0022 [181-458]NB-ARC:3e-60 [877-922]LRR_8:0.00088 [961-1002]LRR_4:0.0015 [1009-1048]LRR_4:0.0053
RC1G0038100	rc01	4945293	4950173	NBS-LRR		P-loop[197-205] Kin-2[271-278] RNBS-B[304-310] GLPL[366-372]	[168-456]NB-ARC:3e-58 [584-638]LRR_8:9e-06
RC1G0038200	rc01	4997244	5004392	TIR-NBS-LRR		P-loop[227-235] Kin-2[301-308] RNBS-B[332-338] GLPL[390-396]	[18-189]TIR:9.3e-41 [206-459]NB-ARC:2.1e-34 [610-628]LRR_3:0.00055 [704-761]LRR_8:0.00073
RC1G0041300	rc01	5325468	5330421	NBS-LRR		P-loop[205-213] Kin-2[280-287] RNBS-B[309-315] GLPL[370-376]	[172-193]AAA_16:0.0076 [194-455]NB-ARC:5.5e-66 [583-635]LRR_8:3.8e-05 [636-679]LRR_8:0.00045 [680-698]LRR_4:0.0018
RC1G0046400	rc01	6001575	6004952	NBS-LRR		P-loop[205-213] Kin-2[279-286] RNBS-B[308-314] GLPL[369-375]	[180-455]NB-ARC:9.8e-56 [583-637]LRR_8:7.1e-05 [637-666]LRR_4:0.009
RC1G0046600	rc01	6015473	6021617	CC-NBS-LRR		P-loop[204-212] Kin-2[288-295] RNBS-B[317-323] GLPL[378-384]	[177-468]NB-ARC:1.1e-63

RC1G0046700	rc01	6022946	6027291	NBS-LRR		P-loop[206-214] Kin-2[281-288] RNBS-B[310-316] GLPL[371-377]	[180-459]NB-ARC:4.1e-63 [584-621]LRR_4:0.0016 [622-635]LRR_4:0.0022
RC1G0054000	rc01	6873096	6882290	NBS-LRR		P-loop[205-213] Kin-2[280-287] RNBS-B[310-316] GLPL[369-375]	[172-194]AAA_16:8.8e-05 [196-457]NB-ARC:4.1e-63 [579-616]LRR_4:0.0073
RC1G0054700	rc01	6918760	6921635	NBS-LRR		P-loop[205-213] Kin-2[281-288] RNBS-B[311-317] GLPL[370-376]	[172-194]AAA_16:2.2e-05 [196-457]NB-ARC:3.5e-63 [580-634]LRR_8:4.1e-05 [634-654]LRR_8:0.00033
RC1G0055000	rc01	7020069	7022309	NBS-LRR		P-loop[205-213] Kin-2[280-287] RNBS-B[310-316] GLPL[369-375]	[172-194]AAA_16:7.2e-06 [195-457]NB-ARC:5.7e-62 [579-633]LRR_8:8.9e-06
RC1G0057100	rc01	7250515	7253199	CC-NBS-LRR		P-loop[199-207] Kin-2[273-280] RNBS-B[303-309] GLPL[361-367]	[166-189]AAA_16:3.7e-06 [190-449]NB-ARC:6.8e-59 [563-572]LRR_8:0.0017 [573-594]LRR_4:0.00075 [595-647]LRR_8:8.5e-05
RC1G0057400	rc01	7348754	7351644	NBS-LRR		P-loop[203-211] Kin-2[278-285] RNBS-B[308-314] GLPL[367-373]	[170-192]AAA_16:1.3e-05 [194-454]NB-ARC:5.6e-63 [572-609]LRR_8:0.0065
RC1G0057600	rc01	7392967	7394847	NBS-LRR		P-loop[106-114] Kin-2[180-187] RNBS-B[210-216] GLPL[268-274]	[73-95]AAA_16:5.5e-05 [96-356]NB-ARC:1.9e-59 [477-500]LRR_8:0.00043 [501-541]LRR_4:4.9e-05
RC1G0058500	rc01	7430559	7433431	NBS-LRR		P-loop[201-209] Kin-2[276-283] RNBS-B[306-312] GLPL[369-375]	[168-190]AAA_16:0.00032 [192-455]NB-ARC:1.1e-63
RC1G0060200	rc01	7583456	7586325	NBS-LRR		P-loop[205-213] Kin-2[279-286] RNBS-B[309-315] GLPL[368-374]	[172-194]AAA_16:8.7e-05 [196-456]NB-ARC:2e-61 [578-632]LRR_8:7.3e-05 [632-652]LRR_8:0.0069
RC1G0061100	rc01	7626425	7629494	NBS-LRR		P-loop[205-213] Kin-2[280-287] RNBS-B[310-316] GLPL[369-375]	[172-194]AAA_16:1.4e-05 [196-456]NB-ARC:2.9e-61 [579-633]LRR_8:7.2e-05
RC1G0061900	rc01	7727136	7730004	CC-NBS-LRR		P-loop[205-213] Kin-2[280-287] RNBS-B[310-316] GLPL[369-375]	[172-194]AAA_16:2.1e-05 [195-456]NB-ARC:1.1e-63 [579-633]LRR_8:0.00012 [640-653]LRR_8:0.0025
RC1G0064300	rc01	8054123	8056050	TIR-NBS		P-loop[133-141] Kin-2[211-218] RNBS-B[238-244] GLPL[297-303]	[3-95]TIR:2.4e-07 [111-121]AAA_16:3.9e-06 [122-365]NB-ARC:1.4e-33
RC1G0065800	rc01	8149862	8157268	NBS-LRR		P-loop[200-208] Kin-2[272-279] RNBS-B[302-308] GLPL[358-364]	[168-190]AAA_16:3.1e-05 [191-446]NB-ARC:7.1e-62 [570-608]LRR_4:3.9e-05
RC1G0069700	rc01	8703984	8706776	NBS-LRR		P-loop[27-35] Kin-2[105-112] RNBS-B[132-138] GLPL[191-197]	[13-261]NB-ARC:2e-28 [409-427]LRR_3:1.8e-05 [477-500]LRR_4:0.00094 [501-557]LRR_8:0.0002 [557-581]LRR_8:0.004
RC1G0073500	rc01	9041245	9043098	TIR-NBS		P-loop[127-135] Kin-2[205-212] RNBS-B[232-238] GLPL[291-297]	[2-93]TIR:9.3e-10 [107-117]AAA_16:4.2e-06 [118-306]NB-ARC:1.2e-24
RC1G0074800	rc01	9109406	9111181	NBS		P-loop[27-35] Kin-2[105-112] RNBS-B[132-138] GLPL[191-197]	[18-258]NB-ARC:5.9e-30 [409-427]LRR_3:1.2e-05
RC1G0102900	rc01	13141019	13142561	NBS-LRR		P-loop[35-43] Kin-2[110-117] RNBS-B[139-145] GLPL[196-202]	[14-284]NB-ARC:4.7e-57 [386-444]LRR_8:1.8e-07
RC1G0105100	rc01	13684527	13694466	CC-NBS-LRR	RPW8	P-loop[904-912] Kin-2[985-992] RNBS-B[1009-1015] GLPL[1063-1069]	[2-134]RPW8:3.7e-28 [172-435]NB-ARC:5e-35 [896-1145]NB-ARC:3.2e-27
RC1G0105300	rc01	13704406	13708236	CC-NBS-LRR	RPW8	P-loop[218-226] Kin-2[302-309] RNBS-B[328-333] GLPL[382-388]	[2-111]RPW8:2.7e-13 [197-469]NB-ARC:3.1e-32 [732-788]LRR_8:0.0027
RC1G0107900	rc01	14058276	14061495	CC-NBS-LRR		P-loop[199-207] Kin-2[274-281] RNBS-B[303-309] GLPL[364-370]	[174-453]NB-ARC:1e-62 [578-632]LRR_8:0.00033

RC1G0110400	rc01	14418616	14420309	CC-NBS		P-loop[199-207] Kin-2[274-281] RNBS-B[304-310] GLPL[362-368]	[164-187]AAA_16:0.00012 [190-447]NB-ARC:2.5e-61
RC1G0116200	rc01	15333635	15336468	NBS-LRR		P-loop[194-202] Kin-2[270-277] RNBS-B[300-306] GLPL[361-367]	[171-446]NB-ARC:4.6e-63 [572-627]LRR_8:3.4e-05
RC1G0119600	rc01	15888685	15896466	CC-TIR-NBS-LRR		P-loop[358-366] Kin-2[433-440] RNBS-B[462-468] GLPL[523-529]	[23-193]TIR:1.8e-43 [332-612]NB-ARC:5.3e-66 [734-789]LRR_8:0.0025
RC1G0122900	rc01	16293738	16299190	NBS-LRR		P-loop[81-89] Kin-2[155-162] RNBS-B[182-188] GLPL[241-247]	[60-312]NB-ARC:7.8e-35 [501-540]LRR_4:0.0012 [541-559]LRR_4:0.0013 [605-646]LRR_4:0.00058
RC1G0123100	rc01	16303980	16307600	NBS-LRR		P-loop[34-42] Kin-2[113-120] RNBS-B[140-146] GLPL[199-205]	[17-273]NB-ARC:3.1e-35 [606-662]LRR_8:0.00016
RC1G0126400	rc01	16721193	16724833	TIR-NBS		P-loop[231-239] Kin-2[306-313] RNBS-B[333-339] GLPL[391-397]	[30-192]TIR:2.5e-44 [210-418]NB-ARC:9.7e-28
RC1G0138100	rc01	18228736	18232954	TIR-NBS-LRR		P-loop[227-235] Kin-2[302-309] RNBS-B[331-337] GLPL[389-395]	[22-187]TIR:2.2e-43 [206-477]NB-ARC:1.4e-52 [576-634]LRR_8:6.1e-06
RC1G0164900	rc01	22907764	22914556	TIR-NBS-LRR	MRP-S25,zf-RVT	P-loop[224-232] Kin-2[306-313] RNBS-B[332-338] GLPL[396-402]	[16-189]TIR:1.1e-46 [217-464]NB-ARC:6.7e-17 [584-632]MRP-S25:0.0048 [775-833]LRR_8:2.6e-05 [833-847]LRR_8:0.00033 [848-904]LRR_8:4.3e-06 [904-927]LRR_8:0.00037 [942-997]LRR_8:0.00036 [1264-1336]zf-RVT:3.6e-16
RC1G0173500	rc01	23919112	23922623	NBS-LRR		P-loop[205-213] Kin-2[278-285] RNBS-B[308-314] GLPL[367-373]	[172-194]AAA_16:0.00016 [196-454]NB-ARC:9.8e-63 [598-638]LRR_4:0.0077
RC1G0188800	rc01	25163338	25166861	CC-TIR-NBS		P-loop[262-270] Kin-2[337-344] RNBS-B[366-372] GLPL[427-433]	[2-89]TIR:1.2e-10 [235-517]NB-ARC:2.5e-68
RC1G0189200	rc01	25203533	25207311	NBS-LRR		P-loop[197-205] Kin-2[272-279] RNBS-B[301-307] GLPL[362-368]	[170-451]NB-ARC:9.7e-66 [589-643]LRR_8:0.00012 [794-825]LRR_4:0.0019
RC1G0202100	rc01	27188454	27191737	CC-NBS		P-loop[121-129] Kin-2[197-204] RNBS-B[224-230] GLPL[284-290]	[103-370]NB-ARC:3.3e-70
RC1G0212800	rc01	28792198	28806550	TIR-NBS-LRR		P-loop[234-242] Kin-2[308-315] RNBS-B[340-346] GLPL[414-420]	[24-192]TIR:1.1e-43 [222-483]NB-ARC:2.8e-22 [634-651]LRR_3:4.2e-05 [730-788]LRR_8:0.00017 [905-939]LRR_8:0.0056
RC1G0222900	rc01	30353802	30356870	CC-NBS		P-loop[186-194] Kin-2[267-274] RNBS-B[295-301] GLPL[359-365]	[164-450]NB-ARC:2e-65
RC1G0226800	rc01	30851240	30853319	NBS-LRR		P-loop[26-34] Kin-2[104-111] RNBS-B[131-137] GLPL[190-196]	[4-256]NB-ARC:2.5e-35 [408-463]LRR_8:0.001 [477-516]LRR_4:0.0044
RC1G0227400	rc01	30924069	30929646	CC-NBS-LRR		P-loop[210-218] Kin-2[285-292] RNBS-B[316-322] GLPL[378-384]	[179-200]AAA_16:0.0038 [202-445]NB-ARC:1.4e-48 [524-548]LRR_8:7.3e-07 [549-602]LRR_8:6.6e-07
RC1G0228100	rc01	31007694	31010755	CC-NBS-LRR		P-loop[197-205] Kin-2[272-279] RNBS-B[301-307] GLPL[362-368]	[171-451]NB-ARC:2.2e-65 [576-630]LRR_8:0.0063
RC1G0243000	rc01	33017453	33020902	NBS-LRR		P-loop[198-206] Kin-2[279-286] RNBS-B[307-313] GLPL[372-378]	[178-472]NB-ARC:7.6e-71
RC1G0243600	rc01	33043255	33047625	NBS		P-loop[270-278] Kin-2[351-358] RNBS-B[379-385] GLPL[444-450]	[250-544]NB-ARC:1.3e-71
RC1G0253600	rc01	34296194	34299052	NBS		P-loop[53-61] Kin-2[134-141] RNBS-B[163-169] GLPL[228-234]	[29-314]NB-ARC:6.1e-64
RC1G0255300	rc01	34455174	34458473	NBS-LRR		P-loop[197-205] Kin-2[278-285] RNBS-B[306-312] GLPL[371-377]	[174-471]NB-ARC:4.5e-67 [583-624]LRR_8:0.0071
RC1G0256100	rc01	34528453	34531707	NBS		P-loop[197-205] Kin-2[278-285] RNBS-B[306-312] GLPL[371-377]	[175-472]NB-ARC:8e-74
RC1G0256400	rc01	34538433	34541505	NBS		P-loop[197-205] Kin-2[278-285] RNBS-B[306-312] GLPL[371-377]	[173-471]NB-ARC:1.3e-66

RC1G0257500	rc01	34582155	34588844	NBS	P-loop[200-208] Kin-2[281-288] RNBS-B[309-315] GLPL[374-380]	[177-475]NB-ARC:5.7e-70
RC1G0258100	rc01	34682821	34686034	NBS	P-loop[168-176] Kin-2[249-256] RNBS-B[277-283] GLPL[342-348]	[146-443]NB-ARC:2.4e-70
RC1G0258500	rc01	34709625	34713095	NBS-LRR	P-loop[198-206] Kin-2[279-286] RNBS-B[307-313] GLPL[369-375]	[175-470]NB-ARC:1e-70 [803-834]LRR_4:0.0045
RC1G0260000	rc01	34855716	34858966	CC-NBS-LRR	P-loop[198-206] Kin-2[273-280] RNBS-B[302-308] GLPL[363-369]	[173-453]NB-ARC:1.5e-61 [573-624]LRR_8:5.5e-05
RC1G0260300	rc01	34910010	34911008	NBS	P-loop[63-71] Kin-2[138-145] RNBS-B[167-173] GLPL[228-234]	[40-305]NB-ARC:1.8e-63
RC1G0260800	rc01	34935325	34938804	CC-NBS-LRR	P-loop[260-268] Kin-2[335-342] RNBS-B[364-370] GLPL[425-431]	[234-516]NB-ARC:9.1e-64 [658-698]LRR_8:2.8e-05
RC1G0261200	rc01	34977136	34979891	NBS-LRR	P-loop[106-114] Kin-2[181-188] RNBS-B[210-216] GLPL[271-277]	[84-360]NB-ARC:9.7e-65 [476-530]LRR_8:9.5e-07 [530-553]LRR_4:0.0097
RC1G0261500	rc01	34992791	34995628	CC-NBS-LRR	P-loop[197-205] Kin-2[272-279] RNBS-B[301-307] GLPL[362-368]	[171-452]NB-ARC:6.2e-65 [570-624]LRR_8:2.9e-05 [624-653]LRR_4:0.00081
RC1G0263800	rc01	35482052	35484165	NBS-LRR	P-loop[1-8] Kin-2[75-82] RNBS-B[104-110] GLPL[165-171]	[1-254]NB-ARC:1.3e-61 [376-430]LRR_8:1.9e-06
RC1G0266700	rc01	35983205	35987660	TIR-NBS-LRR	P-loop[219-227] Kin-2[298-305] RNBS-B[325-331] GLPL[384-390]	[17-180]TIR:1.4e-45 [197-447]NB-ARC:1.8e-30 [611-666]LRR_8:0.00052 [769-808]LRR_8:0.00026
RC1G0267700	rc01	36085877	36095663	NBS-LRR	P-loop[1-8] Kin-2[79-86] RNBS-B[106-112] GLPL[165-171]	[1-227]NB-ARC:1.1e-28 [541-597]LRR_8:2.6e-05
RC1G0274300	rc01	37005938	37008680	NBS-LRR	P-loop[157-165] Kin-2[232-239] RNBS-B[261-267] GLPL[324-330]	[134-414]NB-ARC:8e-65 [537-575]LRR_4:0.00013 [576-594]LRR_8:0.00095
RC1G0274700	rc01	37056770	37059016	NBS-LRR	P-loop[64-72] Kin-2[139-146] RNBS-B[168-174] GLPL[229-235]	[41-319]NB-ARC:1.4e-57 [439-494]LRR_8:3.6e-05
RC1G0276600	rc01	37308983	37312698	CC-TIR-NBS-LRR	P-loop[360-368] Kin-2[435-442] RNBS-B[464-470] GLPL[525-531]	[23-193]TIR:5.6e-46 [329-350]AAA_16:0.0018 [351-617]NB-ARC:3.9e-68 [739-752]LRR_4:0.0075 [753-795]LRR_8:0.0023
RC1G0277100	rc01	37347001	37349814	NBS-LRR	P-loop[194-202] Kin-2[278-285] RNBS-B[305-311] GLPL[369-375]	[171-462]NB-ARC:2.5e-87 [580-636]LRR_8:0.0023 [848-888]LRR_4:0.0039
RC1G0279800	rc01	37721000	37724162	TIR-NBS-LRR	P-loop[228-236] Kin-2[307-314] RNBS-B[334-340] GLPL[393-399]	[23-188]TIR:6.8e-47 [204-457]NB-ARC:3e-30 [621-676]LRR_8:7.5e-05 [677-724]LRR_8:0.00036
RC1G0280200	rc01	37745457	37750723	TIR-NBS-LRR	P-loop[228-236] Kin-2[307-314] RNBS-B[334-340] GLPL[393-399]	[24-188]TIR:4.1e-44 [207-456]NB-ARC:5.1e-30 [621-639]LRR_3:0.0072 [779-830]LRR_8:0.00025
RC1G0280400	rc01	37798453	37800765	TIR-NBS-LRR	P-loop[128-136] Kin-2[207-214] RNBS-B[234-240] GLPL[293-299]	[2-87]TIR:1.9e-15 [104-356]NB-ARC:1.6e-33 [520-576]LRR_8:8.1e-05
RC1G0280700	rc01	37844788	37848991	TIR-NBS-LRR	P-loop[226-234] Kin-2[305-312] RNBS-B[332-338] GLPL[391-397]	[22-183]TIR:8.7e-47 [202-456]NB-ARC:1.9e-33 [610-628]LRR_3:7.8e-05
RC1G0280900	rc01	37882803	37884682	TIR-NBS	P-loop[226-234] Kin-2[305-312] RNBS-B[332-338] GLPL[391-397]	[22-183]TIR:1.3e-45 [202-457]NB-ARC:5.3e-34
RC1G0281100	rc01	37889095	37900487	NBS-LRR	P-loop[65-73] Kin-2[144-151] RNBS-B[171-177] GLPL[230-236]	[43-295]NB-ARC:3.7e-30 [611-666]LRR_8:2.2e-07
RC1G0281700	rc01	37955383	37958948	CC-NBS-LRR	P-loop[180-188] Kin-2[255-262] RNBS-B[284-290] GLPL[346-352]	[154-435]NB-ARC:3.6e-62 [554-609]LRR_8:1.4e-05 [610-638]LRR_4:0.00029 [971-1024]LRR_8:0.0023
RC1G0282300	rc01	38053236	38056766	CC-NBS-LRR	P-loop[180-188] Kin-2[255-262] RNBS-B[284-290] GLPL[346-352]	[156-434]NB-ARC:2.2e-62 [554-609]LRR_8:1.5e-05 [610-

						637]LRR_4:0.00038 [972-1025]LRR_8:0.0039
RC1G0283400	rc01	38244919	38248918	NBS-LRR	P-loop[65-73] Kin-2[144-151] RNBS-B[171-177] GLPL[230-236]	[41-298]NB-ARC:1.6e-30 [459-478]LRR_3:0.0042 [616-670]LRR_8:0.00028
RC1G0288000	rc01	38848444	38859425	TIR-NBS-LRR	P-loop[218-226] Kin-2[296-303] RNBS-B[323-329] GLPL[379-385]	[14-192]TIR:1.1e-47 [193-207]AAA_16:0.0028 [208-446]NB-ARC:3.6e-24 [613-628]LRR_3:0.00089 [654-711]LRR_8:0.0042 [931-987]LRR_8:8.9e-07
RC1G0288100	rc01	38900986	38908393	NBS-LRR	P-loop[26-34] Kin-2[103-110] RNBS-B[130-136] GLPL[186-192]	[5-257]NB-ARC:1.4e-34 [557-579]LRR_4:0.0099 [580-636]LRR_8:0.0078 [651-689]LRR_4:0.0045 [821-875]LRR_8:7e-06
RC1G0292300	rc01	39326948	39330621	CC-NBS-LRR	P-loop[193-201] Kin-2[268-275] RNBS-B[297-303] GLPL[359-365]	[182-449]NB-ARC:2.2e-66 [573-628]LRR_8:6.5e-07
RC1G0300200	rc01	40223859	40231796	NBS-LRR	P-loop[202-210] Kin-2[277-284] RNBS-B[308-314] GLPL[369-375]	[190-458]NB-ARC:6.1e-55 [838-898]LRR_8:0.00016 [1009-1134]LRR_5:4.9e-05
RC1G0329000	rc01	43472577	43474189	TIR-NBS	P-loop[225-233] Kin-2[300-307] RNBS-B[329-335] GLPL[387-393]	[20-182]TIR:2.6e-43 [204-412]NB-ARC:6.6e-40
RC1G0358000	rc01	45960816	45969304	NBS	P-loop[171-179] Kin-2[245-252] RNBS-B[269-275] GLPL[328-334]	[151-415]NB-ARC:1.3e-43
RC1G0363100	rc01	46493639	46504568	NBS-LRR	P-loop[194-202] Kin-2[275-282] RNBS-B[303-309] GLPL[368-374]	[174-467]NB-ARC:7.2e-69 [621-673]LRR_8:0.00042
RC1G0367100	rc01	46770348	46773547	NBS-LRR	P-loop[194-202] Kin-2[275-282] RNBS-B[303-309] GLPL[370-376]	[174-470]NB-ARC:2.8e-69 [767-822]LRR_8:0.0085
RC1G0400700	rc01	50256161	50257511	CC-NBS	P-loop[188-196] Kin-2[265-272] RNBS-B[294-300] GLPL[355-361]	[156-174]AAA_16:0.0039 [175-435]NB-ARC:5e-63
RC1G0404100	rc01	50508504	50510713	NBS-LRR	P-loop[1-8] Kin-2[76-83] RNBS-B[103-109] GLPL[162-163]	[1-229]NB-ARC:1.4e-23
RC1G0435000	rc01	53058281	53067880	TIR-NBS-LRR	P-loop[224-232] Kin-2[283-290] RNBS-B[310-316] GLPL[369-375]	[18-198]TIR:2.1e-47 [203-435]NB-ARC:2e-30 [587-642]LRR_8:0.0055
RC1G0441100	rc01	53471786	53475028	CC-NBS-LRR	P-loop[208-216] Kin-2[285-292] RNBS-B[314-320] GLPL[375-381]	[176-188]AAA_16:0.0056 [189-463]NB-ARC:4.3e-65 [587-642]LRR_8:3.2e-05
RC1G0454600	rc01	54629504	54632323	CC-NBS-LRR	P-loop[206-214] Kin-2[283-290] RNBS-B[312-318] GLPL[373-379]	[174-184]AAA_16:0.00039 [186-459]NB-ARC:3.9e-64 [597-645]LRR_8:0.00017
RC1G0454800	rc01	54650760	54654953	CC-NBS-LRR	P-loop[206-214] Kin-2[283-290] RNBS-B[312-318] GLPL[373-379]	[174-186]AAA_16:6.2e-05 [187-461]NB-ARC:6.8e-65 [560-578]LRR_4:0.002 [587-627]LRR_4:0.00024
RC1G0461500	rc01	55237811	55240714	CC-NBS-LRR	P-loop[212-220] Kin-2[289-296] RNBS-B[318-324] GLPL[380-386]	[180-198]AAA_16:0.00011 [199-467]NB-ARC:9.4e-64 [620-660]LRR_4:1.3e-05 [669-708]LRR_4:0.00022
RC1G0497200	rc01	57900419	57903163	NBS-LRR	P-loop[26-34] Kin-2[104-111] RNBS-B[131-137] GLPL[188-194]	[3-254]NB-ARC:2.8e-29 [430-449]LRR_3:2e-05 [499-540]LRR_4:0.00028 [673-727]LRR_8:2.4e-05
RC1G0497800	rc01	57955390	57958437	NBS-LRR	P-loop[26-34] Kin-2[104-111] RNBS-B[131-137] GLPL[188-194]	[3-255]NB-ARC:2.3e-30 [430-449]LRR_3:3e-07 [674-728]LRR_8:1.7e-06
RC1G0510300	rc01	58639792	58643017	NBS-LRR	P-loop[199-207] Kin-2[274-281] RNBS-B[304-310] GLPL[362-368]	[164-187]AAA_16:1.8e-05 [190-451]NB-ARC:1.5e-61 [566-576]LRR_8:0.00018 [577-616]LRR_4:3.8e-05 [617-651]LRR_8:6.2e-05

RC1G0519100	rc01	59266796	59269332	NBS-LRR		P-loop[199-207] Kin-2[274-281] RNBS-B[304-310] GLPL[362-368]	[188-450]NB-ARC:2.2e-62 [556-569]LRR_8:0.00024 [570-624]LRR_8:1.1e-05 [624-643]LRR_8:0.0068
RC1G0522300	rc01	59490811	59493714	NBS-LRR		P-loop[213-221] Kin-2[295-302] RNBS-B[322-328] GLPL[388-394]	[203-481]NB-ARC:7.5e-77 [601-654]LRR_8:0.0052
RC1G0528100	rc01	59873875	59875920	TIR-NBS		P-loop[218-226] Kin-2[295-302] RNBS-B[322-328] GLPL[379-385]	[14-192]TIR:2.1e-47 [195-442]NB-ARC:1.3e-32
RC1G0528400	rc01	59891985	59893200	NBS		P-loop[19-27] Kin-2[96-103] RNBS-B[123-129] GLPL[180-186]	[5-238]NB-ARC:9.3e-33
RC1G0528700	rc01	59911621	59918597	TIR-NBS-LRR	WRKY	P-loop[222-230] Kin-2[300-307] RNBS-B[327-333] GLPL[384-390]	[18-183]TIR:3.6e-44 [203-451]NB-ARC:1.6e-25 [618-637]LRR_3:4.4e-07 [687-724]LRR_4:0.00096 [725-767]LRR_8:0.0075 [863-915]LRR_8:1.1e-06 [915-925]LRR_4:0.0054 [1275-1335]WRKY:1.3e-23
RC1G0528900	rc01	59925434	59933238	TIR-NBS-LRR		P-loop[1131-1139] Kin-2[1209-1216] RNBS-B[1236-1242] GLPL[1291-1292]	[18-197]TIR:1.1e-39 [201-446]NB-ARC:2.9e-28 [618-637]LRR_3:0.00013 [1107-1316]NB-ARC:4.4e-18 [1511-1530]LRR_3:3.7e-05 [1580-1623]LRR_4:0.0019 [1629-1684]LRR_8:0.00084
RC1G0579300	rc01	63596322	63598477	TIR-NBS		P-loop[124-132] Kin-2[202-209] RNBS-B[229-235] GLPL[288-294]	[4-98]TIR:2e-13 [104-357]NB-ARC:4e-38
RC1G0579500	rc01	63622337	63626256	TIR-NBS-LRR		P-loop[124-132] Kin-2[203-210] RNBS-B[230-236] GLPL[289-295]	[4-86]TIR:2.9e-12 [102-360]NB-ARC:3.2e-37 [503-558]LRR_8:0.00041 [685-727]LRR_4:0.0079
RC1G0581100	rc01	63702553	63706461	CC-TIR-NBS-LRR		P-loop[224-232] Kin-2[302-309] RNBS-B[329-335] GLPL[388-394]	[18-197]TIR:3.9e-50 [206-455]NB-ARC:2.9e-35 [604-659]LRR_8:0.0039
RC1G0581200	rc01	63709713	63715148	NBS-LRR		P-loop[26-34] Kin-2[105-112] RNBS-B[132-138] GLPL[191-197]	[4-254]NB-ARC:1.8e-38 [408-463]LRR_8:0.00074
RC2G0007300	rc02	645051	661704	CC-NBS-LRR	TniB	P-loop[176-184] Kin-2[253-260] RNBS-B[277-283] GLPL[337-343]	[157-424]NB-ARC:8.9e-42 [1272-1282]TniB:0.0021 [1283-1554]NB-ARC:1e-42 [1671-1715]LRR_8:0.0054 [1727-1784]LRR_8:0.0018
RC2G0007700	rc02	674151	678665	CC-NBS-LRR	TniB	P-loop[185-193] Kin-2[265-272] RNBS-B[289-295] GLPL[347-353]	[156-166]TniB:0.0043 [167-426]NB-ARC:1.8e-48 [608-663]LRR_8:0.0011
RC2G0134700	rc02	11227056	11230506	TIR-NBS-LRR		P-loop[226-234] Kin-2[300-307] RNBS-B[327-333] GLPL[386-392]	[20-200]TIR:5.5e-47 [211-454]NB-ARC:7.4e-36
RC2G0148100	rc02	12333147	12335759	NBS	RPW8	P-loop[208-216] Kin-2[282-289] RNBS-B[310-316] GLPL[374-380]	[23-98]RPW8:0.0034 [185-465]NB-ARC:1.3e-89
RC2G0151500	rc02	12581369	12586323	NBS-LRR		P-loop[135-143] Kin-2[212-219] RNBS-B[239-245] GLPL[300-306]	[107-125]AAA_16:0.00053 [126-367]NB-ARC:3.1e-29 [518-536]LRR_3:1.5e-05 [610-667]LRR_8:6.9e-06 [765-822]LRR_8:0.0028
RC2G0155400	rc02	12912578	12916217	CC-NBS-LRR		P-loop[193-201] Kin-2[275-282] RNBS-B[302-308] GLPL[365-371]	[170-457]NB-ARC:1.8e-78 [574-630]LRR_8:1.6e-06 [631-647]LRR_8:0.00012
RC2G0179100	rc02	15325681	15329889	NBS-LRR	RPW8	P-loop[219-227] Kin-2[298-305] RNBS-B[324-330] GLPL[380-386]	[3-136]RPW8:6e-24 [199-467]NB-ARC:9.4e-37
RC2G0179200	rc02	15342873	15347295	NBS-LRR	RPW8	P-loop[203-211] Kin-2[281-288] RNBS-B[307-313] GLPL[362-368]	[3-136]RPW8:3.2e-30 [183-447]NB-ARC:1.9e-25 [710-766]LRR_8:0.0032
RC2G0179300	rc02	15385324	15390125	NBS	RPW8	P-loop[239-247] Kin-2[318-325] RNBS-B[344-350] GLPL[396-402]	[21-157]RPW8:3.5e-31 [219-483]NB-ARC:7.5e-33
RC2G0179400	rc02	15392613	15396430	NBS-LRR	RPW8	P-loop[214-222] Kin-2[293-300] RNBS-B[319-325] GLPL[371-377]	[1-132]RPW8:3.5e-26 [194-457]NB-ARC:1.5e-34

RC2G0179500	rc02	15397426	15402277	NBS	RPW8	P-loop[215-223] Kin-2[294-301] RNBS-B[320-325] GLPL[374-380]	[6-137]RPW8:1e-23 [201-462]NB-ARC:2.9e-30
RC2G0179600	rc02	15402279	15405360	NBS-LRR		P-loop[54-62] Kin-2[134-141] RNBS-B[160-166] GLPL[215-221]	[38-302]NB-ARC:5.6e-27 [540-592]LRR_8:0.0028
RC2G0179800	rc02	15434947	15438315	CC-NBS-LRR	RPW8,Vps53_N	P-loop[231-239] Kin-2[310-317] RNBS-B[335-341] GLPL[389-395]	[5-140]RPW8:4.6e-28 [141-162]Vps53_N:0.0028 [211-475]NB-ARC:3.4e-33 [741-798]LRR_8:5.6e-05
RC2G0180500	rc02	15481969	15485440	CC-NBS-LRR	RPW8	P-loop[230-238] Kin-2[309-316] RNBS-B[334-340] GLPL[388-394]	[5-140]RPW8:1e-26 [210-474]NB-ARC:1.1e-31 [740-797]LRR_8:0.00019
RC2G0180800	rc02	15510723	15513360	CC-NBS	RPW8	P-loop[227-235] Kin-2[306-313] RNBS-B[331-337] GLPL[390-396]	[6-140]RPW8:3e-27 [207-476]NB-ARC:2.7e-30
RC2G0181000	rc02	15515501	15519519	NBS	RPW8	P-loop[213-221] Kin-2[290-297] RNBS-B[317-323] GLPL[372-378]	[8-133]RPW8:8.6e-22 [191-458]NB-ARC:7.2e-36
RC2G0181200	rc02	15537972	15543128	NBS-LRR	RPW8	P-loop[194-202] Kin-2[273-280] RNBS-B[299-305] GLPL[354-360]	[5-139]RPW8:1.4e-24 [175-441]NB-ARC:8.1e-35 [682-737]LRR_8:0.0017
RC2G0181300	rc02	15551313	15554880	CC-NBS	RPW8	P-loop[161-169] Kin-2[240-247] RNBS-B[266-272] GLPL[321-327]	[1-103]RPW8:1.4e-17 [142-407]NB-ARC:1.1e-32
RC2G0181700	rc02	15566602	15570265	CC-NBS	RPW8	P-loop[166-174] Kin-2[245-252] RNBS-B[271-277] GLPL[326-332]	[3-106]RPW8:3.9e-17 [149-412]NB-ARC:1.3e-31
RC2G0181800	rc02	15571593	15574784	NBS-LRR	RPW8	P-loop[199-207] Kin-2[278-285] RNBS-B[306-312] GLPL[361-367]	[11-121]RPW8:1.8e-19 [173-187]AAA_16:0.00063 [188-447]NB-ARC:1.6e-26 [699-746]LRR_8:0.0057 [747-787]LRR_4:0.0016
RC2G0183000	rc02	15720908	15732328	CC-NBS-LRR	RPW8,Pkinase_Tyr	P-loop[417-425] Kin-2[481-488] RNBS-B[507-513] GLPL[562-568]	[5-138]RPW8:6.5e-13 [183-310]RPW8:1.9e-19 [399-648]NB-ARC:4.3e-25 [887-945]LRR_8:0.0039 [1167-1476]Pkinase_Tyr:4.4e-35 [1558-1837]Pkinase_Tyr:1.2e-45
RC2G0184000	rc02	15816412	15826862	CC-NBS-LRR	RPW8,zf-CCCH	P-loop[519-527] Kin-2[598-605] RNBS-B[623-629] GLPL[678-684]	[12-144]RPW8:3.2e-12 [211-328]RPW8:6.9e-22 [439-463]zf-CCCH:2.9e-08 [498-763]NB-ARC:2.3e-41 [1015-1072]LRR_8:7.1e-05
RC2G0184100	rc02	15828907	15835140	NBS	RPW8,Peptidase_C48	P-loop[196-204] Kin-2[275-282] RNBS-B[300-306] GLPL[355-361]	[6-140]RPW8:2.1e-33 [176-442]NB-ARC:1e-24 [1024-1231]Peptidase_C48:6e-30
RC2G0199900	rc02	17674833	17684919	TIR-NBS-LRR		P-loop[260-268] Kin-2[334-341] RNBS-B[365-371] GLPL[426-432]	[56-227]TIR:2.8e-48 [232-241]AAA_16:0.0094 [242-491]NB-ARC:9.8e-33 [894-950]LRR_8:1.2e-05 [1017-1054]LRR_4:3.1e-05 [1152-1204]LRR_8:0.00093 [1244-1280]LRR_8:3.3e-07 [1281-1313]LRR_4:0.00036 [1314-1324]LRR_8:0.0028
RC2G0200100	rc02	17703046	17710202	TIR-NBS-LRR		P-loop[227-235] Kin-2[301-308] RNBS-B[332-338] GLPL[393-399]	[23-194]TIR:4.7e-47 [208-466]NB-ARC:9.1e-33 [716-774]LRR_8:0.0053 [985-1022]LRR_4:0.0007 [1120-1173]LRR_8:0.0011 [1190-1249]LRR_8:5.5e-09 [1250-1282]LRR_4:0.00017 [1283-1293]LRR_8:0.0023

RC2G0200200	rc02	17718777	17727816	TIR-NBS-LRR	P-loop[227-235] Kin-2[305-312] RNBS-B[336-342] GLPL[395-401]	[23-194]TIR:7.8e-49 [205-467]NB-ARC:5e-31 [632-647]LRR_3:0.0018 [891-926]LRR_8:0.0065 [1011-1048]LRR_4:0.00013 [1219-1241]LRR_8:2.6e-06 [1242-1300]LRR_8:6e-12 [1301-1323]LRR_8:2.8e-10 [1324-1333]LRR_8:1.1e-06 [1334-1392]LRR_8:1.7e-09 [1393-1402]LRR_8:2.6e-09 [1403-1448]LRR_8:6e-10 [1449-1507]LRR_8:5.5e-11 [1511-1552]LRR_8:1.6e-05
RC2G0210900	rc02	18878750	18883160	NBS-LRR	P-loop[202-210] Kin-2[277-284] RNBS-B[308-314] GLPL[369-375]	[177-459]NB-ARC:2.8e-63 [562-572]LRR_8:0.0051 [573-629]LRR_8:0.00097 [1120-1159]LRR_4:0.0016
RC2G0219600	rc02	19753419	19761438	NBS-LRR	P-loop[86-94] Kin-2[164-171] RNBS-B[188-194] GLPL[247-253]	[67-333]NB-ARC:5.3e-50 [499-555]LRR_8:0.0016
RC2G0244600	rc02	22875094	22883763	NBS-LRR	P-loop[173-181] Kin-2[250-257] RNBS-B[274-280] GLPL[333-339]	[151-403]NB-ARC:8.4e-36 [591-628]LRR_8:0.0044 [628-652]LRR_8:0.0072
RC2G0255900	rc02	24654280	24655778	NBS	P-loop[178-186] Kin-2[260-267] RNBS-B[288-294] GLPL[343-349]	[148-167]AAA_16:0.0089 [168-355]NB-ARC:4.8e-24
RC2G0285900	rc02	28438869	28441360	CC-NBS-LRR	P-loop[206-214] Kin-2[281-288] RNBS-B[315-321] GLPL[376-382]	[180-464]NB-ARC:5e-59 [584-640]LRR_8:0.00054
RC2G0294800	rc02	29720246	29724405	CC-NBS-LRR	P-loop[270-278] Kin-2[346-353] RNBS-B[375-381] GLPL[437-443]	[254-525]NB-ARC:2.2e-69 [630-649]LRR_8:5.1e-07 [650-705]LRR_8:2.7e-09
RC2G0314400	rc02	32812925	32817044	NBS-LRR	P-loop[206-214] Kin-2[281-288] RNBS-B[315-321] GLPL[376-382]	[180-463]NB-ARC:3.5e-57 [585-639]LRR_8:0.0043
RC2G0318800	rc02	33687657	33689879	NBS-LRR	P-loop[54-62] Kin-2[131-138] RNBS-B[159-165] GLPL[215-221]	[30-306]NB-ARC:8.6e-43 [467-522]LRR_8:5.4e-08
RC2G0319100	rc02	33716915	33720694	CC-NBS-LRR	P-loop[549-557] Kin-2[629-636] RNBS-B[656-662] GLPL[716-722]	[524-803]NB-ARC:3.9e-42 [958-1013]LRR_8:6.1e-05
RC2G0350400	rc02	39412156	39414798	CC-NBS-LRR	P-loop[206-214] Kin-2[281-288] RNBS-B[315-321] GLPL[376-382]	[173-194]AAA_16:0.0035 [195-464]NB-ARC:3.5e-56 [584-638]LRR_8:9.6e-06
RC2G0350700	rc02	39441734	39444415	NBS-LRR	P-loop[206-214] Kin-2[281-288] RNBS-B[315-321] GLPL[376-382]	[178-461]NB-ARC:2.8e-57 [617-655]LRR_4:0.0011
RC2G0356300	rc02	39969343	39973621	NBS-LRR	P-loop[206-214] Kin-2[281-288] RNBS-B[315-321] GLPL[376-382]	[178-462]NB-ARC:4.9e-57 [195-462]NB-ARC:7.7e-56 [584-605]LRR_8:0.0033 [606-645]LRR_4:0.0013
RC2G0358600	rc02	40163047	40168495	NBS-LRR	P-loop[206-214] Kin-2[281-288] RNBS-B[315-321] GLPL[376-382]	[185-462]NB-ARC:5.4e-63 [562-618]LRR_8:1.1e-08 [625-641]LRR_8:0.00058
RC2G0389900	rc02	44543234	44548635	CC-NBS-LRR	P-loop[208-216] Kin-2[283-290] RNBS-B[312-318] GLPL[375-381]	[185-464]NB-ARC:1.3e-64 [568-590]LRR_8:7.4e-07 [591-647]LRR_8:1.6e-07 [788-841]LRR_8:0.0055
RC2G0392700	rc02	44882897	44887968	CC-NBS-LRR	P-loop[208-216] Kin-2[283-290] RNBS-B[312-318] GLPL[375-381]	[174-451]NB-ARC:1.3e-60 [184-464]NB-ARC:7.1e-62 [562-584]LRR_8:1.2e-07 [585-641]LRR_8:7.5e-08
RC2G0394600	rc02	45176707	45181083	NBS	P-loop[198-206] Kin-2[275-282] RNBS-B[305-311] GLPL[366-372]	[1-239]NB-ARC:9.4e-43 [347-396]LRR_8:3.2e-07
RC2G0400800	rc02	46012932	46015626	CC-NBS-LRR	P-loop[208-216] Kin-2[283-290] RNBS-B[312-318] GLPL[375-381]	
RC2G0401500	rc02	46046182	46047530	NBS-LRR	P-loop[1-8] Kin-2[75-82] RNBS-B[104-110] GLPL[167-173]	

RC2G0401600	rc02	46049909	46052803	CC-NBS-LRR		P-loop[208-216] Kin-2[283-290] RNBS-B[312-318] GLPL[375-381]	[184-464]NB-ARC:1.6e-60 [562-584]LRR_8:9.4e-07 [585-641]LRR_8:4.1e-08 [780-833]LRR_8:0.0092
RC2G0401900	rc02	46068087	46070552	NBS-LRR		P-loop[113-121] Kin-2[188-195] RNBS-B[217-223] GLPL[280-286]	[85-367]NB-ARC:4.7e-63 [490-544]LRR_8:1e-08
RC2G0402100	rc02	46079724	46083075	CC-NBS-LRR		P-loop[208-216] Kin-2[283-290] RNBS-B[312-318] GLPL[375-381]	[177-189]AAA_16:0.00095 [190-464]NB-ARC:1.8e-63 [562-584]LRR_8:1.5e-07 [585-640]LRR_8:1.2e-07
RC2G0402400	rc02	46117552	46120801	CC-NBS-LRR		P-loop[208-216] Kin-2[283-290] RNBS-B[312-318] GLPL[375-381]	[186-465]NB-ARC:7.1e-62 [562-584]LRR_8:1.5e-07 [585-641]LRR_8:5.9e-08
RC2G0403100	rc02	46146324	46149074	CC-NBS-LRR		P-loop[208-216] Kin-2[284-291] RNBS-B[313-319] GLPL[376-382]	[185-463]NB-ARC:7.5e-62
RC2G0404000	rc02	46210483	46212510	NBS-LRR		P-loop[1-8] Kin-2[75-82] RNBS-B[104-110] GLPL[167-173]	[1-255]NB-ARC:1.3e-56 [354-376]LRR_8:2.9e-07 [377-433]LRR_8:1e-07
RC2G0422900	rc02	49299023	49302923	CC-NBS-LRR	CSD	P-loop[215-223] Kin-2[292-299] RNBS-B[321-327] GLPL[384-390]	[186-472]NB-ARC:7.2e-62 [567-623]LRR_8:2e-07 [631-654]LRR_4:0.00062 [1004-1069]CSD:7.6e-24
RC2G0424700	rc02	49551738	49556053	CC-NBS		P-loop[208-216] Kin-2[284-291] RNBS-B[313-319] GLPL[375-381]	[191-463]NB-ARC:8.4e-70
RC2G0425100	rc02	49561390	49564576	CC-NBS-LRR		P-loop[200-208] Kin-2[276-283] RNBS-B[305-311] GLPL[368-374]	[179-455]NB-ARC:1.7e-63 [564-580]LRR_8:9.5e-06 [581-633]LRR_8:3.2e-07 [634-659]LRR_8:0.0019
RC2G0428200	rc02	49894772	49895982	CC-NBS		P-loop[203-211] Kin-2[279-286] RNBS-B[308-314] GLPL[371-377]	[171-181]AAA_16:0.0028 [182-386]NB-ARC:7e-45
RC2G0428600	rc02	49927478	49934703	CC-NBS-LRR		P-loop[209-217] Kin-2[285-292] RNBS-B[314-320] GLPL[376-382]	[192-466]NB-ARC:3.4e-71 [587-642]LRR_8:1.4e-08 [657-697]LRR_4:0.0098
RC2G0428800	rc02	49938166	49940232	CC-NBS-LRR		P-loop[216-224] Kin-2[292-299] RNBS-B[322-328] GLPL[384-390]	[199-472]NB-ARC:4.3e-64 [577-626]LRR_8:1.7e-07 [627-647]LRR_8:1.9e-07 [656-671]LRR_8:0.0036
RC2G0429900	rc02	50004991	50007661	CC-NBS-LRR		P-loop[210-218] Kin-2[286-293] RNBS-B[315-321] GLPL[377-383]	[194-465]NB-ARC:2.6e-69 [588-643]LRR_8:6.7e-08
RC2G0430300	rc02	50021196	50024246	CC-NBS-LRR		P-loop[210-218] Kin-2[286-293] RNBS-B[315-321] GLPL[377-383]	[194-465]NB-ARC:3.5e-69 [588-643]LRR_8:8e-08
RC2G0431500	rc02	50128154	50130890	NBS-LRR		P-loop[198-206] Kin-2[280-287] RNBS-B[307-313] GLPL[371-377]	[176-463]NB-ARC:9.6e-83 [557-608]LRR_8:0.00031 [609-630]LRR_8:0.0021
RC2G0432000	rc02	50213957	50215216	NBS		P-loop[18-26] Kin-2[100-107] RNBS-B[127-133] GLPL[191-197]	[5-245]NB-ARC:3.5e-61
RC2G0439500	rc02	51259407	51261938	NBS-LRR		P-loop[134-142] Kin-2[214-221] RNBS-B[243-249] GLPL[306-312]	[105-395]NB-ARC:6.5e-60 [497-543]LRR_8:3.1e-06 [544-562]LRR_8:1.2e-05
RC2G0441000	rc02	51485056	51489326	NBS-LRR		P-loop[194-200] Kin-2[271-278] RNBS-B[300-306] GLPL[359-365]	[184-448]NB-ARC:2.3e-59 [553-562]LRR_8:0.00013 [563-617]LRR_8:1.6e-05 [766-796]LRR_4:0.0049
RC2G0446800	rc02	52027088	52029827	CC-NBS-LRR		P-loop[182-190] Kin-2[260-267] RNBS-B[287-293] GLPL[347-353]	[160-437]NB-ARC:3.9e-87 [518-535]LRR_9:0.0018 [536-594]LRR_8:1.1e-11 [595-624]LRR_4:0.00018
RC2G0474400	rc02	55058308	55061000	CC-NBS-LRR		P-loop[214-222] Kin-2[287-294] RNBS-B[316-322] GLPL[378-384]	[181-203]AAA_16:9.6e-05 [204-467]NB-ARC:1.3e-60 [564-588]LRR_8:2.8e-05 [589-644]LRR_8:2.6e-06 [644-668]LRR_8:0.00052 [778-813]LRR_8:0.00043
RC2G0474900	rc02	55134538	55137227	CC-NBS-LRR		P-loop[215-223] Kin-2[288-295] RNBS-B[317-323] GLPL[379-385]	[182-201]AAA_16:0.00062 [202-468]NB-ARC:2.3e-59 [593-648]LRR_8:5.6e-06 [648-670]LRR_8:0.0023

RC2G0506600	rc02	58862239	58866940	NBS	DAGK_acc	P-loop[18-26] Kin-2[107-114] RNBS-B[148-154] GLPL[221-227]	[11-247]NB-ARC:8.8e-20 [513-617]DAGK_acc:1.2e-10
RC2G0506700	rc02	58868511	58869206	NBS		P-loop[1-8] Kin-2[90-97] RNBS-B[131-137] GLPL[202-208]	[1-221]NB-ARC:3e-19
RC2G0534600	rc02	61705745	61710532	NBS		P-loop[1-8] Kin-2[89-96] RNBS-B[118-124] GLPL[180-186]	[1-268]NB-ARC:6.1e-57
RC2G0587100	rc02	66525159	66528095	CC-NBS-LRR		P-loop[217-225] Kin-2[294-301] RNBS-B[325-331] GLPL[387-393]	[189-476]NB-ARC:7.9e-64 [574-608]LRR_8:0.0082 [610-651]LRR_8:0.0058
RC2G0588700	rc02	66625748	66630124	CC-NBS-LRR		P-loop[216-224] Kin-2[293-300] RNBS-B[324-330] GLPL[385-391]	[188-474]NB-ARC:1.3e-60 [572-629]LRR_8:2.1e-07 [629-653]LRR_8:0.0015
RC2G0589000	rc02	66647790	66651098	CC-NBS-LRR		P-loop[215-223] Kin-2[292-299] RNBS-B[323-329] GLPL[385-391]	[191-474]NB-ARC:7.7e-63 [574-631]LRR_8:1.2e-08 [631-652]LRR_8:2e-07
RC2G0620500	rc02	69511698	69514439	NBS-LRR		P-loop[185-193] Kin-2[258-265] RNBS-B[284-290] GLPL[346-352]	[163-430]NB-ARC:2.5e-51
RC2G0620800	rc02	69557522	69560264	NBS-LRR		P-loop[185-193] Kin-2[258-265] RNBS-B[284-290] GLPL[346-352]	[163-430]NB-ARC:2.4e-51
RC3G0032000	rc03	6974322	6978370	NBS-LRR		P-loop[205-213] Kin-2[280-287] RNBS-B[311-317] GLPL[372-378]	[177-459]NB-ARC:6.1e-61 [539-575]LRR_4:0.0021
RC3G0032300	rc03	7001366	7009066	NBS		P-loop[205-213] Kin-2[280-287] RNBS-B[311-317] GLPL[372-378]	[177-378]NB-ARC:1.3e-42
RC3G0034200	rc03	7189856	7196786	NBS-LRR		P-loop[205-213] Kin-2[280-287] RNBS-B[311-317] GLPL[372-378]	[177-459]NB-ARC:8.2e-61 [539-574]LRR_4:0.0035 [843-903]LRR_8:0.00019
RC3G0042600	rc03	8370125	8377814	TIR-NBS-LRR		P-loop[181-189] Kin-2[260-267] RNBS-B[287-293] GLPL[346-352]	[24-71]TIR:4.5e-10 [72-141]TIR:0.0014 [157-411]NB-ARC:4.7e-33 [706-738]LRR_8:0.00025
RC3G0044100	rc03	8494667	8497519	CC-NBS-LRR		P-loop[212-220] Kin-2[289-296] RNBS-B[318-324] GLPL[379-385]	[181-192]AAA_16:0.00023 [193-467]NB-ARC:2.5e-63 [620-660]LRR_4:0.001
RC3G0047600	rc03	9080520	9088487	TIR-NBS-LRR		P-loop[358-366] Kin-2[433-440] RNBS-B[462-468] GLPL[523-529]	[23-193]TIR:2.9e-46 [327-344]AAA_16:0.00033 [345-613]NB-ARC:6.1e-66 [731-786]LRR_8:3.8e-05
RC3G0062300	rc03	11919385	11921083	NBS-LRR		P-loop[65-73] Kin-2[140-147] RNBS-B[169-175] GLPL[229-235]	[44-320]NB-ARC:1.3e-49 [416-474]LRR_8:2.2e-11
RC3G0070000	rc03	12642166	12647039	NBS	RPW8	P-loop[180-188] Kin-2[279-286] RNBS-B[305-311] GLPL[360-366]	[16-136]RPW8:9e-14 [159-445]NB-ARC:1.1e-33
RC3G0070100	rc03	12670256	12677491	NBS-LRR	RPW8	P-loop[166-174] Kin-2[243-250] RNBS-B[271-277] GLPL[325-331]	[5-111]RPW8:3.9e-13 [151-406]NB-ARC:7.5e-30
RC3G0075200	rc03	13340577	13343332	NBS		P-loop[177-185] Kin-2[251-258] RNBS-B[282-283] GLPL[344-350]	[155-435]NB-ARC:2.7e-60
RC3G0098600	rc03	17063773	17066571	TIR-NBS		P-loop[206-214] Kin-2[284-291] RNBS-B[311-317] GLPL[369-375]	[9-174]TIR:7.4e-48 [182-443]NB-ARC:4.8e-25 [600-615]LRR_3:0.0087
RC3G0111000	rc03	18591350	18592827	NBS-LRR		P-loop[35-43] Kin-2[110-117] RNBS-B[139-145] GLPL[198-204]	[14-281]NB-ARC:1.9e-54 [385-443]LRR_8:2.4e-08
RC3G0123500	rc03	20179686	20181286	TIR-NBS		P-loop[125-133] Kin-2[196-203] RNBS-B[223-229] GLPL[282-288]	[7-100]TIR:2.2e-12 [113-346]NB-ARC:3.2e-36
RC3G0124000	rc03	20217168	20219331	TIR-NBS		P-loop[230-238] Kin-2[302-309] RNBS-B[329-335] GLPL[388-394]	[22-205]TIR:5.5e-47 [208-217]AAA_16:0.0078 [218-468]NB-ARC:2.7e-34 [609-626]LRR_3:0.0038
RC3G0124200	rc03	20245230	20250243	TIR-NBS-LRR		P-loop[230-238] Kin-2[302-309] RNBS-B[329-335] GLPL[388-394]	[22-205]TIR:7.5e-46 [219-456]NB-ARC:1.2e-33 [610-627]LRR_3:0.0008 [842-901]LRR_8:1.9e-05 [901-911]LRR_4:0.001
RC3G0136400	rc03	21740920	21744430	NBS	RPW8	P-loop[161-169] Kin-2[240-247] RNBS-B[266-272] GLPL[321-327]	[1-101]RPW8:3.6e-18 [142-407]NB-ARC:1.3e-31
RC3G0136500	rc03	21762759	21766253	NBS	RPW8	P-loop[139-147] Kin-2[218-225] RNBS-B[244-250] GLPL[299-305]	[3-80]RPW8:1.3e-07 [122-385]NB-ARC:3.1e-30

RC3G0136600	rc03	21808068	21810533	NBS		P-loop[82-90] Kin-2[157-164] RNBS-B[187-193] GLPL[240-244]	[62-325]NB-ARC:6.6e-20
RC3G0145900	rc03	22703075	22704352	CC-NBS		P-loop[178-186] Kin-2[267-274] RNBS-B[308-314] GLPL[371-377]	[169-386]NB-ARC:3e-29
RC3G0199200	rc03	28299616	28301075	NBS-LRR		P-loop[65-73] Kin-2[140-147] RNBS-B[169-175] GLPL[228-234]	[43-319]NB-ARC:3.1e-48 [413-447]LRR_8:5.3e-05
RC3G0200100	rc03	28424037	28425715	NBS-LRR		P-loop[35-43] Kin-2[110-117] RNBS-B[139-145] GLPL[198-204]	[14-289]NB-ARC:8e-54 [383-441]LRR_8:1.1e-09
RC3G0200400	rc03	28514921	28516507	TIR-NBS		P-loop[127-135] Kin-2[202-209] RNBS-B[231-237] GLPL[290-296]	[3-84]TIR:1.1e-07 [105-380]NB-ARC:1.6e-48
RC3G0200800	rc03	28549670	28551783	TIR-NBS		P-loop[160-168] Kin-2[235-242] RNBS-B[264-270] GLPL[323-329]	[2-123]TIR:2.6e-27 [138-413]NB-ARC:1.4e-51
RC3G0201400	rc03	28584130	28585769	NBS-LRR		P-loop[36-44] Kin-2[111-118] RNBS-B[140-146] GLPL[200-206]	[14-292]NB-ARC:1.4e-48 [385-443]LRR_8:1.4e-10
RC3G0207900	rc03	29140368	29142896	CC-NBS-LRR	RPW8	P-loop[184-192] Kin-2[258-265] RNBS-B[287-293] GLPL[344-350]	[15-89]RPW8:0.0049 [154-432]NB-ARC:1.6e-53 [551-605]LRR_8:4.2e-08
RC3G0216100	rc03	30235476	30237794	NBS-LRR		P-loop[74-82] Kin-2[145-152] RNBS-B[173-179] GLPL[226-232]	[56-310]NB-ARC:5.7e-32
RC3G0242300	rc03	33188950	33190098	NBS		P-loop[205-213] Kin-2[280-287] RNBS-B[311-317] GLPL[372-378]	[177-379]NB-ARC:4.9e-39
RC3G0242600	rc03	33200787	33209563	NBS	Cyclin_N	P-loop[204-212] Kin-2[279-286] RNBS-B[310-316] GLPL[371-377]	[176-459]NB-ARC:9.7e-59 [1294-1344]Cyclin_N:6.4e-07 [193-460]NB-ARC:1.7e-55 [532-586]LRR_8:0.00013 [878-936]LRR_8:0.0033 [975-1012]LRR_4:0.00067
RC3G0243600	rc03	33281601	33296322	NBS-LRR		P-loop[200-208] Kin-2[274-281] RNBS-B[305-311] GLPL[370-376]	[194-465]NB-ARC:4.1e-53
RC3G0244300	rc03	33345473	33348282	NBS		P-loop[222-230] Kin-2[296-303] RNBS-B[327-333] GLPL[388-394]	[171-181]AAA_16:9.4e-05 [182-457]NB-ARC:4.8e-62
RC3G0249600	rc03	33811859	33815053	NBS		P-loop[203-211] Kin-2[278-285] RNBS-B[309-315] GLPL[370-376]	[2-280]NB-ARC:6.7e-60 [353-389]LRR_8:0.005
RC3G0252800	rc03	34112771	34115901	NBS-LRR		P-loop[23-31] Kin-2[98-105] RNBS-B[129-135] GLPL[190-196]	[23-182]TIR:4.3e-50 [202-215]AAA_16:0.0022 [216-455]NB-ARC:3.6e-31 [609-626]LRR_3:6.9e-05 [726-782]LRR_8:0.0057 [863-918]LRR_8:0.00023
RC3G0272000	rc03	35710822	35716742	TIR-NBS-LRR		P-loop[227-235] Kin-2[305-312] RNBS-B[332-338] GLPL[391-397]	[181-459]NB-ARC:9e-57
RC3G0277900	rc03	36251527	36255728	CC-NBS-LRR		P-loop[205-213] Kin-2[280-287] RNBS-B[311-317] GLPL[372-378]	[177-459]NB-ARC:7.4e-61 [876-934]LRR_8:0.00093
RC3G0280800	rc03	36402106	36405245	NBS-LRR		P-loop[204-212] Kin-2[279-286] RNBS-B[310-316] GLPL[371-377]	[63-322]NB-ARC:3.2e-35 [664-719]LRR_8:0.00049
RC3G0357100	rc03	42585842	42591797	NBS-LRR		P-loop[79-87] Kin-2[164-171] RNBS-B[191-197] GLPL[250-256]	[185-468]NB-ARC:3e-57 [627-660]LRR_8:0.00083
RC3G0380200	rc03	44011689	44014786	NBS-LRR		P-loop[212-220] Kin-2[291-298] RNBS-B[322-328] GLPL[384-390]	[183-468]NB-ARC:1.6e-54 [574-600]LRR_8:0.0063 [605-635]LRR_4:0.00079 [651-682]LRR_4:0.0008 [1035-1129]LRR_5:0.0031 [1129-1158]LRR_4:0.0038
RC3G0380700	rc03	44048794	44052609	NBS-LRR		P-loop[208-216] Kin-2[289-296] RNBS-B[320-326] GLPL[381-387]	[187-473]NB-ARC:5.7e-57 [603-647]LRR_8:0.0011 [648-665]LRR_4:0.0013 [1016-1134]LRR_5:5.2e-06
RC3G0380800	rc03	44079169	44082987	NBS-LRR		P-loop[214-222] Kin-2[293-300] RNBS-B[324-330] GLPL[386-392]	[180-453]NB-ARC:4.5e-49
RC3G0380900	rc03	44084061	44085554	NBS		P-loop[207-215] Kin-2[286-293] RNBS-B[317-323] GLPL[379-385]	[1-242]NB-ARC:9.9e-33 [440-496]LRR_8:3e-05 [536-558]LRR_8:0.0008 [559-589]LRR_4:0.00014 [637-696]LRR_8:6.8e-05
RC4G0003800	rc04	307316	310088	NBS-LRR		P-loop[6-14] Kin-2[82-89] RNBS-B[109-115] GLPL[168-174]	

RC4G0004700	rc04	366404	371864	NBS-LRR		P-loop[81-89] Kin-2[157-164] RNBS-B[184-190] GLPL[242-248]	[63-309]NB-ARC:3.3e-35 [493-524]LRR_4:0.0054 [666-704]LRR_4:0.001
RC4G0006200	rc04	498278	503605	NBS-LRR		P-loop[81-89] Kin-2[154-161] RNBS-B[181-187] GLPL[240-246]	[66-314]NB-ARC:1.7e-35 [582-638]LRR_8:0.0035 [653-709]LRR_8:0.0022 [724-780]LRR_8:0.0061 [795-851]LRR_8:0.0032 [913-969]LRR_8:0.0049 [1008-1062]LRR_8:0.0074 [1115-1156]LRR_4:0.0019
RC4G0009500	rc04	713187	716014	NBS-LRR		P-loop[2-10] Kin-2[75-82] RNBS-B[102-108] GLPL[161-167]	[2-234]NB-ARC:2.7e-36 [412-447]LRR_4:0.00031
RC4G0018200	rc04	1569721	1571754	NBS-LRR		P-loop[6-14] Kin-2[81-88] RNBS-B[108-114] GLPL[167-173]	[1-232]NB-ARC:5.5e-34 [420-455]LRR_4:0.004
RC4G0026100	rc04	2528716	2531583	CC-NBS-LRR		P-loop[212-220] Kin-2[286-293] RNBS-B[315-321] GLPL[376-382]	[188-461]NB-ARC:3.5e-62 [591-617]LRR_8:0.00056 [618-658]LRR_4:0.00037 [794-826]LRR_4:0.00096
RC4G0026700	rc04	2595101	2603424	TIR-NBS		P-loop[232-240] Kin-2[305-312] RNBS-B[332-338] GLPL[391-397]	[29-190]TIR:5.3e-45 [205-215]AAA_16:0.00018 [216-456]NB-ARC:1.1e-36
RC4G0027200	rc04	2627151	2630401	TIR-NBS-LRR		P-loop[232-240] Kin-2[308-315] RNBS-B[335-341] GLPL[394-400]	[30-188]TIR:3.5e-45 [214-467]NB-ARC:4.5e-38 [649-691]LRR_4:9.7e-05 [694-727]LRR_4:0.0017 [789-845]LRR_8:5.3e-05
RC4G0028300	rc04	2682384	2686107	NBS-LRR		P-loop[6-14] Kin-2[82-89] RNBS-B[109-115] GLPL[168-174]	[1-233]NB-ARC:4.7e-34 [419-451]LRR_4:0.0058 [455-498]LRR_4:3.4e-07 [501-543]LRR_4:1.1e-05 [553-590]LRR_4:0.00034 [711-767]LRR_8:0.00048 [783-838]LRR_8:0.00016 [861-921]LRR_8:2e-06
RC4G0028800	rc04	2707114	2709934	NBS-LRR		P-loop[6-14] Kin-2[82-89] RNBS-B[109-115] GLPL[168-174]	[1-240]NB-ARC:4.6e-34 [411-452]LRR_4:0.00024 [456-498]LRR_4:3.4e-05 [502-545]LRR_4:6e-08 [548-583]LRR_4:0.00089 [643-698]LRR_8:0.0039 [714-767]LRR_8:0.0071
RC4G0032900	rc04	3293893	3296382	NBS		P-loop[178-186] Kin-2[252-259] RNBS-B[280-286] GLPL[344-350]	[155-436]NB-ARC:1.9e-73
RC4G0034000	rc04	3377290	3379078	NBS		P-loop[178-186] Kin-2[232-239] RNBS-B[260-266] GLPL[324-330]	[155-416]NB-ARC:5.7e-58
RC4G0034900	rc04	3445710	3448199	NBS		P-loop[178-186] Kin-2[252-259] RNBS-B[280-286] GLPL[344-350]	[155-436]NB-ARC:1.7e-73
RC4G0058400	rc04	6390210	6394976	NBS-LRR		P-loop[193-201] Kin-2[274-281] RNBS-B[302-308] GLPL[368-374]	[169-465]NB-ARC:4.7e-74 [809-845]LRR_8:0.0017
RC4G0059100	rc04	6456829	6460874	NBS-LRR		P-loop[193-201] RNBS-B[284-290] GLPL[343-349]	[169-439]NB-ARC:1e-60 [766-799]LRR_4:0.0052
RC4G0059600	rc04	6519333	6524016	NBS-LRR		P-loop[193-201] Kin-2[274-281] RNBS-B[302-308] GLPL[368-374]	[169-464]NB-ARC:7.3e-74 [810-842]LRR_4:0.00048
RC4G0076400	rc04	8903303	8907438	CC-NBS-LRR		P-loop[188-196] Kin-2[265-272] RNBS-B[289-295] GLPL[348-354]	[167-415]NB-ARC:1.7e-48 [629-664]LRR_8:0.0015
RC4G0085600	rc04	10344840	10346607	CC-NBS		P-loop[178-186] Kin-2[255-262] RNBS-B[279-285] GLPL[338-344]	[157-411]NB-ARC:1.9e-48
RC4G0088100	rc04	10595425	10611786	CC-NBS-LRR		P-loop[186-194] Kin-2[263-270] RNBS-B[287-293] GLPL[346-352]	[167-413]NB-ARC:2.2e-44 [535-588]LRR_8:0.00012
RC4G0088900	rc04	10659086	10661392	CC-NBS-LRR	DUF677	P-loop[195-203] Kin-2[272-279] RNBS-B[296-302] GLPL[355-361]	[6-110]DUF677:0.00047 [177-439]NB-ARC:3.6e-46 [557-601]LRR_8:0.0036 [635-670]LRR_4:0.0043

RC4G0089900	rc04	10762137	10766873	CC-NBS		P-loop[184-192] Kin-2[262-269] RNBS-B[286-292] GLPL[345-351]	[166-417]NB-ARC:2.6e-46
RC4G0092500	rc04	11062966	11078607	NBS-LRR		P-loop[130-138] Kin-2[207-214] RNBS-B[231-237] GLPL[290-296]	[112-378]NB-ARC:4.3e-44 [491-535]LRR_8:0.00064
RC4G0101000	rc04	12580676	12583891	NBS-LRR		P-loop[186-194] Kin-2[315-322] RNBS-B[342-348] GLPL[402-408]	[163-495]NB-ARC:1.1e-63 [623-667]LRR_8:0.0083
RC4G0131400	rc04	18217613	18221438	TIR-NBS-LRR		P-loop[224-232] Kin-2[303-310] RNBS-B[330-336] GLPL[389-395]	[20-188]TIR:6.3e-49 [201-458]NB-ARC:1.4e-33 [820-875]LRR_8:4e-07 [876-886]LRR_4:0.0011
RC4G0150300	rc04	21839855	21844046	CC-NBS-LRR		P-loop[180-188] Kin-2[258-265] RNBS-B[285-291] GLPL[345-351]	[159-435]NB-ARC:3.2e-84 [532-569]LRR_8:8.9e-08 [579-614]LRR_8:0.00017
RC4G0150700	rc04	21950838	21954395	NBS-LRR		P-loop[186-194] Kin-2[267-274] RNBS-B[294-300] GLPL[359-365]	[162-454]NB-ARC:3e-70 [618-670]LRR_8:0.00066 [783-817]LRR_4:0.0087
RC4G0156700	rc04	22960778	22965591	CC-NBS-LRR		P-loop[346-354] Kin-2[423-430] RNBS-B[447-453] GLPL[506-512]	[326-588]NB-ARC:3.9e-48 [761-816]LRR_8:0.0091
RC4G0161100	rc04	23754452	23761269	NBS-LRR		P-loop[196-204] Kin-2[271-278] RNBS-B[301-307] GLPL[358-364]	[163-184]AAA_16:5.3e-05 [185-448]NB-ARC:6.7e-63 [555-602]LRR_8:0.00015
RC4G0177100	rc04	26269454	26272936	CC-NBS-LRR		P-loop[194-202] Kin-2[276-283] RNBS-B[303-309] GLPL[367-373]	[172-459]NB-ARC:1e-83 [576-631]LRR_8:7.2e-06
RC4G0185400	rc04	27299484	27309739	CC-NBS-LRR	RPW8	P-loop[260-268] Kin-2[337-344] RNBS-B[367-373] GLPL[421-427]	[36-142]RPW8:3.5e-14 [241-508]NB-ARC:2.6e-33 [777-799]LRR_8:0.0087 [800-838]LRR_4:0.0034
RC4G0186600	rc04	27506043	27509702	NBS-LRR		P-loop[35-43] Kin-2[114-121] RNBS-B[141-147] GLPL[200-206]	[17-264]NB-ARC:8.3e-34 [534-554]LRR_8:0.0054 [555-577]LRR_4:0.00055 [578-634]LRR_8:3.7e-07 [640-677]LRR_8:0.0021 [692-747]LRR_8:0.0019
RC4G0188900	rc04	27670968	27676905	TIR-NBS-LRR		P-loop[227-235] Kin-2[306-313] RNBS-B[333-339] GLPL[392-398]	[21-187]TIR:1.7e-47 [206-453]NB-ARC:1.8e-32 [608-663]LRR_8:0.0026 [748-770]LRR_4:0.0077 [771-815]LRR_8:0.00073 [816-855]LRR_4:1.2e-05 [856-872]LRR_8:1.3e-05 [987-1021]LRR_8:0.0082
RC4G0191600	rc04	28026959	28031459	TIR-NBS-LRR		P-loop[219-227] Kin-2[298-305] RNBS-B[325-331] GLPL[384-390]	[14-183]TIR:5.5e-47 [196-450]NB-ARC:1e-30 [833-873]LRR_4:0.00014
RC4G0192500	rc04	28192080	28197651	NBS-LRR		P-loop[204-212] Kin-2[279-286] RNBS-B[310-316] GLPL[371-377]	[173-182]AAA_16:0.0014 [183-460]NB-ARC:4.2e-60 [876-931]LRR_8:0.001 [1156-1195]LRR_4:0.0015
RC4G0206200	rc04	30253977	30257175	NBS-LRR		P-loop[6-14] Kin-2[84-91] RNBS-B[111-117] GLPL[170-176]	[1-234]NB-ARC:2.3e-30 [524-563]LRR_4:0.0015 [570-593]LRR_4:0.0045 [594-640]LRR_8:0.0025 [641-696]LRR_8:0.00059
RC4G0206500	rc04	30288798	30294008	NBS-LRR		P-loop[6-14] Kin-2[84-91] RNBS-B[111-117] GLPL[154-160]	[1-215]NB-ARC:1.4e-19 [488-543]LRR_8:0.00054 [580-636]LRR_8:0.00091 [672-727]LRR_8:0.0013
RC4G0208800	rc04	30532282	30535890	CC-NBS-LRR		P-loop[196-204] Kin-2[272-279] RNBS-B[303-309] GLPL[370-376]	[169-461]NB-ARC:1.5e-59 [568-622]LRR_8:1.8e-05
RC4G0210000	rc04	30659410	30664218	CC-NBS-LRR		P-loop[203-211] Kin-2[278-285] RNBS-B[309-315] GLPL[371-377]	[176-462]NB-ARC:7.5e-62 [521-571]LRR_8:1.8e-06 [895-919]LRR_8:0.00054 [920-978]LRR_8:0.00034 [991-1093]LRR_5:4.1e-07

RC4G0211800	rc04	30991554	30994632	NBS		P-loop[201-209] Kin-2[276-283] RNBS-B[307-313] GLPL[366-372]	[175-419]NB-ARC:8.1e-50 [183-474]NB-ARC:2.1e-61 [577-608]LRR_8:0.0026 [609-647]LRR_8:0.00098
RC4G0232800	rc04	34153012	34155878	NBS-LRR		P-loop[210-218] Kin-2[289-296] RNBS-B[320-326] GLPL[381-387]	[113-404]NB-ARC:4.5e-62 [773-813]LRR_4:0.0048
RC4G0233100	rc04	34202653	34205479	NBS-LRR		P-loop[140-148] Kin-2[219-226] RNBS-B[250-256] GLPL[311-317]	[113-404]NB-ARC:2.1e-58 [503-533]LRR_8:0.00042 [534-573]LRR_8:8.8e-05 [730-806]LRR_5:0.0015
RC4G0233500	rc04	34258520	34261161	NBS-LRR		P-loop[140-148] Kin-2[219-226] RNBS-B[250-256] GLPL[311-317]	[113-402]NB-ARC:3.4e-60 [520-575]LRR_8:0.00017
RC4G0233700	rc04	34301613	34305036	NBS-LRR		P-loop[138-146] Kin-2[217-224] RNBS-B[248-254] GLPL[309-315]	[1-265]NB-ARC:4.1e-58 [387-436]LRR_4:0.00092 [437-452]LRR_8:0.008 [713-735]LRR_8:0.0008 [736-775]LRR_4:0.00023 [877-918]LRR_4:0.0094
RC4G0238500	rc04	34800183	34810214	NBS-LRR		P-loop[5-13] Kin-2[83-90] RNBS-B[114-120] GLPL[175-181]	[187-474]NB-ARC:2.5e-55 [62-353]NB-ARC:8.5e-60 [462-499]LRR_4:0.00048 [500-513]LRR_8:0.00064
RC4G0239200	rc04	34918326	34920024	NBS		P-loop[212-220] Kin-2[290-297] RNBS-B[321-327] GLPL[382-388]	[1-269]NB-ARC:1.6e-58 [373-421]LRR_8:0.0023 [422-439]LRR_4:0.0024 [636-675]LRR_4:0.00071
RC4G0239400	rc04	34935796	34938486	NBS-LRR		P-loop[89-97] Kin-2[168-175] RNBS-B[199-205] GLPL[260-266]	[1-268]NB-ARC:1e-56 [381-422]LRR_4:0.0023 [423-436]LRR_8:0.0039 [59-79]AAA_16:0.0025 [80-349]NB-ARC:6.6e-58
RC4G0239800	rc04	35002789	35005494	NBS-LRR		P-loop[5-13] Kin-2[84-91] RNBS-B[115-121] GLPL[176-182]	[183-473]NB-ARC:2.7e-61 [621-668]LRR_8:0.0074
RC4G0240000	rc04	35027048	35030761	NBS-LRR		P-loop[5-13] Kin-2[83-90] RNBS-B[114-120] GLPL[175-181]	[183-472]NB-ARC:4.8e-64 [582-591]LRR_8:3.8e-05 [592-630]LRR_4:3.3e-05 [631-644]LRR_8:0.00032 [926-965]LRR_4:0.00016
RC4G0240400	rc04	35053190	35054891	NBS		P-loop[89-97] Kin-2[167-174] RNBS-B[198-204] GLPL[259-265]	[182-471]NB-ARC:9.6e-64 [555-593]LRR_4:0.0017 [887-926]LRR_4:0.0021
RC4G0248700	rc04	36192025	36195770	NBS-LRR		P-loop[209-217] Kin-2[287-294] RNBS-B[318-324] GLPL[380-386]	[182-472]NB-ARC:3.1e-64 [713-779]gag_pre-integrs:1.5e-14 [792-904]rve:1.3e-22 [1218-1461]RVT_2:2.1e-96 [1666-1718]LRR_8:0.00019 [1959-2044]LRR_5:0.0016 [2045-2084]LRR_4:0.0015
RC4G0249100	rc04	36239268	36244166	NBS-LRR		P-loop[210-218] Kin-2[288-295] RNBS-B[319-325] GLPL[380-386]	[183-473]NB-ARC:3.1e-64 [582-591]LRR_8:0.00096 [592-629]LRR_4:0.00034 [1043-1101]LRR_8:0.0022 [1126-1235]LRR_5:0.0031
RC4G0249700	rc04	36295031	36299798	NBS-LRR		P-loop[209-217] Kin-2[287-294] RNBS-B[318-324] GLPL[379-385]	[175-186]AAA_16:0.0074 [187-459]NB-ARC:5.2e-57
RC4G0249900	rc04	36308849	36319578	NBS-LRR	gag_pre-integrs,rve, RVT_2	P-loop[209-217] Kin-2[287-294] RNBS-B[318-324] GLPL[379-385]	[1-176]NB-ARC:3.5e-34
RC4G0250200	rc04	36351503	36355784	NBS-LRR		P-loop[210-218] Kin-2[288-295] RNBS-B[319-325] GLPL[380-386]	[177-460]NB-ARC:1.1e-57
RC4G0279600	rc04	39822263	39826573	NBS-LRR		P-loop[205-213] Kin-2[280-287] RNBS-B[311-317] GLPL[372-378]	
RC4G0280400	rc04	39888481	39889072	NBS		P-loop[1-8] Kin-2[75-82] RNBS-B[106-112] GLPL[167-173]	
RC4G0281100	rc04	39962829	39966458	NBS		P-loop[205-213] Kin-2[280-287] RNBS-B[311-317] GLPL[372-378]	

RC4G0281700	rc04	39977671	39984467	NBS-LRR	Apolipoprotein	P-loop[205-213] Kin-2[280-287] RNBS-B[311-317] GLPL[372-378]	[13-137]Apolipoprotein:0.0038 [177-460]NB-ARC:1.8e-57 [910-944]LRR_5:0.0061 [945-985]LRR_4:0.00054 [986-1011]LRR_5:0.0061
RC4G0338200	rc04	45846444	45850390	NBS		P-loop[1-8] Kin-2[78-85] RNBS-B[106-112] GLPL[171-177]	[1-268]NB-ARC:1.1e-66
RC4G0375900	rc04	49192413	49197402	CC-NBS-LRR	RPW8	P-loop[201-209] Kin-2[277-284] RNBS-B[306-312] GLPL[362-368]	[16-90]RPW8:0.005 [177-451]NB-ARC:4.1e-52 [568-618]LRR_8:2e-09
RC4G0479900	rc04	57383168	57385083	NBS		P-loop[83-91] Kin-2[164-171] RNBS-B[191-197] GLPL[252-258]	[61-332]NB-ARC:1.7e-32 [49-315]NB-ARC:3.4e-36 [600-658]LRR_8:0.00011 [741-797]LRR_8:0.00032 [916-971]LRR_8:0.00033
RC4G0480000	rc04	57386756	57392858	NBS-LRR		P-loop[71-79] Kin-2[149-156] RNBS-B[176-182] GLPL[236-242]	
RC5G0010300	rc05	599436	602538	NBS		P-loop[195-203] Kin-2[270-277] RNBS-B[301-302] GLPL[366-372]	[171-455]NB-ARC:9.2e-65
RC5G0010900	rc05	648214	651605	NBS		P-loop[185-193] Kin-2[259-266] RNBS-B[287-293] GLPL[351-357]	[162-446]NB-ARC:4.8e-73 [180-451]NB-ARC:7.4e-56 [545-597]LRR_8:1.9e-05 [885-945]LRR_8:0.00013
RC5G0030200	rc05	2012173	2016350	NBS-LRR		P-loop[193-201] Kin-2[269-276] RNBS-B[300-306] GLPL[365-371]	
RC5G0031700	rc05	2180099	2186355	CC-NBS-LRR		P-loop[211-219] Kin-2[284-291] RNBS-B[314-320] GLPL[376-382]	[188-463]NB-ARC:4e-58 [563-620]LRR_8:1e-05 [792-829]LRR_4:0.0093
RC5G0032000	rc05	2200115	2202139	NBS-LRR		P-loop[102-110] Kin-2[175-182] RNBS-B[205-211] GLPL[267-273]	[79-354]NB-ARC:2.5e-58 [454-478]LRR_8:1.5e-05 [479-517]LRR_4:6.5e-06
RC5G0059300	rc05	4052738	4053379	NBS		P-loop[1-8] Kin-2[88-95] RNBS-B[115-121] GLPL[175-181]	[1-186]NB-ARC:9.2e-26
RC5G0061300	rc05	4199023	4201464	NBS-LRR		P-loop[35-43] Kin-2[124-131] RNBS-B[151-157] GLPL[211-217]	[14-308]NB-ARC:1.3e-46 [408-468]LRR_8:4.4e-09
RC5G0061600	rc05	4224795	4228453	CC-NBS		P-loop[181-189] Kin-2[274-281] RNBS-B[301-307] GLPL[361-367]	[161-465]NB-ARC:1.5e-36
RC5G0127700	rc05	9487723	9492155	TIR-NBS-LRR		P-loop[285-293] Kin-2[363-370] RNBS-B[390-396] GLPL[456-462]	[77-247]TIR:5e-46 [253-279]AAA_16:0.0074 [280-529]NB-ARC:1.6e-20 [727-762]LRR_4:0.006 [868-924]LRR_8:0.0037 [985-1028]LRR_4:0.0002 [1029-1045]LRR_4:0.0058
RC5G0128100	rc05	9506935	9509502	TIR-NBS		P-loop[220-228] Kin-2[298-305] RNBS-B[325-331] GLPL[391-397]	[14-192]TIR:6.2e-47 [193-212]AAA_16:6.1e-05 [213-461]NB-ARC:3.7e-22 [635-650]LRR_3:0.0014
RC5G0149800	rc05	11250263	11252152	NBS-LRR		P-loop[23-31] Kin-2[100-107] RNBS-B[124-130] GLPL[184-190]	[4-266]NB-ARC:2e-46 [383-426]LRR_8:0.0019 [441-497]LRR_8:0.00096
RC5G0167000	rc05	12750787	12755732	NBS-LRR		P-loop[194-202] Kin-2[276-283] RNBS-B[303-309] GLPL[367-373]	[172-459]NB-ARC:1.2e-83 [577-633]LRR_8:6.4e-07
RC5G0169300	rc05	13053055	13055802	CC-NBS-LRR		P-loop[194-202] Kin-2[277-284] RNBS-B[304-310] GLPL[368-374]	[172-460]NB-ARC:2.6e-80 [579-632]LRR_8:6.8e-07
RC5G0169500	rc05	13080742	13083726	CC-NBS-LRR		P-loop[194-202] Kin-2[276-283] RNBS-B[303-309] GLPL[367-373]	[172-459]NB-ARC:2.3e-83 [576-632]LRR_8:3.2e-06
RC5G0169800	rc05	13105656	13115300	NBS-LRR		P-loop[194-202] Kin-2[276-283] RNBS-B[303-309] GLPL[367-373]	[173-459]NB-ARC:7.9e-85 [576-632]LRR_8:7.3e-06 [633-649]LRR_8:0.00054
RC5G0227800	rc05	18936361	18942066	TIR-NBS		P-loop[220-228] Kin-2[298-305] RNBS-B[326-332] GLPL[386-392]	[15-194]TIR:1.1e-48 [196-455]NB-ARC:5.7e-35 [618-634]LRR_3:0.0089

RC5G0228700	rc05	19071300	19075405	TIR-NBS-LRR		P-loop[220-228] Kin-2[300-307] RNBS-B[328-334] GLPL[386-392]	[15-185]TIR:2.1e-48 [197-457]NB-ARC:2.4e-29 [620-636]LRR_3:0.00036 [646-701]LRR_8:0.009 [713-745]LRR_8:0.0068
RC5G0231700	rc05	19480303	19485750	TIR-NBS		P-loop[219-227] Kin-2[298-305] RNBS-B[326-332] GLPL[384-390]	[15-193]TIR:2.4e-49 [195-459]NB-ARC:1.8e-25 [620-635]LRR_3:0.00053
RC5G0245000	rc05	20532298	20535069	NBS-LRR		P-loop[196-204] Kin-2[274-281] RNBS-B[301-307] GLPL[365-371]	[175-458]NB-ARC:1.4e-65 [600-653]LRR_8:1.2e-05
RC5G0254700	rc05	21614563	21616935	TIR-NBS		P-loop[218-226] Kin-2[297-304] RNBS-B[324-330] GLPL[383-389]	[14-177]TIR:7.4e-51 [200-460]NB-ARC:3.3e-26
RC5G0327400	rc05	30163102	30167202	CC-NBS-LRR		P-loop[191-199] Kin-2[269-276] RNBS-B[296-302] GLPL[354-360]	[170-446]NB-ARC:3.4e-65 [538-595]LRR_8:1e-08 [609-665]LRR_8:1.4e-07
RC5G0343100	rc05	32481329	32483874	NBS-LRR		P-loop[106-114] Kin-2[181-188] RNBS-B[210-216] GLPL[271-277]	[80-358]NB-ARC:1.1e-61 [479-517]LRR_4:0.00021 [525-562]LRR_4:0.0049
RC5G0343400	rc05	32499168	32502401	CC-NBS-LRR		P-loop[203-211] Kin-2[278-285] RNBS-B[307-313] GLPL[368-374]	[177-454]NB-ARC:9.7e-61 [566-575]LRR_8:0.0081 [577-631]LRR_8:0.00027
RC5G0343500	rc05	32505090	32506001	NBS		P-loop[88-96] Kin-2[165-172] RNBS-B[194-200] GLPL[255-261]	[62-289]NB-ARC:1.4e-47
RC5G0343700	rc05	32507785	32512256	CC-NBS-LRR		P-loop[201-209] Kin-2[276-283] RNBS-B[305-311] GLPL[366-372]	[175-452]NB-ARC:3e-64 [577-633]LRR_8:8.8e-06
RC5G0346300	rc05	32787576	32790430	CC-NBS-LRR	RPW8	P-loop[203-211] Kin-2[278-285] RNBS-B[307-313] GLPL[368-374]	[4-88]RPW8:0.0071 [177-454]NB-ARC:8e-66 [575-616]LRR_8:0.00014
RC5G0370200	rc05	36020158	36024058	CC-NBS-LRR		P-loop[202-210] Kin-2[277-284] RNBS-B[306-312] GLPL[367-373]	[176-453]NB-ARC:7.7e-62 [561-571]LRR_8:0.0013 [572-626]LRR_8:0.00047
RC5G0370400	rc05	36049700	36058870	CC-NBS-LRR		P-loop[182-190] Kin-2[257-264] RNBS-B[286-292] GLPL[347-353]	[156-436]NB-ARC:1.3e-62 [552-573]LRR_8:3.2e-06 [574-632]LRR_8:2.4e-06
RC5G0370800	rc05	36124042	36132140	NBS-LRR		P-loop[184-192] Kin-2[259-266] RNBS-B[288-294] GLPL[346-352]	[158-432]NB-ARC:7.7e-64 [553-607]LRR_8:2.2e-06
RC5G0371100	rc05	36172573	36178226	CC-NBS-LRR	RPW8	P-loop[206-214] Kin-2[281-288] RNBS-B[310-316] GLPL[370-376]	[4-88]RPW8:0.0014 [180-461]NB-ARC:1.2e-70 [588-626]LRR_4:8.7e-05
RC5G0376400	rc05	36979080	36981422	CC-NBS-LRR	RPW8	P-loop[204-212] Kin-2[270-277] RNBS-B[299-305] GLPL[344-348]	[4-98]RPW8:1.4e-05 [181-433]NB-ARC:9.7e-43 [556-610]LRR_8:2e-05
RC5G0380200	rc05	37680567	37683462	NBS-LRR		P-loop[234-242] Kin-2[310-317] RNBS-B[340-346] GLPL[401-407]	[203-212]AAA_16:0.00014 [213-489]NB-ARC:4.2e-62 [608-641]LRR_4:0.00037
RC5G0403300	rc05	40299954	40303988	CC-NBS-LRR		P-loop[182-190] Kin-2[257-264] RNBS-B[286-292] GLPL[347-353]	[156-433]NB-ARC:8.7e-63 [536-587]LRR_8:1.1e-05
RC5G0435500	rc05	45625860	45628523	NBS		P-loop[19-27] Kin-2[98-105] RNBS-B[125-131] GLPL[182-188]	[5-246]NB-ARC:3.1e-29
RC5G0441600	rc05	46313610	46317073	NBS-LRR		P-loop[206-214] Kin-2[281-288] RNBS-B[315-321] GLPL[376-382]	[178-464]NB-ARC:1e-56 [586-639]LRR_8:0.0015
RC5G0451400	rc05	48176707	48179831	NBS-LRR		P-loop[194-202] Kin-2[276-283] RNBS-B[303-309] GLPL[367-373]	[172-459]NB-ARC:2e-80 [580-636]LRR_8:2.7e-06
RC5G0451800	rc05	48195161	48198638	NBS-LRR		P-loop[197-205] Kin-2[279-286] RNBS-B[306-312] GLPL[370-376]	[175-461]NB-ARC:1.3e-82 [587-643]LRR_8:4.5e-07
RC5G0452200	rc05	48274304	48277639	NBS-LRR		P-loop[194-202] Kin-2[276-283] RNBS-B[303-309] GLPL[367-373]	[172-459]NB-ARC:4.1e-81 [580-636]LRR_8:8.1e-06
RC5G0452700	rc05	48338371	48341154	NBS-LRR		P-loop[194-202] Kin-2[276-283] RNBS-B[303-309] GLPL[367-373]	[172-459]NB-ARC:4.1e-82 [580-636]LRR_8:6.7e-08
RC5G0489900	rc05	55379318	55386672	TIR-NBS-LRR		P-loop[243-251] Kin-2[322-329] RNBS-B[349-355] GLPL[409-415]	[37-204]TIR:3.7e-48 [221-476]NB-ARC:8.2e-29

RC5G0490600	rc05	55468667	55471769	TIR-NBS-LRR		P-loop[199-207] Kin-2[276-283] RNBS-B[303-309] GLPL[362-368]	[36-165]TIR:2.1e-26 [175-189]AAA_16:0.00067 [190-432]NB-ARC:2.6e-28 [580-598]LRR_3:0.0002 [672-729]LRR_8:6.1e-06
RC5G0491400	rc05	55585356	55590552	TIR-NBS-LRR		P-loop[129-137] Kin-2[200-207] RNBS-B[227-233] GLPL[286-292]	[3-95]TIR:7.2e-12 [120-351]NB-ARC:9.2e-34 [503-520]LRR_3:0.0035 [756-815]LRR_8:6.2e-05
RC5G0511300	rc05	58633590	58636220	CC-NBS-LRR		P-loop[206-214] Kin-2[281-288] RNBS-B[315-321] GLPL[376-382]	[181-463]NB-ARC:1.2e-59 [584-605]LRR_8:0.0098 [606-645]LRR_4:0.0016
RC5G0511600	rc05	58675227	58680594	TIR-NBS-LRR		P-loop[175-183] Kin-2[250-257] RNBS-B[279-285] GLPL[338-344]	[2-131]TIR:1.2e-30 [153-429]NB-ARC:6e-52 [524-580]LRR_8:9.3e-09 [581-591]LRR_4:0.0015
RC5G0528800	rc05	61147231	61150828	NBS-LRR		P-loop[20-28] Kin-2[81-88] RNBS-B[110-116] GLPL[169-175]	[4-255]NB-ARC:1.1e-34 [377-435]LRR_8:4.4e-08
RC5G0529000	rc05	61157136	61161309	TIR-NBS-LRR		P-loop[219-227] Kin-2[280-287] RNBS-B[309-315] GLPL[368-374]	[14-187]TIR:1.1e-42 [199-459]NB-ARC:2.9e-36 [569-627]LRR_8:9.3e-06 [627-637]LRR_4:0.00059
RC5G0529400	rc05	61185509	61186618	NBS		P-loop[20-28] Kin-2[81-88] RNBS-B[110-116] GLPL[171-177]	[1-258]NB-ARC:1.5e-36
RC5G0550500	rc05	64286509	64289637	TIR-NBS-LRR		P-loop[231-239] Kin-2[306-313] RNBS-B[335-341] GLPL[403-409]	[22-193]TIR:6.3e-44 [211-489]NB-ARC:6.2e-48 [589-647]LRR_8:7.7e-10
RC5G0550800	rc05	64342396	64347751	CC-TIR-NBS-LRR	NAP	P-loop[317-325] Kin-2[391-398] RNBS-B[420-426] GLPL[478-484]	[101-274]TIR:1e-46 [296-567]NB-ARC:1.7e-50 [665-724]LRR_8:2.3e-09 [728-768]LRR_8:0.0006 [1209-1450]NAP:1.9e-68
RC5G0551300	rc05	64363055	64364261	TIR-NBS		P-loop[179-187] Kin-2[254-261] RNBS-B[283-289] GLPL[342-348]	[2-137]TIR:2.4e-29 [160-352]NB-ARC:2.8e-34
RC5G0551600	rc05	64416135	64418578	TIR-NBS		P-loop[288-296] Kin-2[371-378] RNBS-B[400-406] GLPL[459-465]	[78-249]TIR:5.8e-46 [267-548]NB-ARC:8.1e-46
RC5G0551800	rc05	64429958	64436745	TIR-NBS-LRR		P-loop[232-240] Kin-2[307-314] RNBS-B[336-342] GLPL[395-401]	[25-188]TIR:7.8e-44 [212-488]NB-ARC:2.2e-46 [586-643]LRR_8:6.3e-09 [650-666]LRR_4:0.0053
RC5G0555100	rc05	64897229	64898989	TIR-NBS		P-loop[134-142] Kin-2[209-216] RNBS-B[236-242] GLPL[295-301]	[20-109]TIR:2.8e-10 [121-372]NB-ARC:3.2e-34
RC5G0555900	rc05	65041864	65043564	TIR-NBS		P-loop[125-133] Kin-2[200-207] RNBS-B[227-233] GLPL[286-292]	[5-100]TIR:9.3e-12 [110-361]NB-ARC:9e-35
RC5G0568600	rc05	66603387	66605777	TIR-NBS		P-loop[227-235] Kin-2[299-306] RNBS-B[326-332] GLPL[385-391]	[20-189]TIR:1.4e-46 [213-455]NB-ARC:2.6e-35
RC5G0569800	rc05	66766343	66770979	TIR-NBS-LRR		P-loop[216-224] Kin-2[294-301] RNBS-B[321-327] GLPL[388-394]	[11-181]TIR:1.4e-48 [186-208]AAA_16:0.0004 [209-457]NB-ARC:4e-25 [622-637]LRR_3:3.7e-05 [736-789]LRR_8:0.0062
RC5G0600200	rc05	69891742	69900734	TIR-NBS-LRR		P-loop[232-240] Kin-2[307-314] RNBS-B[336-342] GLPL[395-401]	[23-189]TIR:9.8e-42 [211-479]NB-ARC:5e-51 [574-632]LRR_8:8.5e-07 [645-685]LRR_4:0.00049 [686-700]LRR_8:0.0087
RC5G0600300	rc05	69902585	69913939	CC-TIR-NBS-LRR		P-loop[233-241] Kin-2[308-315] RNBS-B[337-343] GLPL[396-402]	[18-190]TIR:1.8e-40 [213-480]NB-ARC:3.9e-53 [585-643]LRR_8:1.7e-08
RC5G0675300	rc05	78464769	78465971	TIR-NBS		P-loop[122-130] Kin-2[197-204] RNBS-B[226-232] GLPL[284-290]	[5-72]TIR:1.6e-06 [101-371]NB-ARC:1.2e-46
RC5G0675800	rc05	78567578	78569079	NBS-LRR		P-loop[20-28] Kin-2[95-102] RNBS-B[124-130] GLPL[181-187]	[10-269]NB-ARC:6.9e-52 [367-425]LRR_8:2.3e-12 [434-473]LRR_8:0.00049

RC5G0687100	rc05	79582027	79588091	TIR-NBS-LRR		P-loop[256-264] Kin-2[331-338] RNBS-B[360-366] GLPL[419-425]	[52-221]TIR:1.2e-40 [235-509]NB-ARC:5.6e-51 [608-665]LRR_8:2.7e-09
RC5G0687500	rc05	79603288	79605968	TIR-NBS-LRR	bHLH-MYC_N	P-loop[451-459] Kin-2[526-533] RNBS-B[555-561] GLPL[613-619]	[15-195]bHLH-MYC_N:7.5e-55 [242-407]TIR:1.6e-41 [430-702]NB-ARC:4.4e-52 [782-838]LRR_8:0.00037
RC5G0688900	rc05	79846207	79853071	TIR-NBS-LRR		P-loop[1076-1084] Kin-2[1151-1158] RNBS-B[1180-1186] GLPL[1238-1244]	[5-81]TIR:9.7e-07 [101-372]NB-ARC:3.9e-51 [470-526]LRR_8:1.2e-06 [1055-1330]NB-ARC:3e-46 [1421-1479]LRR_8:2.3e-09
RC5G0689200	rc05	79887787	79891821	TIR-NBS-LRR	bHLH-MYC_N	P-loop[454-462] Kin-2[529-536] RNBS-B[558-564] GLPL[616-622]	[16-195]bHLH-MYC_N:2.6e-53 [245-409]TIR:8e-41 [433-705]NB-ARC:9.5e-52 [804-862]LRR_8:1e-07 [876-930]LRR_8:0.0096 [1096-1128]LRR_4:0.0064
RC5G0689800	rc05	79921071	79925722	TIR-NBS-LRR		P-loop[284-292] Kin-2[359-366] RNBS-B[388-394] GLPL[446-452]	[76-241]TIR:2.8e-45 [264-530]NB-ARC:6.5e-49 [669-728]LRR_8:9.9e-09
RC5G0692400	rc05	80217334	80218912	NBS-LRR		P-loop[14-22] Kin-2[90-97] RNBS-B[119-125] GLPL[178-184]	[5-287]NB-ARC:3.4e-36 [378-434]LRR_8:2.2e-07 [435-445]LRR_4:0.00012 [446-464]LRR_4:0.00037 [465-480]LRR_8:0.0041
RC5G0693200	rc05	80412660	80413992	NBS		P-loop[35-43] Kin-2[110-117] RNBS-B[139-145] GLPL[196-202]	[14-286]NB-ARC:2.1e-54
RC5G0693300	rc05	80481072	80482660	NBS-LRR		P-loop[20-28] Kin-2[95-102] RNBS-B[124-130] GLPL[181-187]	[1-269]NB-ARC:4e-49 [370-427]LRR_8:6.9e-11
RC5G0693800	rc05	80551223	80552865	NBS-LRR		P-loop[16-24] Kin-2[91-98] RNBS-B[120-126] GLPL[178-184]	[4-265]NB-ARC:1.4e-46 [362-420]LRR_8:1.8e-10
RC5G0694500	rc05	80684718	80686586	NBS-LRR	TniB	P-loop[43-51] Kin-2[118-125] RNBS-B[147-153] GLPL[206-212]	[16-25]TniB:0.004 [26-288]NB-ARC:4.5e-52 [392-450]LRR_8:9e-09 [450-463]LRR_4:0.0039 [464-519]LRR_8:1.8e-07
RC5G0694800	rc05	80695805	80701646	NBS-LRR		P-loop[33-41] Kin-2[108-115] RNBS-B[137-143] GLPL[195-201]	[12-282]NB-ARC:1.3e-53 [381-439]LRR_8:1.8e-09
RC5G0695300	rc05	80730554	80736129	TIR-NBS-LRR		P-loop[229-237] Kin-2[304-311] RNBS-B[333-339] GLPL[392-398]	[23-190]TIR:6.4e-42 [210-477]NB-ARC:3.8e-55 [579-637]LRR_8:5e-05
RC5G0695400	rc05	80792576	80794250	NBS-LRR		P-loop[14-22] Kin-2[89-96] RNBS-B[118-124] GLPL[177-183]	[5-285]NB-ARC:1.5e-35 [377-433]LRR_8:1.3e-07 [434-444]LRR_4:0.00023 [445-463]LRR_4:0.0014 [464-479]LRR_8:0.0022
RC5G0697200	rc05	80998711	81009255	TIR-NBS-LRR		P-loop[465-473] Kin-2[540-547] RNBS-B[569-575] GLPL[628-634]	[259-425]TIR:8.5e-45 [447-719]NB-ARC:1.6e-48 [817-874]LRR_8:2.7e-08
RC5G0698000	rc05	81141362	81152942	TIR-NBS-LRR		P-loop[2668-2676] Kin-2[2743-2750] RNBS-B[2772-2778] GLPL[2830-2836]	[15-280]NB-ARC:5.1e-52 [384-440]LRR_8:1.6e-07 [456-510]LRR_8:0.00022 [988-1153]TIR:1.6e-41 [1172-1446]NB-ARC:3.7e-48 [1537-1698]TIR:6.4e-37 [1722-1990]NB-ARC:5.5e-51 [2088-2146]LRR_8:1.6e-06 [2649-2920]NB-ARC:6.5e-47 [3034-3090]LRR_8:4.7e-08
RC5G0698100	rc05	81165421	81169898	TIR-NBS-LRR		P-loop[126-134] Kin-2[201-208] RNBS-B[230-236] GLPL[288-294]	[6-82]TIR:5.8e-06 [105-377]NB-ARC:5.8e-52 [476-534]LRR_8:7.6e-08 [768-800]LRR_4:0.0046

RC5G0699100	rc05	81344789	81350645	TIR-NBS-LRR	P-loop[222-230] Kin-2[297-304] RNBS-B[326-332] GLPL[384-390]	[18-194]TIR:4.5e-39 [200-472]NB-ARC:1.9e-53 [575-633]LRR_8:2.2e-07 [912-948]LRR_4:0.0089
RC5G0699900	rc05	81493380	81497501	NBS-LRR	P-loop[36-44] Kin-2[111-118] RNBS-B[140-146] GLPL[199-205]	[19-281]NB-ARC:4.7e-51 [385-443]LRR_8:4.2e-09 [457-512]LRR_8:3.7e-07
RC5G0700800	rc05	81678593	81683206	TIR-NBS-LRR	P-loop[461-469] Kin-2[536-543] RNBS-B[565-571] GLPL[624-630]	[17-182]TIR:7.7e-40 [258-420]TIR:4.4e-43 [441-732]NB-ARC:4.6e-39 [824-879]LRR_8:1.7e-07 [880-926]LRR_8:0.00097
RC5G0700900	rc05	81694590	81695899	NBS-LRR	P-loop[16-24] Kin-2[91-98] RNBS-B[120-126] GLPL[178-184]	[6-266]NB-ARC:6.3e-54 [364-408]LRR_8:7.3e-05
RC5G0701600	rc05	81772931	81775477	TIR-NBS-LRR	P-loop[272-280] Kin-2[347-354] RNBS-B[376-382] GLPL[437-443]	[68-232]TIR:5.2e-41 [251-524]NB-ARC:9.2e-51 [589-647]LRR_8:1.9e-10
RC5G0703200	rc05	81915928	81920392	TIR-NBS-LRR	P-loop[465-473] Kin-2[540-547] RNBS-B[569-575] GLPL[628-634]	[28-193]TIR:1.3e-38 [262-428]TIR:1.2e-44 [445-734]NB-ARC:5.2e-39 [828-884]LRR_8:8.9e-08 [885-895]LRR_4:0.00021 [896-905]LRR_4:0.0054
RC5G0703900	rc05	82019665	82022336	TIR-NBS-LRR	P-loop[278-286] Kin-2[353-360] RNBS-B[382-388] GLPL[440-446]	[74-239]TIR:9.8e-43 [258-529]NB-ARC:3.9e-53 [626-684]LRR_8:2.5e-05
RC5G0704100	rc05	82052760	82054580	NBS-LRR	P-loop[33-41] Kin-2[108-115] RNBS-B[137-143] GLPL[195-201]	[12-283]NB-ARC:4.9e-57 [381-438]LRR_8:4.2e-08 [448-484]LRR_8:0.00025
RC5G0704400	rc05	82106576	82108154	NBS-LRR	P-loop[20-28] Kin-2[95-102] RNBS-B[124-130] GLPL[185-191]	[1-273]NB-ARC:1.6e-50 [372-430]LRR_8:2.2e-10
RC5G0707000	rc05	82427759	82432941	TIR-NBS-LRR	P-loop[126-134] Kin-2[216-223] RNBS-B[245-251] GLPL[304-310]	[4-82]TIR:5.8e-06 [107-394]NB-ARC:3.4e-38 [492-548]LRR_8:0.00014
RC5G0707800	rc05	82510963	82516475	TIR-NBS-LRR	P-loop[26-34] Kin-2[102-109] RNBS-B[129-135] GLPL[185-191]	[3-251]NB-ARC:5.5e-27 [252-314]TIR:9.7e-08 [346-516]TIR:5.5e-27 [547-697]TIR:6.5e-26 [734-999]NB-ARC:3.8e-49 [1100-1156]LRR_8:1.1e-06
RC5G0716100	rc05	83403364	83404578	TIR-NBS	P-loop[125-133] Kin-2[204-211] RNBS-B[231-237] GLPL[288-294]	[2-88]TIR:1.5e-15 [104-294]NB-ARC:2.1e-21
RC5G0717400	rc05	83546016	83547738	NBS	P-loop[19-27] Kin-2[98-105] RNBS-B[125-131] GLPL[185-191]	[5-251]NB-ARC:7.3e-37
RC5G0718200	rc05	83610483	83613250	TIR-NBS	P-loop[223-231] Kin-2[302-309] RNBS-B[329-335] GLPL[388-394]	[23-183]TIR:3e-48 [199-454]NB-ARC:1.5e-30
RC6G0005500	rc06	717905	722131	TIR-NBS-LRR	P-loop[215-223] Kin-2[292-299] RNBS-B[319-325] GLPL[378-384]	[12-182]TIR:7.5e-50 [204-443]NB-ARC:4.2e-33 [666-725]LRR_8:0.0021 [997-1053]LRR_8:7.9e-06
RC6G0006000	rc06	738780	743774	TIR-NBS-LRR	P-loop[215-223] Kin-2[292-299] RNBS-B[319-325] GLPL[378-384]	[12-182]TIR:2.9e-49 [203-429]NB-ARC:1.4e-31 [642-682]LRR_4:0.0024 [831-886]LRR_8:2.7e-06
RC6G0010700	rc06	1085292	1090720	TIR-NBS-LRR	P-loop[222-230] Kin-2[299-306] RNBS-B[326-332] GLPL[385-391]	[12-192]TIR:9.5e-43 [198-212]AAA_16:3.3e-05 [213-452]NB-ARC:7.4e-31 [603-621]LRR_3:3.8e-06 [695-752]LRR_8:8.4e-06 [860-903]LRR_4:0.00025 [904-914]LRR_8:0.0015
RC6G0012000	rc06	1203564	1208147	TIR-NBS-LRR	P-loop[221-229] Kin-2[293-300] RNBS-B[320-326] GLPL[379-385]	[20-181]TIR:3.5e-34 [199-445]NB-ARC:5.1e-30 [595-613]LRR_3:0.004 [854-912]LRR_8:0.0001 [912-922]LRR_4:0.00053

RC6G0019700	rc06	1964771	1968620	NBS-LRR		P-loop[37-45] Kin-2[113-120] RNBS-B[145-151] GLPL[206-212]	[14-271]NB-ARC:5.9e-39 [437-452]LRR_3:0.0035 [577-630]LRR_8:0.0052
RC6G0046600	rc06	4748698	4750511	TIR-NBS		P-loop[221-229] Kin-2[298-305] RNBS-B[325-331] GLPL[384-390]	[18-188]TIR:2.9e-47 [209-449]NB-ARC:1.5e-30
RC6G0052000	rc06	5413192	5415967	NBS-LRR		P-loop[27-35] Kin-2[105-112] RNBS-B[132-138] GLPL[191-197]	[18-262]NB-ARC:7.6e-31 [409-427]LRR_3:1.9e-06 [501-557]LRR_8:1.9e-05 [646-669]LRR_8:0.0052 [670-713]LRR_4:0.00028
RC6G0093200	rc06	10156940	10162501	CC-NBS-LRR	RPW8	P-loop[187-195] Kin-2[264-271] RNBS-B[293-299] GLPL[355-361]	[22-93]RPW8:0.00035 [166-445]NB-ARC:6.7e-57 [574-627]LRR_8:3.2e-05
RC6G0107000	rc06	11477082	11479066	NBS-LRR		P-loop[172-180] Kin-2[247-254] RNBS-B[279-285] GLPL[338-344]	[153-423]NB-ARC:2.8e-55 [524-583]LRR_8:1.6e-09 [592-629]LRR_8:0.00025
RC6G0123900	rc06	13531770	13533972	CC-NBS-LRR		P-loop[186-194] Kin-2[268-275] RNBS-B[295-301] GLPL[354-360]	[164-444]NB-ARC:1.8e-67 [544-601]LRR_8:1.3e-06 [618-670]LRR_8:2.4e-05
RC6G0124200	rc06	13557623	13561228	CC-NBS-LRR	YqeY	P-loop[222-230] Kin-2[304-311] RNBS-B[331-337] GLPL[390-396]	[109-162]YqeY:0.0033 [200-480]NB-ARC:1.1e-64 [581-637]LRR_8:5e-09 [655-708]LRR_8:0.0081
RC6G0157600	rc06	16429923	16432940	TIR-NBS		P-loop[117-125] Kin-2[196-203] RNBS-B[223-229] GLPL[283-289]	[4-79]TIR:1.8e-08 [95-354]NB-ARC:6.4e-34
RC6G0160400	rc06	16755259	16771333	TIR-NBS-LRR		P-loop[252-260] Kin-2[331-338] RNBS-B[358-364] GLPL[416-422]	[24-145]TIR:2.9e-40 [243-482]NB-ARC:1.7e-29 [687-726]LRR_4:0.0036
RC6G0160500	rc06	16774763	16779151	TIR-NBS-LRR		P-loop[217-225] Kin-2[296-303] RNBS-B[323-329] GLPL[382-388]	[11-177]TIR:6.2e-49 [193-446]NB-ARC:1.9e-31 [624-657]LRR_4:0.0065 [720-758]LRR_4:0.0014 [759-775]LRR_8:0.0041
RC6G0183500	rc06	20403767	20408944	TIR-NBS		P-loop[222-230] Kin-2[301-308] RNBS-B[328-334] GLPL[387-393]	[17-186]TIR:1.6e-48 [198-455]NB-ARC:1.9e-23
RC6G0197000	rc06	22624488	22628680	TIR-NBS-LRR		P-loop[262-270] Kin-2[341-348] RNBS-B[368-374] GLPL[430-436]	[33-189]TIR:8.8e-48 [250-494]NB-ARC:1.1e-29 [647-702]LRR_8:0.00061 [740-763]LRR_8:0.0017 [764-820]LRR_8:1.6e-05
RC6G0197300	rc06	22658497	22666183	TIR-NBS-LRR		P-loop[229-237] Kin-2[308-315] RNBS-B[335-341] GLPL[394-400]	[26-191]TIR:7.1e-43 [212-460]NB-ARC:4.6e-30 [635-673]LRR_4:0.0007 [674-697]LRR_4:0.001 [730-767]LRR_4:0.0031 [768-785]LRR_8:0.0047
RC6G0202400	rc06	23439171	23442402	TIR-NBS-LRR		P-loop[226-234] Kin-2[305-312] RNBS-B[332-338] GLPL[392-398]	[23-185]TIR:5.6e-45 [204-461]NB-ARC:6.1e-31 [655-693]LRR_4:0.00058
RC6G0203300	rc06	23594062	23598587	NBS-LRR		P-loop[1-8] Kin-2[72-79] RNBS-B[102-108] GLPL[164-170]	[1-250]NB-ARC:3.6e-51 [355-385]LRR_8:0.00032 [386-440]LRR_8:0.00014
RC6G0214000	rc06	25147821	25151340	CC-NBS-LRR		P-loop[200-208] Kin-2[287-294] RNBS-B[316-322] GLPL[378-384]	[195-465]NB-ARC:4.1e-60 [586-631]LRR_8:0.0013 [632-667]LRR_4:0.0011 [999-1056]LRR_8:0.004
RC6G0216200	rc06	25400339	25403357	NBS-LRR	RPW8	P-loop[181-189] Kin-2[256-263] RNBS-B[285-291] GLPL[347-353]	[3-58]RPW8:0.0025 [154-434]NB-ARC:3.5e-63 [556-610]LRR_8:0.0011

RC6G0224800	rc06	26889034	26894819	TIR-NBS-LRR		P-loop[221-229] Kin-2[299-306] RNBS-B[326-332] GLPL[383-389]	[15-195]TIR:3.9e-46 [197-445]NB-ARC:3.6e-32 [666-685]LRR_3:4.9e-05 [784-806]LRR_4:0.0076 [807-846]LRR_4:0.0045 [997-1037]LRR_4:0.0066 [1091-1131]LRR_4:0.0075 [1350-1405]LRR_8:9.9e-05
RC6G0241800	rc06	30458368	30464847	TIR-NBS-LRR		P-loop[233-241] Kin-2[312-319] RNBS-B[339-345] GLPL[398-404]	[29-194]TIR:2.1e-50 [210-221]ATPase_2:0.00028 [222-463]NB-ARC:1.8e-31 [615-634]LRR_3:0.00016 [755-811]LRR_8:0.0034 [865-920]LRR_8:0.0041
RC6G0256400	rc06	33268274	33273327	NBS-LRR		P-loop[193-201] Kin-2[275-282] RNBS-B[302-308] GLPL[366-372]	[173-458]NB-ARC:1.1e-83 [600-654]LRR_8:0.00027
RC6G0259700	rc06	33714369	33715887	NBS-LRR		P-loop[65-73] Kin-2[140-147] RNBS-B[169-175] GLPL[228-234]	[43-317]NB-ARC:3.6e-51 [413-470]LRR_8:4.5e-08
RC6G0262100	rc06	34010916	34013831	CC-NBS-LRR		P-loop[210-218] Kin-2[286-293] RNBS-B[315-321] GLPL[377-383]	[199-464]NB-ARC:1.7e-68 [590-644]LRR_8:2.6e-09
RC6G0265700	rc06	34555768	34566304	TIR-NBS-LRR		P-loop[227-235] Kin-2[306-313] RNBS-B[333-339] GLPL[392-398]	[23-189]TIR:4.2e-49 [209-459]NB-ARC:2.7e-31 [838-877]LRR_4:4.6e-05
RC6G0270900	rc06	35315757	35318664	TIR-NBS		P-loop[225-233] Kin-2[305-312] RNBS-B[332-338] GLPL[391-397]	[21-186]TIR:1.4e-50 [203-456]NB-ARC:6.1e-31
RC6G0271200	rc06	35365251	35371062	NBS		P-loop[35-43] Kin-2[115-122] RNBS-B[142-148] GLPL[201-207]	[13-266]NB-ARC:1.8e-31
RC6G0276500	rc06	36143986	36148656	TIR-NBS-LRR		P-loop[230-238] Kin-2[309-316] RNBS-B[336-342] GLPL[395-401]	[22-195]TIR:8.5e-47 [202-214]AAA_16:0.0025 [215-462]NB-ARC:9.4e-37 [620-639]LRR_3:4.4e-05 [665-705]LRR_4:0.0025 [900-940]LRR_4:0.0099
RC6G0284500	rc06	37427969	37431126	CC-NBS-LRR		P-loop[232-240] Kin-2[314-321] RNBS-B[341-347] GLPL[405-411]	[209-498]NB-ARC:1.5e-84 [637-693]LRR_8:4.2e-06 [884-926]LRR_4:0.0037
RC6G0290600	rc06	38547981	38551114	NBS-LRR		P-loop[194-202] Kin-2[276-283] RNBS-B[303-309] GLPL[367-373]	[172-459]NB-ARC:1.9e-82 [571-627]LRR_8:5e-05 [628-645]LRR_8:0.00018
RC6G0314900	rc06	41749290	41755946	CC-NBS-LRR		P-loop[180-188] Kin-2[254-261] RNBS-B[279-285] GLPL[339-345]	[160-429]NB-ARC:5.2e-50 [607-662]LRR_8:6.4e-05
RC6G0322100	rc06	42577765	42580401	TIR-NBS		P-loop[222-230] Kin-2[301-308] RNBS-B[328-334] GLPL[388-394]	[18-186]TIR:1e-46 [201-454]NB-ARC:2e-29 [613-631]LRR_3:0.0022
RC6G0323100	rc06	42663725	42665265	NBS		P-loop[1-8] Kin-2[79-86] RNBS-B[106-112] GLPL[166-172]	[1-231]NB-ARC:6.6e-24 [398-413]LRR_3:0.00056
RC6G0323700	rc06	42727143	42728649	CC-NBS		P-loop[60-68] Kin-2[134-141] RNBS-B[161-167] GLPL[220-226]	[41-303]NB-ARC:8.7e-42
RC6G0362300	rc06	47266486	47268853	TIR-NBS		P-loop[219-227] Kin-2[298-305] RNBS-B[325-331] GLPL[384-390]	[16-180]TIR:6.1e-46 [196-447]NB-ARC:3e-33
RC6G0374500	rc06	48557514	48566076	TIR-NBS		P-loop[218-226] Kin-2[297-304] RNBS-B[324-330] GLPL[383-389]	[16-185]TIR:3.5e-41 [201-456]NB-ARC:5e-33 [610-628]LRR_3:2.2e-05
RC6G0478700	rc06	57862436	57865361	NBS	RPW8	P-loop[213-221] Kin-2[290-297] RNBS-B[313-319] GLPL[370-376]	[9-131]RPW8:2.8e-15 [197-455]NB-ARC:6.2e-35
RC7G0023600	rc07	1475070	1477290	NBS-LRR		P-loop[202-210] Kin-2[278-285] RNBS-B[312-318] GLPL[374-380]	[192-465]NB-ARC:1.9e-63 [589-644]LRR_8:1.5e-07
RC7G0033200	rc07	2131265	2134171	NBS-LRR		P-loop[85-93] Kin-2[159-166] RNBS-B[193-199] GLPL[254-260]	[53-67]AAA_16:0.00068 [68-342]NB-ARC:1.9e-62 [465-519]LRR_8:9.7e-05
RC7G0033400	rc07	2140917	2144390	CC-NBS-LRR		P-loop[204-212] Kin-2[278-285] RNBS-B[312-318] GLPL[373-379]	[172-183]AAA_16:0.0022 [184-462]NB-ARC:1.7e-64 [584-639]LRR_8:0.00017

RC7G0133900	rc07	10173706	10179266	TIR-NBS-LRR	P-loop[226-234] Kin-2[305-312] RNBS-B[332-338] GLPL[392-398]	[23-187]TIR:1.9e-47 [204-458]NB-ARC:1e-33 [604-630]LRR_8:0.0025 [631-666]LRR_4:0.00099
RC7G0225300	rc07	18963510	18972518	CC-NBS	P-loop[258-266] Kin-2[333-340] RNBS-B[357-363] GLPL[415-421]	[238-498]NB-ARC:7.4e-44
RC7G0235900	rc07	20055775	20061940	CC-NBS-LRR	P-loop[179-187] Kin-2[256-263] RNBS-B[280-286] GLPL[338-344]	[160-416]NB-ARC:2.8e-38 [596-652]LRR_8:0.0068
RC7G0244700	rc07	21016051	21020571	CC-NBS-LRR	P-loop[184-192] Kin-2[260-267] RNBS-B[284-290] GLPL[343-349]	[164-425]NB-ARC:1.2e-44 [608-664]LRR_8:9.2e-05
RC7G0245500	rc07	21075666	21080081	NBS-LRR	P-loop[19-27] Kin-2[95-102] RNBS-B[119-125] GLPL[178-184]	[2-260]NB-ARC:1.1e-42 [436-492]LRR_8:0.00016
RC7G0252400	rc07	21761370	21763976	CC-NBS-LRR	P-loop[242-250] Kin-2[316-323] RNBS-B[340-346] GLPL[399-405]	[221-481]NB-ARC:4e-44 [657-713]LRR_8:0.00017
RC7G0257200	rc07	22347270	22350134	CC-NBS	P-loop[204-212] Kin-2[279-286] RNBS-B[310-316] GLPL[371-377]	[187-460]NB-ARC:1.4e-59
RC7G0284000	rc07	25389959	25391583	NBS	P-loop[23-31] Kin-2[101-108] RNBS-B[128-134] GLPL[188-194]	[14-259]NB-ARC:1.4e-32
RC7G0284100	rc07	25432425	25434875	TIR-NBS	P-loop[251-259] Kin-2[330-337] RNBS-B[357-363] GLPL[417-423]	[46-213]TIR:5.4e-46 [228-491]NB-ARC:4.1e-37
RC7G0309000	rc07	28256648	28259491	NBS-LRR	P-loop[195-203] Kin-2[277-284] RNBS-B[304-310] GLPL[366-372]	[172-461]NB-ARC:1.1e-74 [576-598]LRR_8:0.0033 [599-649]LRR_8:0.00046
RC7G0319700	rc07	29485761	29488529	NBS-LRR	P-loop[199-207] Kin-2[281-288] RNBS-B[308-314] GLPL[370-376]	[177-463]NB-ARC:1.3e-76
RC7G0319900	rc07	29491118	29495220	NBS-LRR	P-loop[199-207] Kin-2[281-288] RNBS-B[308-314] GLPL[370-376]	[176-465]NB-ARC:2.8e-77 [605-655]LRR_8:0.0027
RC7G0320000	rc07	29512402	29515306	NBS-LRR	P-loop[196-204] Kin-2[278-285] RNBS-B[305-311] GLPL[367-373]	[173-462]NB-ARC:6.3e-76 [600-650]LRR_8:0.0027
RC7G0320100	rc07	29517534	29521547	NBS-LRR	P-loop[196-204] Kin-2[278-285] RNBS-B[305-311] GLPL[367-373]	[175-462]NB-ARC:1.8e-75 [600-650]LRR_8:0.0015
RC7G0320300	rc07	29539288	29542140	CC-NBS-LRR	P-loop[192-200] Kin-2[276-283] RNBS-B[303-309] GLPL[365-371]	[171-458]NB-ARC:7.7e-75 [579-634]LRR_8:0.00019 [635-652]LRR_8:0.0016
RC7G0320600	rc07	29549108	29551951	NBS	P-loop[192-200] Kin-2[274-281] RNBS-B[301-307] GLPL[363-369]	[170-456]NB-ARC:4.6e-70
RC7G0320900	rc07	29558456	29561305	CC-NBS-LRR	P-loop[192-200] Kin-2[276-283] RNBS-B[303-309] GLPL[365-371]	[171-458]NB-ARC:1.6e-75 [601-651]LRR_8:0.0043
RC7G0321100	rc07	29566741	29569691	NBS-LRR	P-loop[121-129] Kin-2[205-212] RNBS-B[232-238] GLPL[294-300]	[100-386]NB-ARC:6.6e-74 [507-562]LRR_8:9.1e-05 [563-580]LRR_8:0.0014
RC7G0321400	rc07	29647957	29650613	NBS-LRR	P-loop[121-129] Kin-2[205-212] RNBS-B[232-238] GLPL[294-300]	[100-387]NB-ARC:2.6e-71 [507-562]LRR_8:4.6e-05 [563-580]LRR_8:0.0011
RC7G0321800	rc07	29682960	29685842	CC-NBS-LRR	P-loop[198-206] Kin-2[282-289] RNBS-B[309-315] GLPL[370-376]	[190-463]NB-ARC:3.3e-72 [583-638]LRR_8:2.3e-05 [639-656]LRR_8:0.00045
RC7G0321900	rc07	29688306	29691152	NBS-LRR	P-loop[191-199] Kin-2[275-282] RNBS-B[302-308] GLPL[364-370]	[170-458]NB-ARC:1.9e-75 [577-632]LRR_8:7.3e-06 [633-650]LRR_8:0.0011
RC7G0322000	rc07	29706420	29708997	NBS-LRR	P-loop[101-109] Kin-2[176-183] RNBS-B[205-211] GLPL[263-269]	[81-347]NB-ARC:4.6e-49 [449-508]LRR_8:6.9e-10 [509-518]LRR_4:0.0021
RC7G0335300	rc07	31329692	31331125	NBS	P-loop[186-194] Kin-2[265-272] RNBS-B[292-298] GLPL[353-359]	[165-441]NB-ARC:2.1e-75
RC7G0400300	rc07	40886140	40891483	CC-TIR-NBS	P-loop[230-238] Kin-2[305-312] RNBS-B[334-340] GLPL[393-399]	[17-188]TIR:5.6e-47 [209-479]NB-ARC:8.3e-51
RC7G0416400	rc07	43459766	43467338	TIR-NBS-LRR	P-loop[226-234] Kin-2[304-311] RNBS-B[330-336] GLPL[389-395]	[22-194]TIR:2.1e-51 [204-454]NB-ARC:1.5e-31 [607-626]LRR_3:0.00018 [864-885]LRR_4:0.0079 [889-928]LRR_4:8.8e-05

RC7G0421200	rc07	44042650	44045331	NBS-LRR		P-loop[16-24] Kin-2[91-98] RNBS-B[120-126] GLPL[179-185]	[6-261]NB-ARC:1.8e-46 [368-426]LRR_8:7.3e-08 [459-495]LRR_8:0.00084
RC7G0421300	rc07	44047157	44048711	TIR-NBS		P-loop[171-179] Kin-2[246-253] RNBS-B[275-281] GLPL[333-339]	[1-135]TIR:2.5e-32 [152-418]NB-ARC:3.3e-49
RC7G0429300	rc07	45382761	45384998	NBS-LRR		P-loop[1-8] Kin-2[75-82] RNBS-B[106-112] GLPL[168-174]	[1-257]NB-ARC:4.3e-59 [348-388]LRR_8:1.9e-05 [401-436]LRR_8:0.0072
RC7G0429700	rc07	45486721	45489588	CC-NBS-LRR	DUF3656	P-loop[210-218] Kin-2[285-292] RNBS-B[316-322] GLPL[378-384]	[15-79]DUF3656:0.0047 [185-467]NB-ARC:5.8e-63 [558-598]LRR_8:2.6e-05 [611-646]LRR_8:0.0096
RC7G0429900	rc07	45552832	45555696	CC-NBS-LRR		P-loop[210-218] Kin-2[285-292] RNBS-B[316-322] GLPL[378-384]	[183-467]NB-ARC:5.4e-62 [558-598]LRR_8:4.7e-06
RC7G0452100	rc07	49220915	49227770	CC-TIR-NBS-LRR		P-loop[233-241] Kin-2[308-315] RNBS-B[335-341] GLPL[394-400]	[27-195]TIR:2.8e-47 [209-464]NB-ARC:3.1e-36 [641-696]LRR_8:0.00042 [716-742]LRR_8:0.00015 [743-783]LRR_4:0.00012
RC7G0452700	rc07	49282300	49289216	TIR-NBS-LRR		P-loop[232-240] Kin-2[308-315] RNBS-B[335-341] GLPL[394-400]	[27-186]TIR:2.9e-48 [209-461]NB-ARC:1.9e-32 [612-668]LRR_8:0.00036 [754-809]LRR_8:0.00045 [825-865]LRR_4:0.0011
RC7G0454900	rc07	49474139	49476752	CC-NBS-LRR		P-loop[222-230] Kin-2[299-306] RNBS-B[330-336] GLPL[392-398]	[213-482]NB-ARC:2.3e-63 [571-613]LRR_8:3.2e-06 [614-656]LRR_8:0.00019
RC7G0460600	rc07	50106007	50108856	CC-NBS-LRR		P-loop[211-219] Kin-2[286-293] RNBS-B[317-323] GLPL[379-385]	[180-191]AAA_16:0.0042 [192-464]NB-ARC:6e-61 [595-649]LRR_8:4.7e-07
RC7G0461100	rc07	50173383	50178731	CC-NBS-LRR		P-loop[210-218] Kin-2[285-292] RNBS-B[317-323] GLPL[379-385]	[179-190]AAA_16:0.0083 [191-464]NB-ARC:1.8e-61 [596-651]LRR_8:1.1e-06
RC7G0463700	rc07	50685389	50689356	NBS-LRR		P-loop[64-72] Kin-2[139-146] RNBS-B[170-176] GLPL[232-238]	[36-319]NB-ARC:1.7e-61 [410-453]LRR_8:1.4e-06 [454-496]LRR_8:1.7e-06
RC7G0463900	rc07	50732972	50735776	NBS-LRR	DUF3656	P-loop[205-213] Kin-2[280-287] RNBS-B[311-317] GLPL[373-379]	[24-79]DUF3656:0.0054 [177-462]NB-ARC:9e-61 [557-598]LRR_8:9.7e-06
RC7G0464500	rc07	50812770	50814191	CC-NBS	DUF3656	P-loop[205-213] Kin-2[282-289] RNBS-B[313-319] GLPL[375-381]	[20-79]DUF3656:0.0027 [180-460]NB-ARC:2.5e-58
RC7G0465100	rc07	50857572	50862536	CC-NBS-LRR		P-loop[214-222] Kin-2[289-296] RNBS-B[320-326] GLPL[382-388]	[183-192]AAA_16:0.00042 [193-470]NB-ARC:1.6e-63 [561-604]LRR_8:2.3e-07 [605-650]LRR_8:4.3e-06
RC7G0465900	rc07	50945167	50948053	CC-NBS-LRR		P-loop[218-226] Kin-2[295-302] RNBS-B[326-332] GLPL[388-394]	[193-474]NB-ARC:2.1e-57 [567-608]LRR_8:1.2e-06 [625-659]LRR_8:0.0015
RC7G0466400	rc07	50969677	50971132	NBS		P-loop[184-192] Kin-2[266-273] RNBS-B[294-300] GLPL[360-366]	[174-374]NB-ARC:3.8e-25
RC7G0466700	rc07	50980655	50990938	CC-NBS-LRR		P-loop[215-223] Kin-2[290-297] RNBS-B[321-327] GLPL[383-389]	[189-470]NB-ARC:1.3e-60 [557-599]LRR_8:1.9e-07 [607-650]LRR_8:0.0032
RC7G0467400	rc07	51045826	51049263	CC-NBS-LRR		P-loop[222-230] Kin-2[297-304] RNBS-B[328-334] GLPL[390-396]	[185-216]AAA_16:0.0077 [214-477]NB-ARC:4.3e-61 [571-603]LRR_8:0.00031 [604-659]LRR_8:0.00027
RC7G0468200	rc07	51139885	51140885	NBS		P-loop[96-104] Kin-2[178-185] RNBS-B[206-212] GLPL[272-278]	[63-84]AAA_16:0.00016 [86-286]NB-ARC:2.1e-27
RC7G0468400	rc07	51151640	51153007	CC-NBS	DUF3656	P-loop[205-213] Kin-2[282-289] RNBS-B[313-319] GLPL[375-381]	[21-79]DUF3656:0.0031 [179-454]NB-ARC:3.7e-60

RC7G0469000	rc07	51206574	51209390	CC-NBS-LRR	DUF3656	P-loop[204-212] Kin-2[281-288] RNBS-B[312-318] GLPL[374-380]	[19-79]DUF3656:0.005 [179-463]NB-ARC:8.6e-62 [560-615]LRR_8:2.6e-07 [616-640]LRR_8:8.9e-05
RC7G0469600	rc07	51262264	51265140	CC-NBS-LRR		P-loop[214-222] Kin-2[289-296] RNBS-B[320-326] GLPL[382-388]	[186-469]NB-ARC:1.3e-63 [564-603]LRR_8:5.8e-06 [616-652]LRR_8:0.00051
RC7G0470500	rc07	51326238	51328673	CC-NBS-LRR	DUF3656	P-loop[204-212] Kin-2[282-289] RNBS-B[313-319] GLPL[375-381]	[19-79]DUF3656:0.0072 [179-462]NB-ARC:7.9e-63 [554-595]LRR_8:2.1e-05 [603-647]LRR_8:0.0022
RC7G0470700	rc07	51341530	51343590	CC-NBS-LRR		P-loop[214-222] Kin-2[289-296] RNBS-B[320-326] GLPL[382-388]	[186-469]NB-ARC:1.1e-61 [561-602]LRR_8:8.7e-07 [613-654]LRR_8:0.003
RC7G0471000	rc07	51430939	51431977	CC-NBS		P-loop[96-104] Kin-2[178-185] RNBS-B[206-212] GLPL[272-278]	[63-84]AAA_16:0.00031 [86-286]NB-ARC:8.4e-26
RC7G0471600	rc07	51471327	51473867	NBS-LRR		P-loop[102-110] Kin-2[177-184] RNBS-B[208-214] GLPL[270-276]	[78-359]NB-ARC:5.3e-61 [464-521]LRR_8:2.7e-09
RC7G0475200	rc07	51830046	51831773	CC-NBS	DUF3656	P-loop[210-218] Kin-2[287-294] RNBS-B[318-324] GLPL[380-386]	[22-79]DUF3656:0.0083 [173-204]AAA_16:0.0042 [201-467]NB-ARC:1.4e-63
RC7G0484900	rc07	53080293	53083711	CC-NBS-LRR		P-loop[210-218] Kin-2[287-294] RNBS-B[318-324] GLPL[380-386]	[184-467]NB-ARC:4e-61 [561-603]LRR_8:6.7e-06 [604-649]LRR_8:6.7e-05
RC7G0486200	rc07	53255434	53258352	CC-NBS-LRR		P-loop[207-215] Kin-2[295-302] RNBS-B[326-332] GLPL[389-395]	[185-477]NB-ARC:7.7e-58 [587-635]LRR_8:2.7e-09
RC7G0486400	rc07	53319282	53321738	CC-NBS-LRR		P-loop[208-216] Kin-2[284-291] RNBS-B[315-321] GLPL[378-384]	[184-466]NB-ARC:4.8e-60 [576-623]LRR_8:1.7e-08 [631-655]LRR_4:0.0057
RC7G0486600	rc07	53337335	53338855	NBS-LRR		P-loop[55-63] Kin-2[131-138] RNBS-B[162-168] GLPL[225-231]	[31-308]NB-ARC:1.2e-57 [423-472]LRR_8:1.4e-08 [480-497]LRR_8:0.00047
RC7G0486900	rc07	53398628	53401504	CC-NBS-LRR		P-loop[208-216] Kin-2[285-292] RNBS-B[316-322] GLPL[379-385]	[184-466]NB-ARC:4.7e-57 [577-626]LRR_8:1.2e-07
RC7G0487800	rc07	53556508	53558706	CC-NBS-LRR		P-loop[207-215] Kin-2[283-290] RNBS-B[314-320] GLPL[377-383]	[183-465]NB-ARC:1.9e-61 [575-623]LRR_8:3e-09
RC7G0488000	rc07	53612846	53615618	CC-NBS-LRR		P-loop[209-217] Kin-2[304-311] RNBS-B[335-341] GLPL[397-403]	[185-484]NB-ARC:8.8e-59 [595-643]LRR_8:7e-08 [651-674]LRR_4:0.002
RC7G0488200	rc07	53658690	53661166	CC-NBS-LRR		P-loop[209-217] Kin-2[290-297] RNBS-B[321-327] GLPL[384-390]	[185-472]NB-ARC:4.5e-59 [582-598]LRR_8:6e-07 [599-654]LRR_8:5.2e-08
RC7G0488400	rc07	53703331	53706225	CC-NBS-LRR		P-loop[207-215] Kin-2[284-291] RNBS-B[315-321] GLPL[378-384]	[183-466]NB-ARC:2e-61 [576-625]LRR_8:5.3e-07 [626-654]LRR_4:0.0031
RC7G0488900	rc07	53790542	53792110	CC-NBS-LRR		P-loop[1-8] Kin-2[81-88] RNBS-B[112-118] GLPL[175-181]	[1-262]NB-ARC:9.7e-57 [373-422]LRR_8:1.1e-10 [423-446]LRR_4:0.00021
RC7G0497000	rc07	54968789	54971929	NBS-LRR		P-loop[62-70] Kin-2[137-144] RNBS-B[166-172] GLPL[227-233]	[35-314]NB-ARC:5.4e-60 [440-495]LRR_8:1.9e-06 [495-519]LRR_4:0.00038
RC7G0497100	rc07	55007186	55010884	CC-NBS-LRR	RPW8	P-loop[250-258] Kin-2[325-332] RNBS-B[354-360] GLPL[415-421]	[4-95]RPW8:0.0029 [223-502]NB-ARC:1.7e-65 [625-680]LRR_8:9.4e-05 [680-709]LRR_4:0.00049
RC7G0507600	rc07	56734367	56738253	TIR-NBS-LRR		P-loop[214-222] Kin-2[293-300] RNBS-B[320-326] GLPL[379-385]	[13-177]TIR:4.4e-47 [191-446]NB-ARC:5.8e-32 [643-701]LRR_8:0.00076
RC7G0508000	rc07	56794636	56797637	TIR-NBS-LRR		P-loop[128-136] Kin-2[207-214] RNBS-B[234-240] GLPL[292-298]	[1-84]TIR:5.7e-13 [104-359]NB-ARC:2.1e-37 [512-567]LRR_8:0.00046

RC7G0511800	rc07	57337077	57340131	TIR-NBS-LRR	P-loop[252-260] Kin-2[331-338] RNBS-B[358-364] GLPL[417-423]	[48-210]TIR:2.7e-45 [228-482]NB-ARC:1.9e-32 [652-690]LRR_8:0.00054
RC7G0527800	rc07	59327412	59329960	CC-NBS	P-loop[179-187] Kin-2[255-262] RNBS-B[279-285] GLPL[338-344]	[160-422]NB-ARC:5.7e-44
RC7G0530500	rc07	59779621	59782561	NBS-LRR	P-loop[197-205] Kin-2[272-279] RNBS-B[302-308] GLPL[363-369]	[169-450]NB-ARC:1.3e-62 [581-635]LRR_8:2.3e-06
RC7G0567300	rc07	65553075	65558854	TIR-NBS-LRR	P-loop[299-307] Kin-2[376-383] RNBS-B[402-408] GLPL[462-468]	[96-267]TIR:7.1e-49 [276-535]NB-ARC:1.2e-37 [681-700]LRR_3:0.0004 [926-984]LRR_8:0.00057
RC7G0567700	rc07	65614421	65619817	NBS-LRR	P-loop[26-34] Kin-2[103-110] RNBS-B[129-135] GLPL[189-195]	[3-259]NB-ARC:1.9e-37 [500-523]LRR_8:0.0047 [524-580]LRR_8:0.0003 [642-700]LRR_8:0.00065

Supplementary figures

Supp. Fig. 1 Evaluation zone and rating scale of black spot disease in rose

From 0 (no symptoms) to 5 (total defoliation of the plant) with a score of 1 for less than 25% of infected leaflets, a score of 2 for infection between 25 and 50%, a score of 3 for infection between 50 and 75% of infected leaflets and 4 for infection of 75% to 100% and partial defoliation.

Evaluation zone

Absence of symptoms

0 < x ≤ 25% of infected leaflets

25 < x ≤ 50% of infected leaflets

50 < x ≤ 75% of infected leaflets

75 < x ≤ 100% of infected leaflets + Partial defoliation

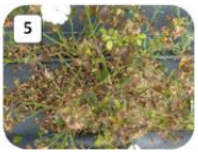

Total defoliation

Supp. Fig. 2 Overall mean of black spot disease (BSD) scores for three rose populations over several locations and years under natural infections in field

In the box plots, the boundaries of the box indicate the 25th percentile (on the lower part) and the 75th percentile (on the upper part). A thick line within the box marks the median, and a dot within the box marks the mean. Lines above and below the box indicate the 10th and 90th percentiles. Points above and below the whiskers indicate outliers outside the 10th and 90th percentiles. A: Data description for different years for OW population in Angers, B: Data description for different years for FW population in Angers, C: Data description for different years for HW population in Angers, Bellegarde and Diémoz. A Kruskal-Wallis test was used to compare the scoring years for HW and OW populations, and a Wilcoxon test was used to compare the two scoring years 2014-2018 for FW. For HW population, locations were considered separately. P-values of the tests are displayed on the graphs for all populations.

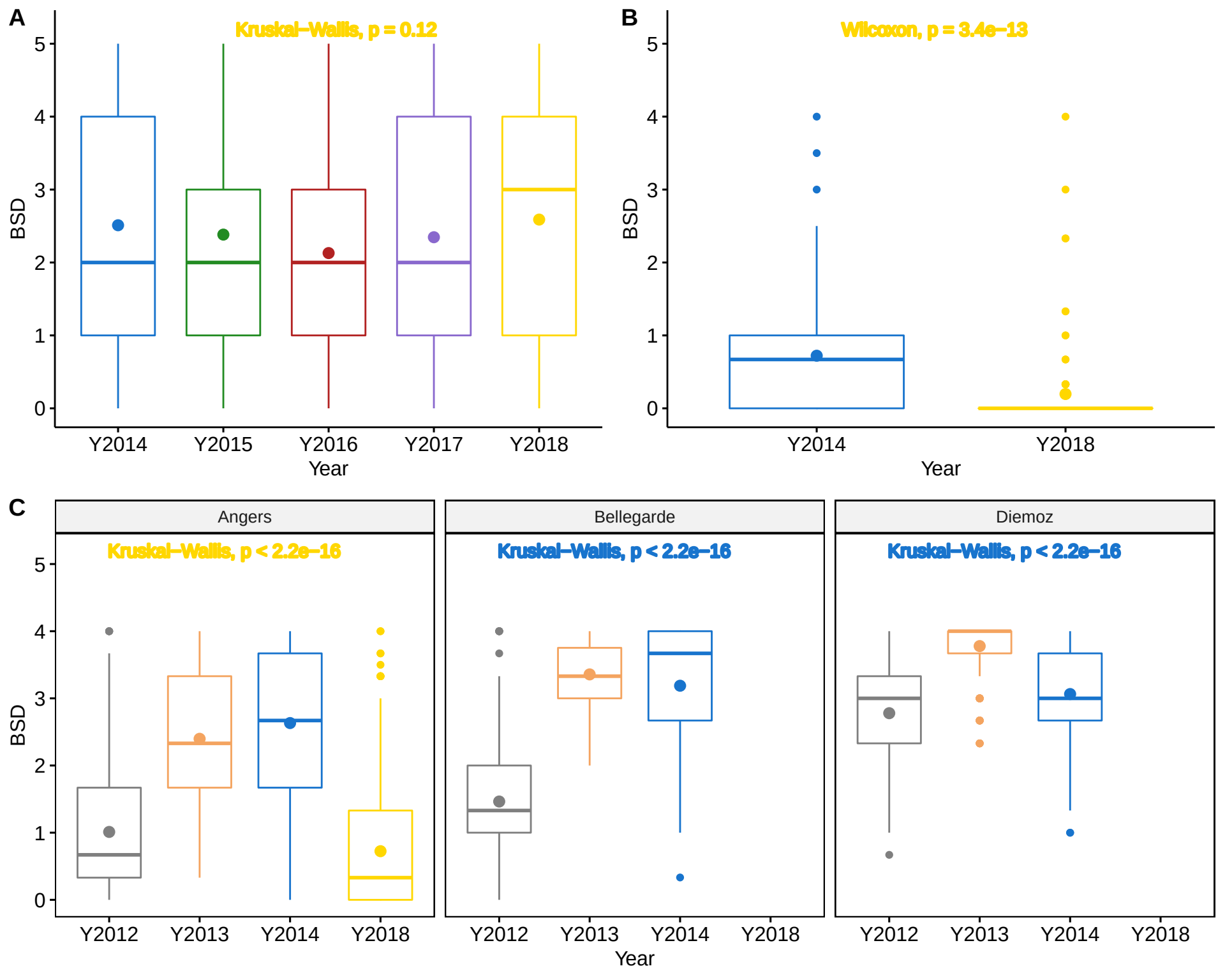
A
Kruskal–Wallis, p = 0.12
BSD
Year
Y2014
Y2015
Y2016
Y2017
Y2018
B
Wilcoxon, p = 3.4e−13
BSD
Year
Y2014
Y2018
C
Angers
Kruskal–Wallis, p < 2.2e−16
Bellegarde
Kruskal–Wallis, p < 2.2e−16
Diemoz
Kruskal–Wallis, p < 2.2e−16
BSD
Year
Y2012
Y2013
Y2014
Y2018

Supp. Fig. 3 Genetic linkage map of the male parent hybrid, *Rosa wichurana*, for OW population

Linkage groups (LG) names for the male map (B1 to B7) are placed above the corresponding linkage groups according to Spiller et al. 2011. Locus names are indicated on the right side of each LG. When several markers were mapped at a same position, one or two markers were reported corresponding to the unique loci or markers with different phases. SSR markers are indicated in red. Genetic distances (cM) are indicated on the left side of each LG.

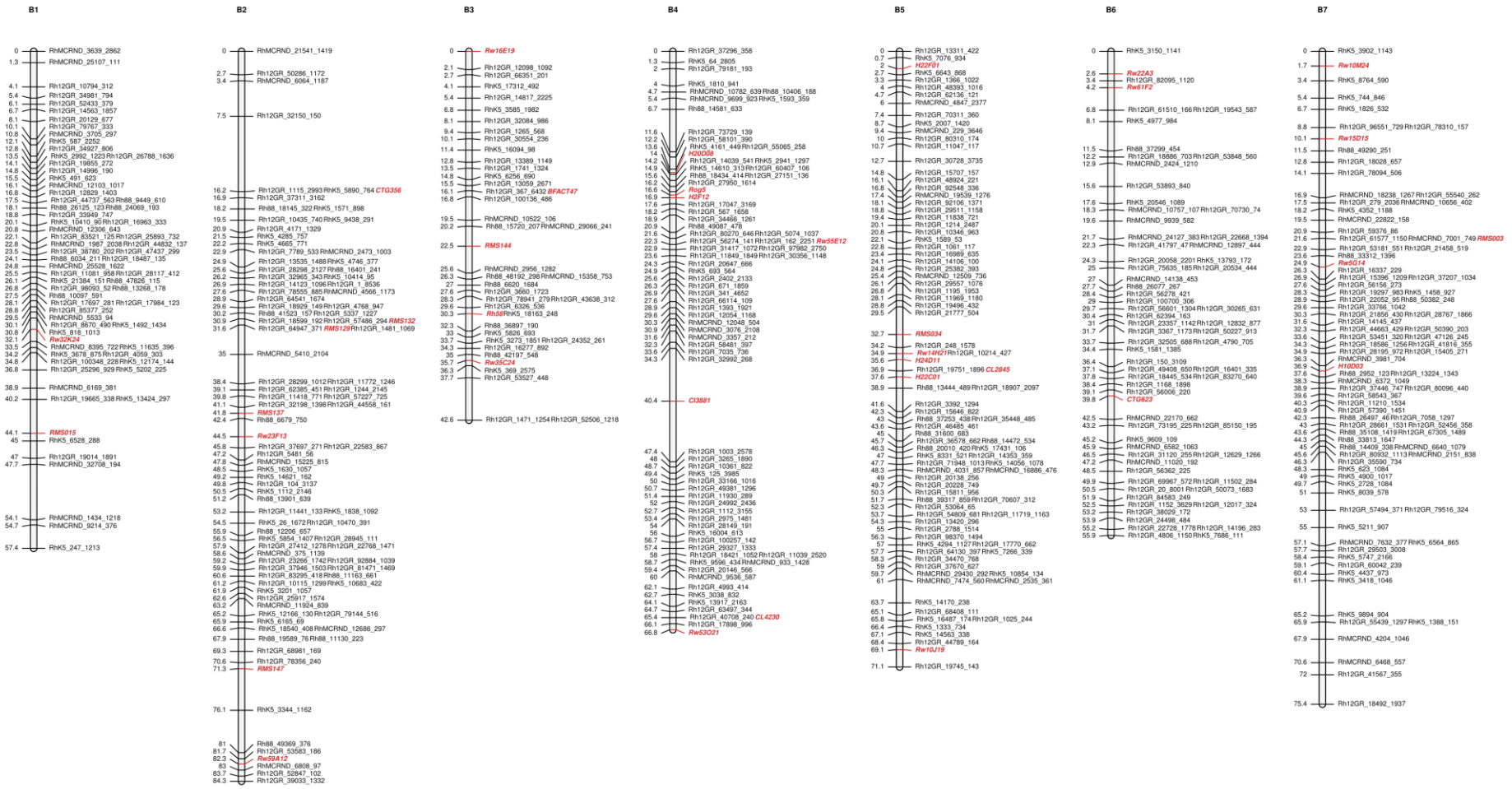

Supplementary figure 3: Genetic linkage map of the male parent hybrid, *Rosa wichurana*, for OW population

Supp. Fig. 4 Genetic linkage map of the female parent, *Rosa chinensis* 'Old Blush', for OW population

Linkage groups (LG) names for the female map (A1 to A7) are placed above the corresponding linkage groups. Locus names are indicated on the right side of each LG. When several markers were mapped at the same position, one or two markers were reported corresponding to the unique loci or markers with different phases. SSR markers are indicated in red. Genetic distances (cM) are indicated on the left side of each LG.

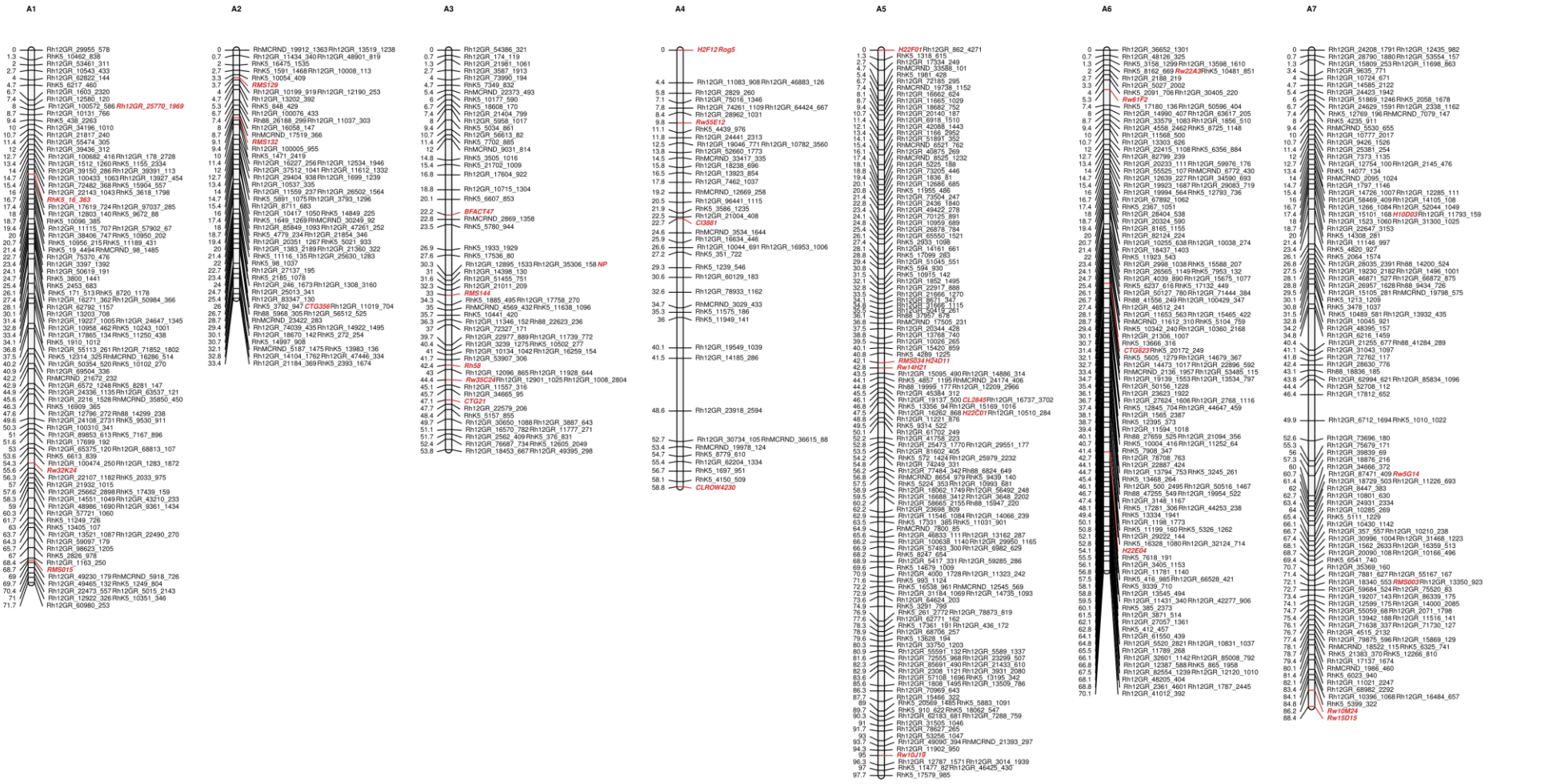

Supplementary figure 4: Genetic linkage map of the female parent, Rosa chinensis 'Old Blush', for OW population

Supp. Fig. 5 QTL mapping associated with black spot disease (BSD) resistance using a normal model with an CIM analysis for OW population for the male map

Linkage groups are named as follows: “B” for the male map and the number of the linkage group. LOD score for each year and the mean of all years are calculated using a Composite Interval Mapping method (CIM) and are displayed with different colors. The same set of colors is used to represent the α=0.05 LOD threshold for declaring significant QTL based on 1,000 permutations.

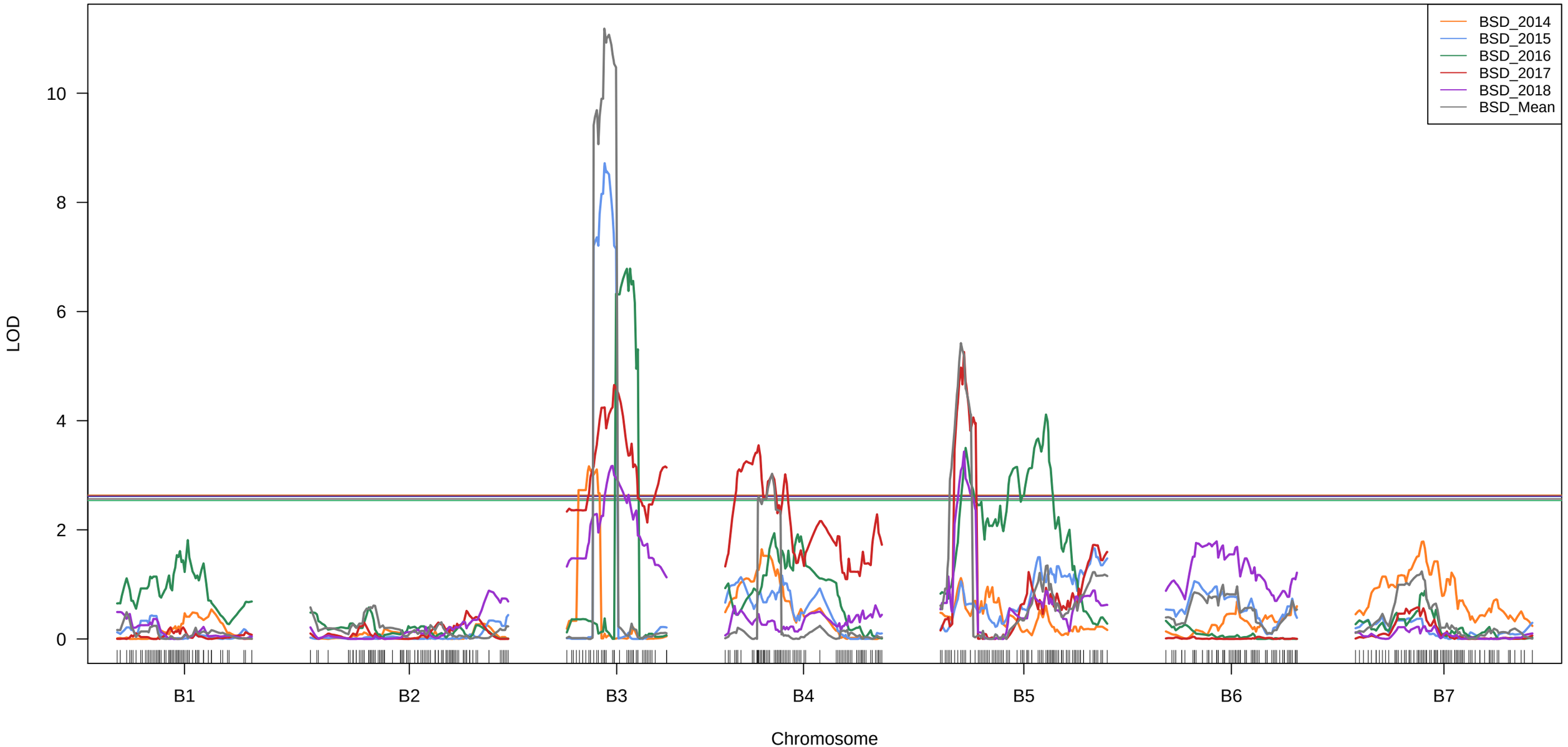
BSD_2014
BSD_2015
BSD_2016
BSD_2017
BSD_2018
BSD_Mean
LOD
0
2
4
6
8
10
B1
B2
B3
B4
B5
B6
B7
Chromosome

Supp. Fig. 6 QTL mapping associated with black spot disease resistance using a two-part model approach for non-normally distributed data of FW population for the male map

A and B: LOD curves for the two-part model for 2014 (A) and 2018 (B); LOD.π (penetrance, equivalent to binary model) displayed in blue, LOD.μ (severity, equivalent to normal model for non-spike phenotypes) displayed in green and LOD.π.μ (sum, representing the complete model) displayed in black; LOD thresholds are displayed in red with α=0.05 for declaring significant QTL based on 1,000 permutations.

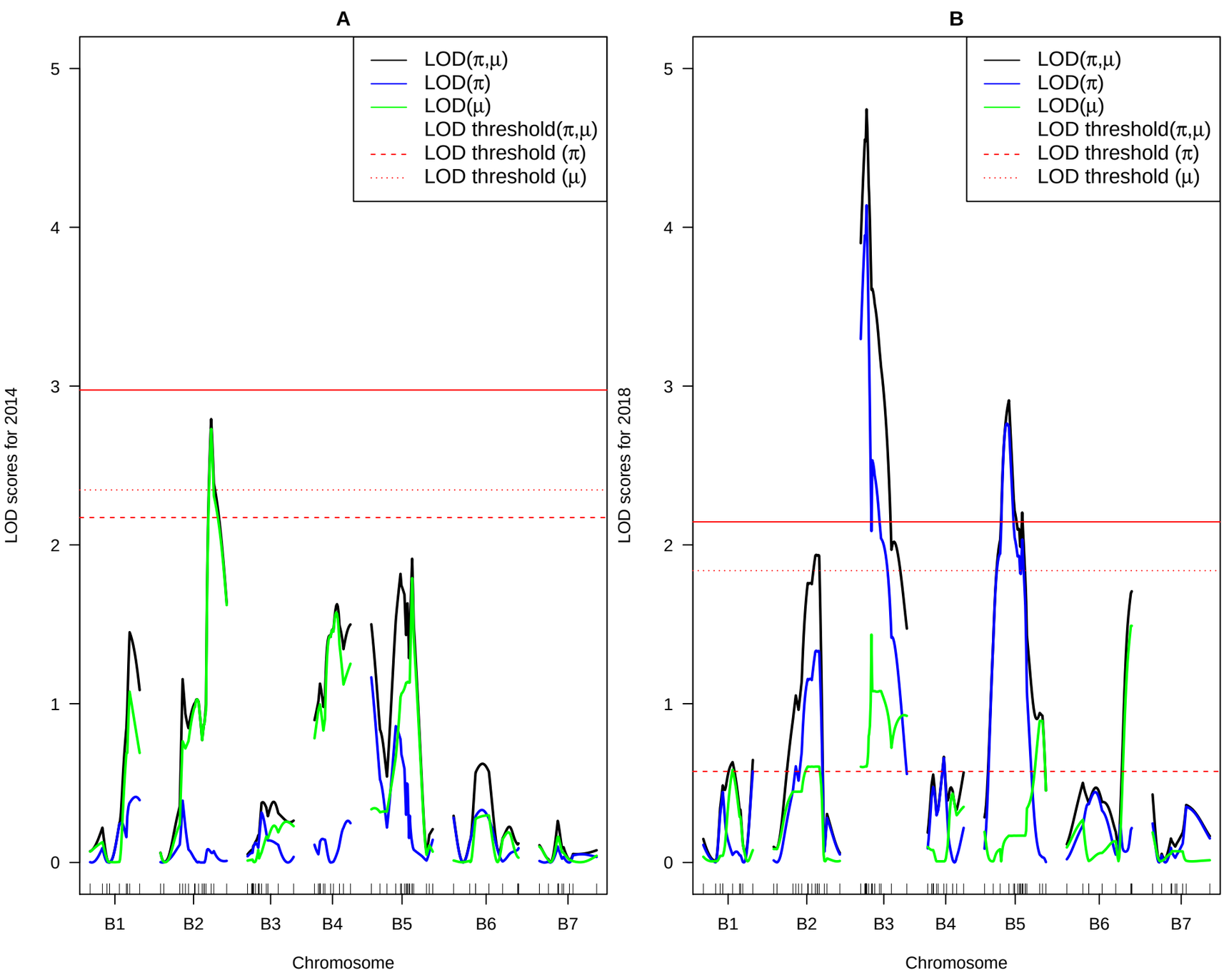
A
B
LOD(π,μ)
LOD(π)
LOD(μ)
LOD threshold(π,μ)
LOD threshold (π)
LOD threshold (μ)
LOD scores for 2014
LOD scores for 2018
0
1
2
3
4
5
B1
B2
B3
B4
B5
B6
B7
Chromosome

Supp. Fig. 7 QTL mapping associated with black spot disease (BSD) resistance for normally distributed data of HW population using a normal model with CIM analysis for the male map

Linkage groups are named as follow: “B” for the male map and the number of the linkage group. For HW population, BSD was scored in three locations: (A) Angers, (B) Bellegarde and (C) Diémoz. LOD score for each year and the mean of all years were calculated using a Composite Interval Mapping (CIM) method. The same set of colors is used to represent the different scoring years in the different locations. α=0.05 LOD threshold was used for declaring significant QTL based on 1,000 permutations.

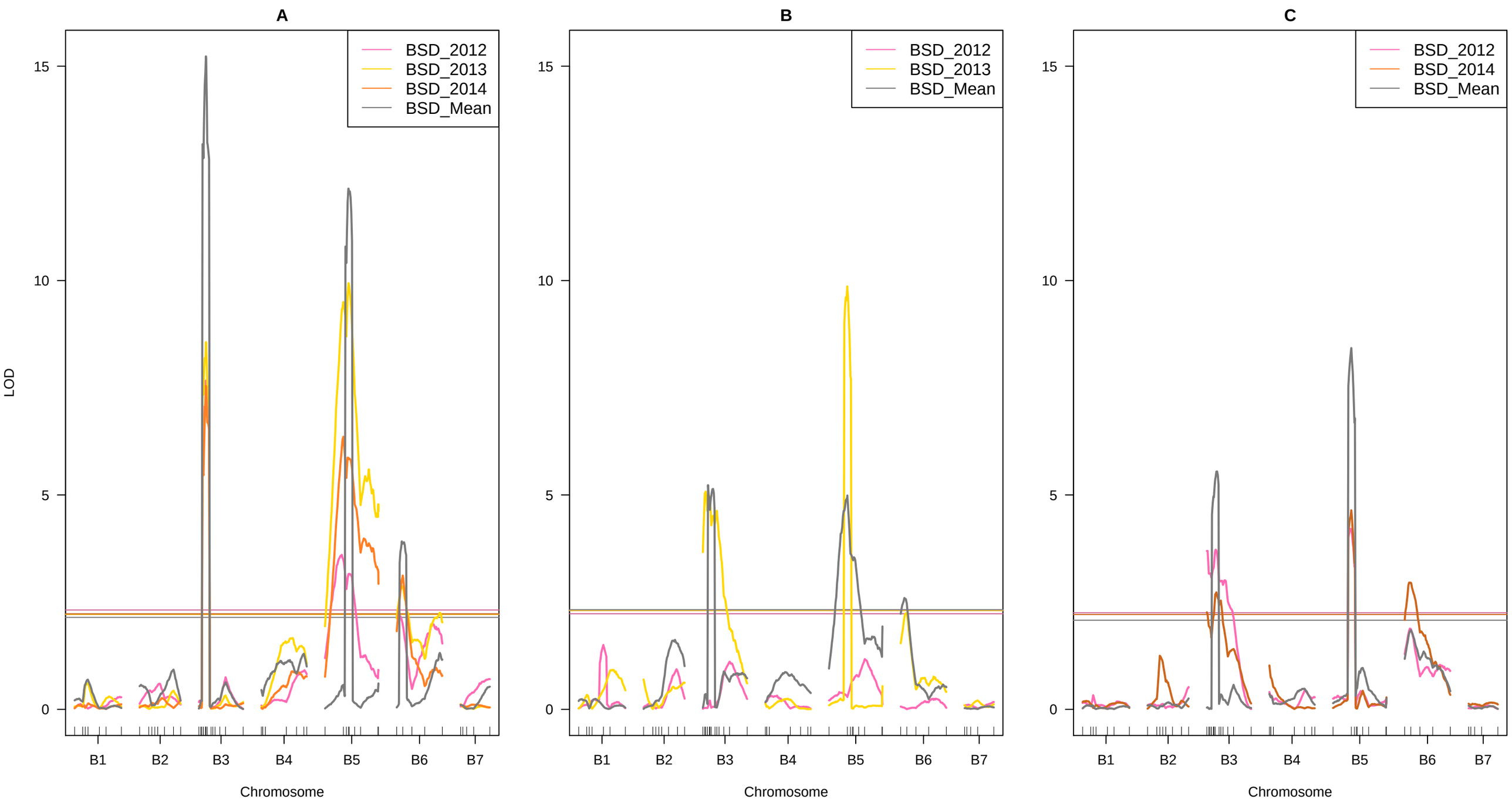
A
B
C
BSD_2012
BSD_2013
BSD_2014
BSD_Mean
LOD
15
10
5
0
B1
B2
B3
B4
B5
B6
B7
Chromosome

Supp. Fig. 8 QTL mapping with black spot disease (BSD) resistance using a two-part model approach for non-normally distributed data of HW population for the male map

Linkage groups are named as follows: “B” for the male map and the number of the linkage group. A to C: LOD curves of the two-part model analysis for spike-like distribution of HW BSD scoring years (Angers-2018 (A), Bellegarde-2014 (B) and Diémoz-2013 (C)); LOD.π (penetrance, equivalent to binary model) displayed in blue, LOD.μ (severity, equivalent to normal model for non-spike phenotypes) displayed in green and LOD.π.μ (sum, representing the complete model) displayed in black; LOD thresholds are displayed in red with α=0.05 for declaring significant QTL based on 1,000 permutations.

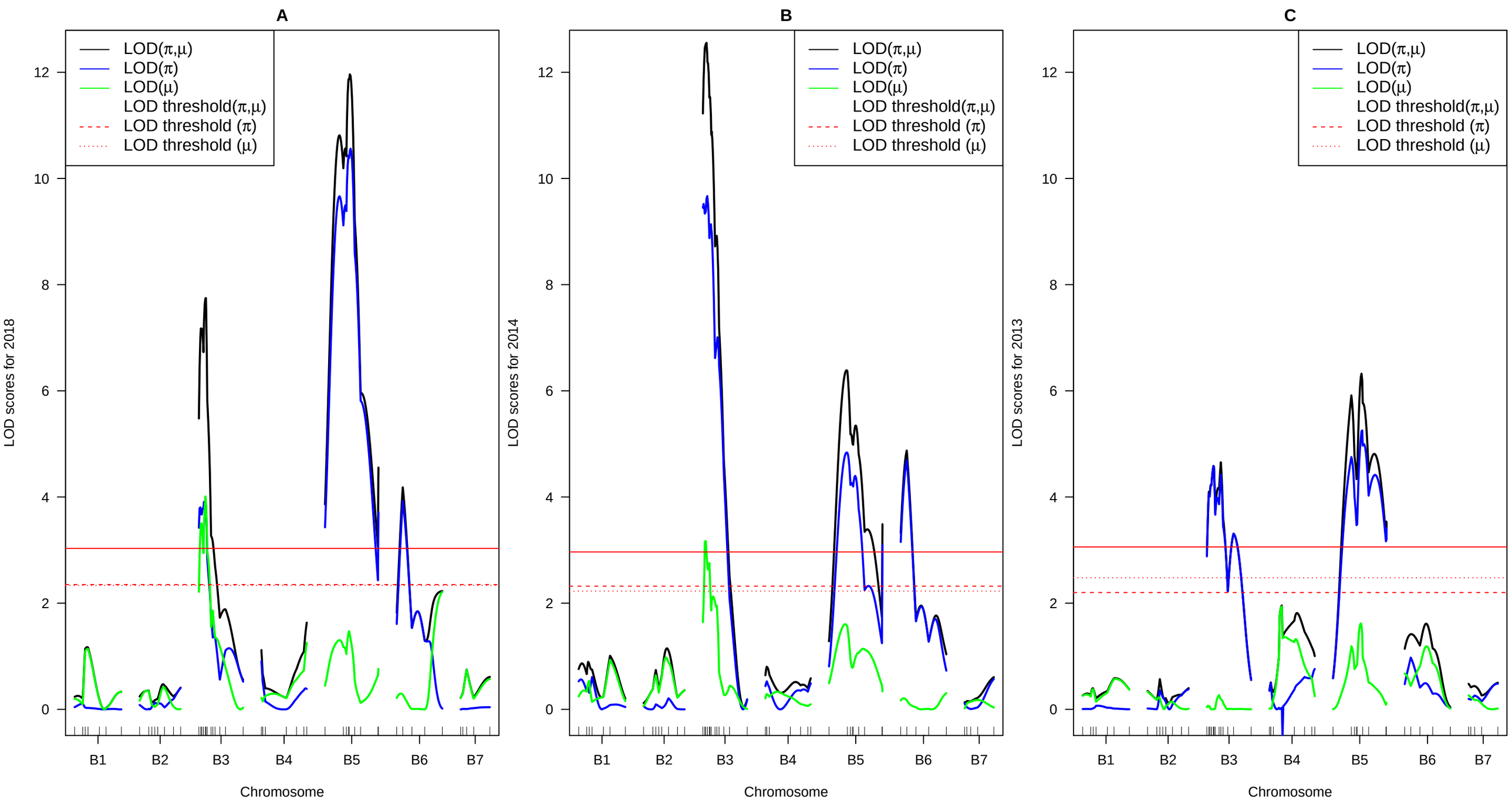
A
B
C
LOD(π,μ)
LOD(π)
LOD(μ)
LOD threshold(π,μ)
LOD threshold (π)
LOD threshold (μ)
LOD scores for 2018
LOD scores for 2014
LOD scores for 2013
0
2
4
6
8
10
12
B1
B2
B3
B4
B5
B6
B7
Chromosome

Supp. Fig. 9 QTL mapping with black spot disease resistance using a two-part model approach for non-normally distributed data of FW and HW populations for the female maps

A: LOD curves for the two-part model for FW population using 2018 scoring year in Angers; B: LOD curves for the two-part model for HW population using scoring year 2014 in Bellegarde; LOD.π (penetrance, equivalent to binary model) displayed in blue, LOD.μ (severity, equivalent to normal model for non-spike phenotypes) displayed in green and LOD.π.μ (sum, representing the complete model) displayed in black; LOD thresholds are displayed in red with α=0.05 for declaring significant QTL based on 1,000 permutations.

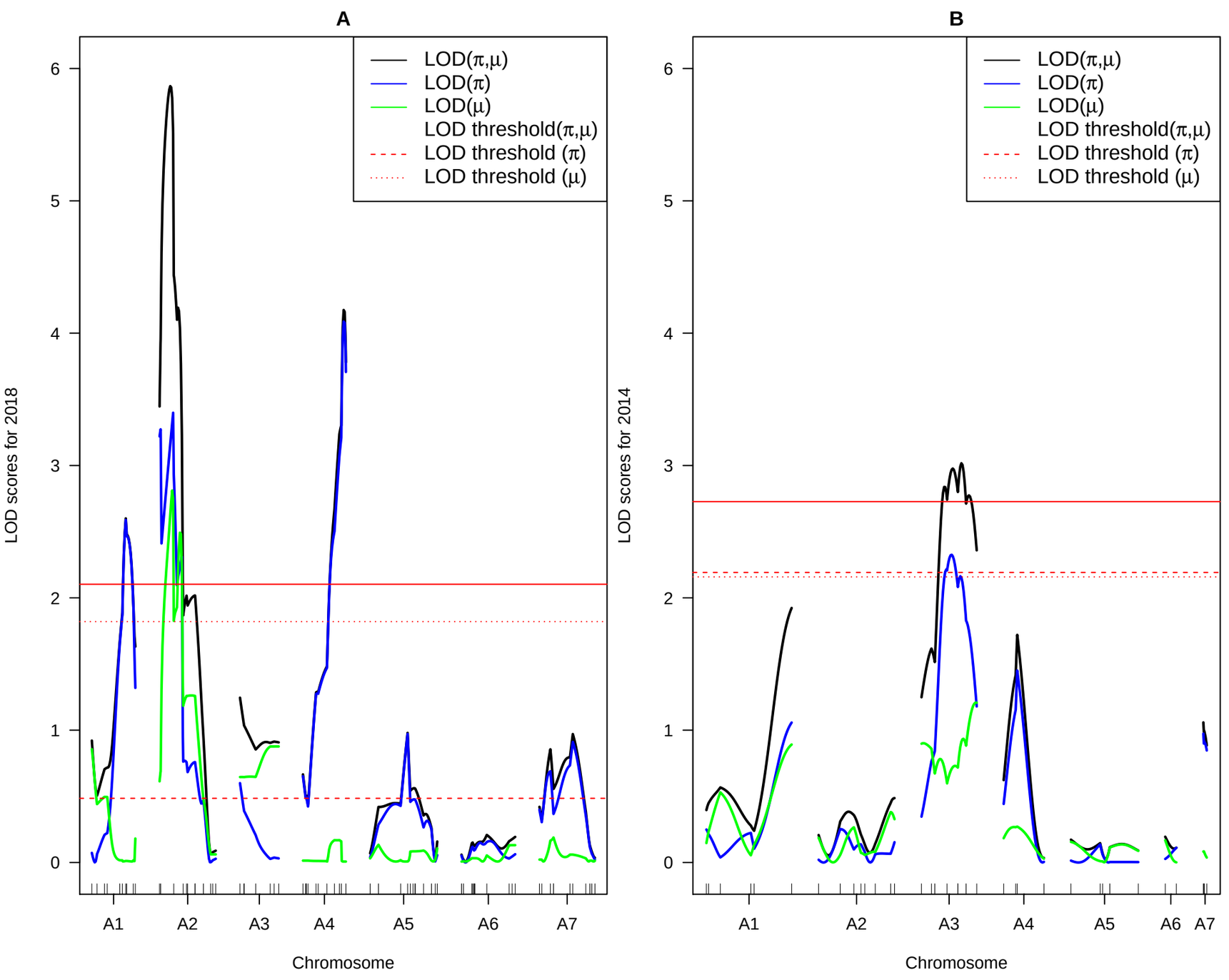
A
LOD(π,μ)
LOD(π)
LOD(μ)
LOD threshold(π,μ)
LOD threshold (π)
LOD threshold (μ)
LOD scores for 2018
0
1
2
3
4
5
6
A1
A2
A3
A4
A5
A6
A7
Chromosome

B
LOD(π,μ)
LOD(π)
LOD(μ)
LOD threshold(π,μ)
LOD threshold (π)
LOD threshold (μ)
LOD scores for 2014
0
1
2
3
4
5
6
A1
A2
A3
A4
A5
A6
A7
Chromosome

Supp. Fig. 10 Co-localization of the *Rdr1* genes cluster with the QTLs on A1 from OW and FW female maps

Linkage groups (LG) names from female genetic maps are placed above the LG and named A1 - “population name” and the corresponding chromosome is placed in the middle. Names of markers are on the right and the genetic distances (in cM) on the left. For the chromosome from the physical map, physical distances are expressed in mega-base (Mb). TNLs genes and clusters (OB2-A, OB-B, Cluster1 and Cluster2, Menz et al. 2020) are shown in black. The markers peaks of each QTL are displayed in grey. The active form of *Rdr1* resistance gene (*muRdr1A*) is located on the cluster2 (Menz et al. 2020). QTLs widest confidence intervals are represented in plain colors on the linkage groups: blue for the OW female map, yellow for the FW female map and green for the equivalent common widest region on the physical map.

A1−OB

0 Rh12GR_29955_578
1.3 RhK5_10462_838
2 Rh12GR_53461_311
2.7 Rh12GR_10543_433
4 Rh12GR_62822_144
4.7 RhK5_6217_460
6.7 Rh12GR_1603_2320
7.4 Rh12GR_12580_120
8 Rh12GR_100572_586 Rh12GR_25770_1969
8.7 Rh12GR_10131_766
9.4 RhK5_438_2263
10 Rh12GR_34196_1010
10.7 Rh12GR_21817_240
11.4 Rh12GR_55474_305
12 Rh12GR_39436_312
12.7 Rh12GR_100682_416 Rh12GR_178_2728
13.4 Rh12GR_1512_1260 RhK5_1155_2334
14 Rh12GR_39150_286 Rh12GR_39391_113
14.7 Rh12GR_100433_1063 Rh12GR_13927_454
15.4 Rh12GR_72482_368 RhK5_15904_557
16 Rh12GR_22143_1043 RhK5_3618_1798
16.7 RhK5_16_363
17.4 Rh12GR_17619_724 Rh12GR_97037_285
18 Rh12GR_12803_140 RhK5_9672_88
18.7 RhK5_10096_385
19.4 Rh12GR_11115_707 Rh12GR_57902_67
20 Rh12GR_38406_747 RhK5_10950_202
20.7 RhK5_10956_215 RhK5_11189_431
21.4 RhK5_19_4494 RhMCRND_98_1485
22.7 Rh12GR_75370_476
23.4 Rh12GR_3397_1392
24.1 Rh12GR_50619_191
24.7 RhK5_3800_1441
25.4 RhK5_2453_683
26.1 RhK5_171_513 RhK5_8720_1178
27.4 Rh12GR_16271_362 Rh12GR_50984_366
28.1 Rh12GR_62792_1157
30.1 Rh12GR_13203_708
31.4 Rh12GR_19227_1005 Rh12GR_24647_1345
32.8 Rh12GR_10958_462 RhK5_10243_1001
33.4 Rh12GR_17865_134 RhK5_11250_438
34.1 RhK5_1910_1012
36.8 Rh12GR_55113_261 Rh12GR_71852_1802
37.5 RhK5_12314_325 RhMCRND_16286_514
40.2 Rh12GR_50354_520 RhK5_10102_270
40.9 Rh12GR_69504_336
42.2 RhMCRND_21672_232
42.9 *Rh12GR_6572_1248* RhK5_8281_147
44.9 Rh12GR_24336_1135 Rh12GR_63537_121
45.6 Rh12GR_2216_1528 RhMCRND_35850_450
46.3 RhK5_16909_365
47.6 Rh12GR_12796_272 Rh88_14299_238
49.6 Rh12GR_24108_2731 RhK5_9530_911
50.3 Rh12GR_100310_341
51 Rh12GR_89853_613 RhK5_7167_896
51.6 Rh12GR_17699_192
53 Rh12GR_65375_120 Rh12GR_68813_107
53.6 RhK5_6613_839
54.3 *Rh12GR_100474_250* Rh12GR_1283_1872
55.6 Rw32K24
56.3 Rh12GR_22107_1182 RhK5_2033_975
57 Rh12GR_21932_1015
57.6 Rh12GR_25662_2898 RhK5_17439_159
58.3 Rh12GR_14551_1049 Rh12GR_43210_233
59 Rh12GR_48986_1690 Rh12GR_9361_1434
60.3 *Rh12GR_57721_1060*
61.7 RhK5_11249_726
63 RhK5_13405_107
63.7 Rh12GR_13521_1087 Rh12GR_22490_270
64.3 Rh12GR_59097_179
65.7 Rh12GR_98623_1205
67 RhK5_2826_978
68.4 Rh12GR_1163_250
68.7 *RMS015*
69 Rh12GR_49230_179 RhMCRND_5918_726
69.7 Rh12GR_49465_132 RhK5_1249_804
70.4 Rh12GR_22473_557 Rh12GR_5015_2143
71 Rh12GR_12922_326 RhK5_10351_346
71.7 Rh12GR_60980_253

Chr1

1 begenningChr1
10.5 OB2_A
30.9 OB2_B
42.2 *TE_F2MCf83*
51.2 *Rw34L6*
51.6 *Rh12GR_6572_1248*
53 Cluster1 (OB2_C to OB2_H)
57.2 *Rh12GR_100474_250*
59.7 *Rh12GR_57721_1060*
62.5 *RMS015*
62.6 Cluster2 (OB2_J to OB2_S)
64.8 endChr1

A1−TF

0 RhAB92
5.4 Rw25J16
13.1 RoSOC1
15.9 *TE_F2MCf83*
28.8 H23O17
31.5 RoLEa
35 *Rw34L6*
36 Rw32K24
42.7 RoTFL1b
44.9 *RMS015*

Acknowledgement

This work was financially supported by RFI Objectif Végétal, the BAP department of the “Institut National de la Recherche Agronomique et Environnement” (INRAE) and Région Pays de la Loire (support by the CASDAR project ROGER n° C-2014-06 from the French Ministry of Agriculture, Agrifood and Forestry). The invaluable collaboration and work of the ANAN platform (SFR Quasav) for SSR analysis as well as INRA Horticulture Experimental Facility (Beaucouzé, France), for plant management in experimental fields are gratefully acknowledged. We thank Martin Leduc for his work on OW maps, Kévin Debray for his work on SNP positioning in the genome and Briana Gastaldello for the final proofreading of the article.

Material & correspondence

Any request for correspondence and materials should be sent to Diana Carolina Lopez Arias (diana.lopez-arias@inrae.fr).